UNIVERSITÉ DE BOURGOGNE
Laboratoire Interdisciplinaire Carnot de Bourgogne UMR CNRS 5209

NATIONAL ACADEMY OF SCIENCES OF ARMENIA
Institute for Physical Research

GENERATION AND INTERFACING OF SINGLE-PHOTON LIGHT WITH MATTER AND CONTROL OF ULTRAFAST ATOMIC DYNAMICS FOR QUANTUM INFORMATION PROCESSING

by

ANAHIT GOGYAN

A Thesis in Physics
Submitted for the Degree of
Doctor of Philosophy

Date of Defense: October 11, 2010

The Jury:

Yuri MALAKYAN	Professor Institute for Physical Research, NAS, Ashtarak	*Supervisor*
Stéphane GUERIN	Professor ICB, Université de Bourgogne, Dijon	*Supervisor*
Armen MELIKYAN	Professor Russian-Armenian (Slavonic) University, Erevan	*Referee*
Hamlet AVETISSIAN	Professor Yerevan State University, Erevan	*Referee*
Wolfgang LANGE	Professor University of Sussex, Sussex	*Referee*
Claude LEROY	Maître de Conférences ICB, Université de Bourgogne, Dijon	*Examiner*

**Génération et interfaçage de lumière à photon unique
et contrôle de la dynamique atomique ultra-rapide pour l'information quantique**

Résumé

Nous développons un mécanisme robuste et réaliste pour la génération de photons uniques indiscernables avec des impulsions de fréquence et de polarisation identiques. Ils sont produits à la demande à partir d'un système couplé atome-cavité double-Raman en interaction avec une séquence d'impulsions laser de pompe. Ce processus combine un rendement élevé, la capacité de produire une séquence d'impulsions de photons uniques à bande étroite avec un retard déterminé seulement par le taux de répétition de la pompe, avec la simplicité du système libre de complications comme le repompage et le déphasage de l'environnement.

Nous proposons et analysons un schéma simple de conversion paramétrique de fréquence pour l'information quantique optique dans des ensembles atomiques froids. Ses propriétés remarquables sont des pertes réduites, une distorsion de la forme des impulsions minimale, ainsi que la persistance de la cohérence quantique et de l'intrication. Une conversion efficace de fréquence entre les différentes régions spectrales est montrée. Une méthode de génération d'états caractérisant des photons uniques intriqués en fréquence est discutée.

Nous proposons un mécanisme robuste et simple d'excitation cohérente de molécules et d'atomes en une superposition d'états pré-sélectionnés par un train d'impulsions laser femtoseconde, combinée avec un champ de couplage à largeur de bande étroite.

La théorie des battements quantiques pour la génération du rayonnement ultra-violet par mélange à quatre ondes dans des expériences pompe-sonde est développée. Les résultats sont en bon accord avec les données expérimentales observées dans la vapeur de Rb lorsque les fluctuations de phase laser sont importantes.

Mots clefs : Electrodynamique quantique en cavité, génération de photons uniques, conversion de fréquence quantique, interaction paramétrique, excitation sélective, cohérence atomique, battements quantiques, processus de mélange à quatre ondes.

Generation and interfacing of single-photon light with matter and control of ultrafast atomic dynamics for quantum information processing

Abstract

We develop a robust and realistic mechanism for the generation of indistinguishable single-photon (SP) pulses with identical frequency and polarization. They are produced on demand from a coupled double-Raman atom-cavity system driven by a sequence of laser pump pulses. This scheme features a high efficiency, the ability to produce a sequence of narrow-band SP pulses with a delay determined only by the pump repetition rate, and simplicity of the system free from complications such as repumping process and environmental dephasing.

We propose and analyze a simple scheme of parametric frequency conversion for optical quantum information in cold atomic ensembles. Its remarkable properties are minimal losses and distortion of the pulse shape, and the persistence of quantum coherence and entanglement. Efficient conversion of frequency between different spectral regions is shown. A method for the generation of frequency-entangled single photon states is discussed.

We suggest a robust and simple mechanism for the coherent excitation of molecules or atoms to a superposition of pre-selected states by a train of femtosecond laser pulses, combined with narrow-band coupling field.

The theory of quantum beatings in the generation of ultra-violet radiation via a four wave mixing in pump-probe experiments is developed. The results are in good agreement with experimental data observed in Rb vapor when the laser phase fluctuations are significant.

Remerciements

J'aimerais exprimer ma grande considération à mes Directeurs de thèse, les Professeurs Yuri Malakyan et Stéphane Guérin pour leur soutien et leur patience.

Je remercie l'Ambassade de France en Arménie pour son aide financière, notamment la bourse No. 2007-4703 en tant que Boursière du Gouvernement Français. Ce financement m'a aussi permis de découvrir les traditions françaises et de m'initier à l'apprentissage de la langue française.

Je voudrais aussi remercier tous mes collègues et tout le personnel de l'Institute for Physical Research de l'Académie des sciences d'Arménie et du Laboratoire Interdisciplinaire Carnot de Bourgogne de l'université de Bourgogne pour leur aide et leur chaleureuse camaraderie.

Acknowledgments

I would like to express my sincere consideration to my supervisors Profs. Yuri Malakyan and Stéphane Guérin for their support and patience.

I acknowledge the support of French Embassy in Armenia for Grant No. 2007-4703 as Boursière du Gouvernement Français . This grant allowed me to discover the French traditions and to begin the French language learning.

I would also like to thank all the co-workers and staff of the Institute for Physical Research of National Academy of Sciences and Laboratoire Interdisciplinaire Carnot de Bourgogne of University of Bourgogne for the kindly and warmhearted attitude.

Research conducted in the scope of the International Associated Laboratory IRMAS.

Contents

Introduction

The relevance of the subject

This thesis relates to one of the most promising and rapidly developing areas of modern physics- quantum-information science. The ultimate goal of research in this field is the development of quantum computers and quantum communication networks. Unlike traditional "classical" information, quantum information is incomparably more powerful, allowing to solve mathematical problems which are fundamentally impossible to solve using classical computers. In a quantum network (QN) the carriers of information are photons, which due to their very weak interaction with the environment can be distributed over long distances. The use of photons provides a totally secret transfer of information, eliminating eavesdropping from outside, because unlike classical methods for the transfer of sensitive information the security of quantum information is not based on mathematical complexity, but on the quantum properties of photons whose state cannot be cloned, and hence a quantum information cannot be copied without its distortion that can be easily detected.

Huge achievements have been recorded in this field during the last two decades. In particular, quantum cryptography and teleportation of quantum states of photons over distances of several hundred kilometers have been implemented. However, for the ultimate realization of quantum networks, including quantum computers, many fundamental questions still remain unsolved. First, however weak is the interaction of photon with the environment, the bottleneck for communication between distant nodes of quantum networks is the scaling of the probability errors with the length of the channel connecting the nodes. For channels such

as an optical fiber, the losses grow exponentially with the length of the fiber. The problem of exponential attenuation of the losses can be overcome by using quantum repeaters at certain points in the communication channel, which store, process and retrieve quantum information. As a quantum repeater can serve individual atoms, ions, coherent atomic ensembles, quantum dots, solid states doped with resonant atoms, etc. Secondly, although the interaction of photons with atoms is weak, it must be strong enough to ensure effective conversion (storage) of quantum information recorded in the medium. A particular problem is the fact that, in the telecommunication waveguides, photons display minimal losses at a wavelength of around 1.5μm, while atomic-based quantum memories operate efficiently at the wavelengths in the visible domain of spectrum, so mechanisms must be developed for converting quantum information between telecom and visible wavelengths at the single photon level. Thirdly, in many applications of quantum optics, including quantum computing, quantum cryptography, teleportation, etc., the deterministic sources of single-photon pulses of the same frequency and polarization and a given shape are necessary, since the latter processes and schemes are based on photonic interference processes and thus are very sensitive to the parameters of single-photon wave packets. Finally, for fast quantum information processing an efficient selective excitation of target atomic states or their superposition in femtosecond timescale is required.

To address these problems, we propose and develop theoretically new mechanisms and present the schemes for their experimental implementation.

*The **main objectives** of the thesis are:*

- to develop a mechanism for deterministic generation of a train of single-photon pulses having the same frequency, polarization and a given identical shape of wave-packets.

- to analyze and present realistic schemes for experimental implementation of the proposed mechanism.

- to solve the problem of quantum frequency conversion in cold atomic ensembles on the basis of strong parametric interaction between two narrow-band single-photon pulses.

- to generalize the proposed QFC technique to transform a telecom wavelength qubit into another at a visible domain and vise versa with maintaining the coherence of initial state.

- to develop a new mechanism combining constant coupling fields and ultrashort laser pulses for selective excitation of atomic and molecular states and their coherent superposition.

- to use the quantum beating technique for elaboration of a sensitive method for experimental verification of the proposed selective excitation mechanism.

The main statements of the thesis

- A mechanism of deterministic production of a a train of indistinguishable single-photon pulses in a single atom-cavity QED system, its quantum theory and scheme of experimental realization.

- A new scheme of quantum frequency conversion of quantum information, based on parametric coupling between single-photon pulses in a slow-light cold atomic medium.

- A new mechanism to generate single-photon frequency-entangled state.

- Quantum frequency conversion of quantum field at telecom wavelength into another at a visible domain.

- A new mechanism to selectively excite the atoms or molecules by ultrashort pulses combined with constant coupling fields in both weak and strong fields regimes and a sensitive method for experimental verification of selective excitation.

- Theory of quantum beating in ultraviolet field intensity generated via four-wave-mixing in femtosecond pump-probe experiments.

Scientific Novelty and Practical Importance

- A new efficient and robust mechanism is proposed to produce deterministically a train of indistinguishable single-photon pulses in a multilevel single atom-cavity QED system. The generated photons have the same frequency, polarization and easily controlled spatio-temporal profile. The proposed mechanism allows to change the repetition rate of the non-entangled single-photons freely. One of the most important applications of this property

is to generate Fock states with a programmable number of photons.This is of fundamental importance for quantum information processing and secure quantum communication.

• For the first time a method is proposed for efficient frequency conversion of quantum information based on strong parametric coupling between two single-photon pulses propagating in a slow-light three-level atomic medium at different group velocities. An incoming quantum field frequency is converted into another frequency in a lossless and shape-conserving manner while keeping the initial quantum coherence and entanglement. It is possible to generate a narrow-band single-photon frequency-entangled state. Moreover, slightly modified scheme enables transformation of an input qubit at telecom wavelength into another at a visible domain with near-unity efficiency. This is a desirable tool for interfacing of quantum communication lines with photon memory units.

• In this thesis we have proposed a robust and efficient method for population transfer to a desired superposition in multilevel atomic or molecular systems using a train of femtosecond pump pulses or pump-probe technique combined with control lasers. This is of a great importance not only for fast quantum information processing, but also for the control of chemical and biological processes, which occur in femtosecond time-scales. It has been considered two weak-field and strong-field regimes. For the first time quantum beats (QB) in the Stokes radiation generated in the stimulated electronic Raman scattering (SERS) process are studied theoretically. The theory of the QBs in the hyper-Raman scattering and four-wave mixing is developed as well with and without taking into account the laser phase fluctuations.

Approbation of the Thesis Statements

The statements of the thesis were presented and discussed at the Theoretical Physics Laboratory's seminars at the Institute for Physical Research of Armenian NAS; at the seminars of the Institute for Physical Research of Armenian NAS; at the Laboratoire Interdisciplinaire Carnot de Bourgogne at the University of Bourgogne, as well as reported at the conferences "European Young Scientists Conference on Quantum Information" (Vienna, Austria, 2007),

"International School on Quantum Electronics-2008" (Bourgas, Bulgaria 2008), "Advances in Foundations of Quantum Mechanics and Quantum Information with atoms and photons and IQIS 2010" (Turin, Italy, 2010), CAMEL-VI (Varna, Bulgaria, 2010), "Les Journées des Ecoles Doctorales-2009" (Dijon, France, 2009), "Les Journées des Ecoles Doctorales-2010" (Besancon, France, 2010), "Laser Physics - 2007, 2008" (Ashtarak-2, Armenia, 2007, 2008), "International Advanced Research Workshop on Modern Problems in Optics and Photonics" (Yerevan, Armenia, 2009), "ECAMP-2010" (Salamanca, Spain).

The main results of this dissertation have been published as articles in 8 peer reviewed journals and 9 abstracts in the conference Book of Abstracts.

The thesis, which consists of introduction, four chapters and References, comprises 124 pages, contains 28 figures and 147 references.

In the **_Chapter I_** an overview of literature on the subjects, discussed in the thesis is given. Particularly, key works on previous mechanisms to produce single-photon pulses is presented, quantum frequency conversion schemes are discussed and hitherto listed, techniques to selectively excite atoms or molecules by ultrashort laser pulses is given. The advantages and drawbacks of previously suggested and realized schemes are discussed.

In the **_Chapter II_** of this thesis we present a mechanism to produce indistinguishable single-photon pulses on demand from an optical cavity. The sequences of two laser pulses generate, at the two Raman transitions of a four-level atom, the same cavity-mode photons without repumping of the atom between photon generations. Photons are emitted from the cavity with near-unity efficiency in well-defined temporal modes of identical shapes controlled by the laser fields.

In the **_Chapter III_** a novel method for frequency conversion of quantum states of light and redistribution of optical information between different quantum fields is developed based on the parametric interaction between two single-photon pulses propagating in a resonantly driven nonabsorbing cold atomic ensembles at low group velocities. The absorption reduction and slowing of the pulses are achieved by means of electromagnetically induced

transparency realized for both quantum fields. We analyze the quantum properties of the frequency conversion process and show how a partial conversion leads to a generation of the frequency-entangled single-photon state.

A method for efficient conversion of the quantum information frequency between different regions of a spectrum of light is given. It is shown that an input qubit at telecom wavelength is transformed into another at a visible domain in a lossless and shape-conserving manner while keeping the initial quantum coherence and entanglement.

In the **_Chapter IV_** a mechanism to prepare the atoms or molecules to a coherent superposition of pre-selected states of atoms or molecules has been theoretically proposed for two cases. In a weak field regime the atomic or molecular system is interacting with a train of ultrashort femtosecond laser pulses, whose spectrum is wide enough to overlap all the upper states, while a narrow-band weak laser couples the level we don't need to be populated with an auxiliary state. By adjusting the repetition rate of the pump pulses and the intensity of the coupling laser, one can suppress a transition, while simultaneously enhancing the desired transitions. As an example various superpositions of states of the K_2 molecule are shown. In a strong field regime atom or molecule is excited with pump and probe femtosecond laser pulses and selectivity in this case is also achieved by constant coupling field, which cancels the undesired transition.

For the first time QBs in the Stokes radiation generated in the SERS process are studied theoretically. For this purpose, at first it is considered a simple model of a four-level atom and then a more realistic situation in the cases of hyper-Raman scattering and four-wave mixing, where QBs were observed experimentally both in the Stokes signal and in the parametric generation of UV radiation.

Chapter 1

Literature overview

One of the fastest developing and promising areas of modern physics is the quantum information (QI) science, which represents an extension of classical information to a domain in which quantum effects are important and therefore quantum mechanics must be used as the underlying physical theory. Over the last few decades QI science has emerged to consider what additional power and functionality can be realized in the encoding, transmission and processing of information by specifically harnessing quantum mechanical effects [1]. The ideal carriers of quantum information are photons, since they travel long distances through the medium without high losses due to their weak interaction with environment. The ability to manipulate photon states enables us to perform tasks that would be unachievable in a classical context, such as unconditionally secure transmission of information, ruling out further eavesdropping [2]. The reason is that unlike the classical methods of information transmission, the security of quantum information is based not on a mathematical complexity leading to time consuming resolutions, but on the intrinsic property of quantum states, that cannot be cloned: the information cannot be copied without its demolition, which can be easily found out. Another anticipated technologies include quantum metrology [3], which allows more precise measurements than could ever be achieved without quantum mechanics, and quantum lithography [4], which could enable fabrication of devices with features much smaller than the wavelength of light. Perhaps the most startling and powerful future quan-

tum technology is a quantum computer, which promises exponentially faster computation for particular tasks which are, in principle, unsolvable with classical computers in a reasonable time [1, 5].

Great advances have been recorded in the field during the last two decades, including dense coding and teleportation [6], which demonstrate our ability to control coherently individual quantum systems. Nevertheless, for the ultimate realization of quantum networks, which play an important role, both for the formal analysis and the physical implementation of quantum computation and secure quantum communication, many fundamental problems still remain unsolved. To create a quantum network, quantum information is generated, processed, and stored locally in quantum nodes. These nodes are linked by quantum channels that transport quantum states from site to site with high fidelity and that distribute entanglement across the entire network. The first problem is the scaling of the error probability with the length of the channel connecting the nodes, no matter how small is the interaction of photon with the environment. For channels such as an optical fiber, the losses grow exponentially with the length of the fiber. The problem of exponential attenuation can be overcome by using quantum repeaters at certain points in the communication channel, which store, process and retrieve quantum information. As a quantum repeater can serve individual atoms, ions, coherent atomic ensembles, quantum dots, solid states, etc. Thus, a central issue in realization of quantum networks is the effective atom-light interaction; namely it should be strong enough to ensure effective storage and conversion of quantum information recorded in the medium. A particular problem is that, in the telecommunication waveguide, photons display minimal losses at a wavelength of around 1.5μm, while atomic-based quantum memories operate efficiently at the wavelengths in the visible domain of spectrum of light, thus impeding the interfacing of quantum communication lines with photon-memory units. Secondly, in many applications of quantum optics, including quantum computing, quantum cryptography, teleportation, etc., deterministic sources of single-photon (SP) pulses with well-defined identical shapes, frequency and polarization are necessary, as these schemes based on photon interference effects are very sensitive to the parameters of SP pulses. The last

problem to be considered in the thesis relates to the challenging task of implementation of fast quantum gates in the femtosecond (fs) timescale, which are an important ingredient of fast quantum information processing, as opposed to more standard techniques developed in nano- or microsecond timescales. The first step to solve this problem is the efficient selective excitation of target states of atoms and molecules by fs pump pulses.

In the thesis we propose and develop the robust mechanisms to solve the above mentioned problems, namely: (a) a mechanism for generation with high efficiency a train of indistinguishable single-photon pulses in a four-level atom-cavity QED system; (b) a scheme of photon frequency conversion between infrared (telecom) and visible regions of spectrum of light based on the efficient parametric coupling between two single-photon pulses propagating in a slow-light medium; (c) new mechanisms for selective coherent excitation of multilevel atoms and molecules by ultrashort laser pulses. It is worth noting that ultra-fast excitation of atoms and molecules is of significance in its own right, as it is well adopted for the control of chemical and biological processes, that usually occur in this fs range. In this Chapter we present a summary of the state of the art of these problems.

1.1   Generation of identical single-photon pulses in a cavity-quantum electrodynamics system

Motivated by developments in quantum information science, much recent effort has been directed toward producing single photons on demand for implementation of functional nodes of a quantum network, where the emitters serve as processing nodes and photons are used for long-distance quantum communication [7]. For many of these practical applications, it is important that outgoing single photons have desired frequency and bandwidth, enabling quantum computing with linear optics [8, 9], nonlinear optical switching at a single photon level [10], entanglement swapping [11] and long-distance transmission over telecommunications wavelengths [12]. Most quantum information processing schemes involve interference

between the photons [13], in which the indistinguishability of photons is a fundamental and critical requirement. Any distinguishability will reduce the visibility of interference and the fidelity of quantum computation protocol [14]. It will also directly affect the other applications with photon interference, such as quantum key distribution [2] and high precision quantum phase measurement [15]. Moreover, photon indistinguishability is fundamental to stimulated emission [16, 17] and has been applied in quantum cloning [18, 19] and entanglement measure [20]. Thus, for these protocols, a basic requirement is to have SP wave packets with well-defined identical shapes, frequency and polarization. An ideal SP source has to ensure a pure SP state without mixture from both the multi-photon and zero-photon states and to prevent the entanglement between the photons which degrades the purity of the SP state. Since the individual photons are usually emitted during the spontaneous decay of atomic systems, the SP sources must be immune to the environmental effects that induce the dephasing of atomic transitions. In addition, a good source supports an on-demand generation of single photons at a high repetition rate with a Fourier-transform-limited spectrum for a given spatio-temporal mode. This is possible, if the SP pulses are generated by a unitary, reversible process based on a deterministic and unitary energy exchange between a single emitter, e.g. an atom, and a single mode of the quantized radiation field, as is the case in the resonant optical microcavities (cavity QED) [21, 22, 23]. During the last years many different types of SP sources have been proposed and demonstrated [24, 25, 26, 27, 28]. However, most of the schemes to produce single photons on demand from solid state single emitters [29], organic molecules [30, 31], and quantum dots [21, 32] do not satisfy all the above requirements. Besides, they do not offer a high efficiency because of the isotropic nature of fluorescence that prevents to collect the photons, not to mention the spectral dephasing and inhomogeneity of solid-state emitters. Deterministic sources of single photons on the basis of electromagnetically induced transparency (EIT) [33] are realized also in cold atomic ensembles with feedback circuit [34, 35]. But these schemes are not suitable to generate SP train with an arbitrary repetition rate because of strong temporary bounds caused by the feedback and write-read processes.

At present, all the requirements mentioned above can be achieved together with a Λ-type atom trapped in high-finesse optical cavities [36, 23, 37, 38], where the single photons are generated via vacuum-stimulated Raman scattering of a classical laser field into a cavity mode. These systems not only provide a strong interaction between a photon and an atom, but also support very high collection efficiency due to the fact that the photons leave the cavity through one mirror with a transmissivity incomparably larger than that of the opposite one, thus forming a single-photon pulse propagating in a well-defined direction in space. By carefully adjusting the parameters of the laser pulse one can also easily control the waveform of output single photons. However, the main disadvantage of these schemes is the necessity to use a repumping field to transfer the population of the atom to its initial state after the generation of a cavity photon and only then to generate the next one.

In the Chapter II of this thesis we propose a scheme featuring a double Raman atomic configuration, which is able to deterministically generate a stream of identical SP pulses without using the repumping field, while maintaining the high generation efficiency, as well as providing simple control of the output photon waveforms. The removal of the repumping field is a principal task, because its usage strongly restricts the process: the repetition rate of emitting photons is limited by the acting time of the repumping field. Unlike this, our mechanism allows to freely change the repetition rate of the single-photon pulses up to zero, because even in this case non-entangled single-photons are generated. One of the most important applications of this property is to generate Fock states with a programmable number of photons. Moreover, in the good-cavity limit our scheme can serve as an one-atom laser with a controllable statistics of generated photons that provides the quantitative study of the quantum-to-classical transition in our system raised with gradual change of the parameters. It is worth noting that a similar scheme without repumping field was employed in [39] for generating a sequence of single photons of alternating polarization. We calculated the second order correlation function that reveals the single-photon nature of the source. We also present a realistic setup for the experimental implementation of our scheme.

1.2 Quantum frequency conversion

Nonlinear optical frequency conversion is widely used in fields as diverse as ultrahigh-resolution imaging and telecommunications, as it allows for the generation of light in regions of the spectrum for which there are no convenient sources or detectors. Common implementations include optical parametric oscillators to make tunable fs lasers in the infrared. Recently, nonlinear photonic crystal cavities [40, 41, 42] have emerged as promising systems in which similar nonlinear functionalities can be achieved at micron scales, which would enable the miniaturization of optical devices onto integrated platforms. While the majority of such work focuses on conversion of classical fields, these systems are now being applied to quantum optics and quantum information science. The up- or down-conversion of frequency of photons termed as quantum frequency conversion (QFC) [43] has been attracting attention as a way to connect quantum information systems with photons of various wavelengths. The transmission of qubits (qubit is the quantum analogue of the classical bit and is defined in a two-dimensional Hilbert space) in quantum networks, especially over large distances, would most easily be accomplished by telecom-band photons at 1550nm, which has the highest transmission through fiber optics. However, the storage or processing of qubits require photons in the visible spectrum, e.g. corresponding to some atomic transition, and so a method must be developed for converting between wavelengths at the single photon level while coherently maintaining the polarization state [44]. Quantum frequency upconversion (QFUC) [45, 46, 47, 48, 49, 50] has been employed to convert a photon of telecom-wavelength to a visible-band photon that is important not only for utilizing single photon detector technologies in the visible wavelength bands, but also for interfacing quantum communication lines of different wavelength (e.g. fiber-optical and open-air) between each other and with memory-based quantum repeaters [51]. For complete realization of quantum networks, containing communication channels between atomic-memory elements, the reversible mapping between photons and atoms is required and, hence, the quantum frequency downconversion (QFDC) is also necessary that has been realized only recently [52, 53] because of the difficulties to detect

infrared photons - detectors at $\sim 1.5 \mu$m are more noisy than those at $\sim 0.8 \mu$m. The basic requirement for reliable implementation of quantum interface between light and matter is the ability of all QFC schemes to preserve any polarization state of the incoming photons, since the content of information is encoded in the polarization degree of freedom of single photon states. As opposed to the reproduction of classical information between different systems, it is not possible to merely measure the properties of a given quantum system and replicate them accordingly, as a result of the no-cloning theorem [54]. Nevertheless, it is possible to transfer the quantum information based on an interaction, which maintains the coherence properties of atomic and photon qubits. QFC has been hitherto realized in the nonlinear crystals, basically in periodically poled lithium niobate, using the process of parametric up- [45, 46, 47, 48, 49, 55, 56] and downconversions [52]. For implementation of QFC in atomic ensembles, a technique for light storage and its subsequent retrieval [57] at another optical frequency under the conditions of EIT was employed. However, despite the success of proof-of-principle experiments performed in a four-level double Λ-type atomic medium [58, 59], to date no true demonstration of information preserving frequency conversion has been given. The major difficulties inherent to these schemes are unavoidable losses and shape distortion of a weak (quantum) light pulse during its storage and retrieval by means of EIT.

In the Chapter III, a protocol for QFC in atomic ensembles free from the above drawbacks has been proposed. It makes use of recently demonstrated [60] efficient parametric coupling between two single-photon pulses propagating in a slow-light medium. The latter is an ensemble of atoms which interact with two quantum fields in a V-type configuration, while the upper electric-dipole forbidden transition is driven by a classical and constant field inducing a magnetic dipole or an electric quadruple transition between the two upper levels (Fig.3.1). The role of classical field is twofold. First, it creates parametric coupling between the photons and, second, it induces medium transparency for the intensity values where the EIT conditions are fulfilled for both quantum fields. It is clear, however, that implementation of the medium transparency leads evidently to degradation of parametric interaction between the fields. Nevertheless, an incoming signal-photon state is efficiently converted under EIT conditions

into second optical mode in a lossless manner conserving at the same time the pulse shape and initial entanglement. The easiest way to realize this is obviously the case of equal group velocities of quantum fields, which, however, is almost never met in practice (see below). Meanwhile, for realistic atomic systems, we predict the conversion efficiency as high as $\sim 90\%$. In essence, while the process involves only one photon at a time, this system allows for the realization of strong interaction of individual photons with each other, even if the two pulses propagate in the medium with different group velocities. Our approach offers another important advantage: unlike the previous proposals for QFC based on the light storage and its retrieval, we apply here only one and, moreover, constant driving field for control the conversion efficiency that makes our method much favorable for future applications. One obvious limitation of considered process is that it is effective in a relatively narrow frequency range associated with specific atoms. We note, however, that recently a source of narrow-band, frequency tunable single photons with properties allowing exciting the narrow atomic resonances has been created [61, 62, 34, 63].

1.3 Coherent excitation of atoms and molecules by ultrashort laser pulses

Quantum communication is based on the distribution of photonic entangled states [2], while quantum computing relies on quantum gates (quantum "logic gates" are simple unitary operations on qubits [5, 64]) in the linear-optics approach [8] or in measurement carried out on complex cluster entangled states [65]. These tasks require the fast implementation of operation conditioned on single photon measurements. An important figure of merit to evaluate a specific physical implementation is the ratio between the gate operation time and the coherence time characteristic of the system. In this sense, for a given quantum memory coherence time and gate error rate, faster gates are of course highly preferable [66, 67, 68, 69, 70]. Since the preparation and rotations of single atomic qubits associated

with long-lived internal states can be performed by addressing individual atoms with laser radiation, shaped femtosecond laser pulses act as extremely fast quantum gates and can be designed by applying optimal control theory. Therefore, it is a fundamental problem to prepare atoms or molecules in specific quantum states via selective population transfer by ultrashort laser pumping. Such a scheme allows one to control coherently the atomic and molecular dynamics needed for fast quantum information processing. Besides, efficient excitation of atoms and molecules to a coherent superposition state is an urgent need for efficient implementation of chemical and biological processes [71, 72, 73, 74]. The time scale of the latter is usually in the femtosecond range, which stipulates the use of ultrashort laser pulses with a comparable or smaller duration to excite a medium very rapidly. As a result, laser fields having a wide spectrum can simultaneously excite a large number of close-lying upper levels of atoms or molecules, thus forming a coherent superposition of two and more atomic eigenstates. The spatial probability distribution of such atomic wave packets (WP) is strongly localized as compared to the classical size of atoms or the internuclear distance in molecules. Therefore, the study of the temporal evolution of WPs provides the possibility of retracing the chemical processes, particularly of observing directly the dissociation of the molecules or formation of chemical bonds between them [75].

To produce a superposition of two states in atoms and molecules, different mechanisms have been hitherto employed including the π-pulse techniques [76, 77, 78, 79], brute-force optimal control [80], and adiabatic passage in nanosecond regime [81, 79, 82]. Several of these mechanisms have been verified experimentally [83, 84, 85]. Extending these techniques to an ultrafast (fs) regime and for molecular systems is of particular interest. Another ultrafast spectroscopic technique is Impulsive Stimulated Raman Scattering (ISRS). Rotational, electronic, and spin excitations via ISRS plays an important role in fs pulse interactions with molecules, crystals, glasses (including optical fibers), semiconductors, and metals [86]. This is an effective approach to determine also the dynamics of vibrational molecular motion with high temporal and spectral resolution [86, 87, 88, 89].

In this thesis, we propose an alternate robust and efficient method for population transfer

17

to a desired superposition in multilevel systems using a train of pump pulses or pump-probe technique combined with control lasers. Recent progress has allowed the development of mode-locked laser systems producing mutually phase-coherent ultrashort laser pulses of high intensity with arbitrary adjustable amplitudes of stable frequency and, what is more important, of controllable delay time (see for instance [90, 91]). Theoretical [92, 93, 94] and experimental [95, 96] analysis in a few level systems have shown that a resonant π-pulse (or generalized π-pulse [78, 79]) can be split into trains of fractional π-pulses and can lead to the accumulation of population in a target state for appropriate delays. The main point is that weak pulses can then be used preventing detrimental destructive effects such as ionization. For more complicated systems, populating some chosen states among a set of levels all within the broad ultrashort pulse spectrum is a major issue. However we can exploit one of the main properties of the associated frequency comb, that is its extremely high resolution, given by the width of the combs teeth in the frequency domain, much better than the one determined by the Fourier transform of a single pulse in the train. High degree of population transfer to a single vibrational state of an electronic excited state has been indeed numerically shown by a train of fs laser pulses by choosing the pulse repetition period as non-integer multiple of the vibrational period [97]. Recently a so-called piecewise adiabatic passage method, based on the combination of adiabatic passage, trains of pulses, and pulse-shaping techniques, has been proposed [98, 99]. To prepare the atoms or molecules to a coherent superposition of preselected states of atoms and molecules we considered two cases of: (a) weak coupling field using a train of fs pump-laser pulses [135] and (b) strong coupling field in pump-probe experiments [139]. These regimes are discussed in the §1 and §2 of the **Chapter IV**, respectively. In both cases the selectivity of the upper-lying levels is realized using constant coupling fields that allowed one to find the analytical formulas in the impulsive and perturbative regimes for the ultrashort pump pulses.

To verify these schemes experimentally, we suggest in §3 of the Chapter IV a sensitive method based on quantum beating technique. First, the pump laser pulse generates a WP in an atom or molecule, which is then observed by the second pulse coming after a certain time

delay τ_d. Due to the Ramsey-type interference [100] of the two WPs, generated by the pump and probe pulses, periodic changes or QB appear in the τ_d dependence of any detected signal. Evidently, the coherent violation of WP owing to interaction with the coupling field strongly modifies the QB pattern. Moreover, under certain conditions the QB disappears that provides the possibility of ensuring the selective excitation of excited atomic and molecular levels by fs laser pulses. The QB technique has been tested in a number of previous studies. It is worth mentioning that due to the fact that the frequency of QB is proportional to the difference in energy between the excited states, the QB technique has been applied successfully for measurement of small frequency shifts, in particular, of the fine and hyperfine splitting of high-lying atomic levels [101]. In early experiments, a photoionization signal has been used for detection of WP by the QB technique [100, 102, 103, 104]. However, for well-known reasons, the temporal resolution and the efficiency of this approach are low. A much higher efficiency can obviously be achieved, when the wave packets are detected by a coherent narrow-band signal, for example, by Stokes field generated via stimulated electronic Raman scattering (SERS) of ultrashort laser pulses. Such experiments were recently carried out in K and Rb vapors [105, 106, 107], where QB has been observed in the intensities of Stokes and ultraviolet (UV) fields generated on the basis of hyper-Raman scattering (HRS) and four-wave mixing (FWM) [108], respectively. It is worth noting that the QB in the Stokes signal at a wavelength $\lambda \sim 4 \div 8 \mu m$ was used for detection of the motion of atomic fragments in the dissociation of diatomic molecules [107]. In the thesis we apply this technique to detect the selective excitation of a given atomic upper level by measuring the QB in UV intensity. We have developed the full theory of quantum beating in UV generation and demonstrated its excellent agreement with the experimental data.

Chapter 2

Generation of a train of indistinguishable single-photon pulses

In this chapter we present a mechanism to produce indistinguishable single-photon pulses on demand from an optical cavity [133]. The sequences of two laser pulses generate, at the two Raman transitions of a four-level atom, the same cavity-mode photons without repumping of the atom between photon generations. Photons are emitted from the cavity with near-unity efficiency in well-defined temporal modes of identical shapes controlled by the laser fields. The second order correlation function reveals the single-photon nature of the proposed source. A realistic setup for the experimental implementation is presented.

2.1   Four-level atom. Problem statement

All the requirements for ideal source to generate a train of indistinguishable single-photon pulses can be achieved in a scheme featuring a double Raman atomic configuration, which is able to deterministically generate a stream of identical SP pulses without using any repumping field, while maintaining the high generation efficiency, as well as providing simpler control of the output photon waveforms. It is interesting to note that a repumping field is not required also in a similar scheme for generating a sequence of single photons of alternating polarization
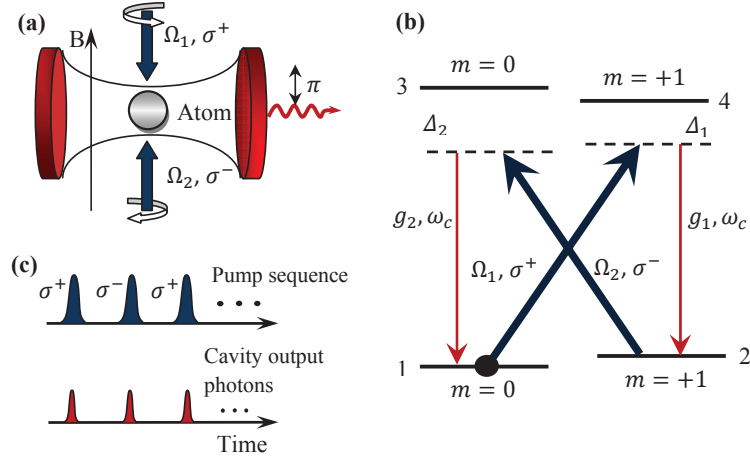
[39].

Figure 2.1: Schematic setup. (a) A single atom trapped in a high-Q cavity is driven by two laser pulses. b) Relevant atomic level structure in an external magnetic field. The case is shown, when the Landé g_L-factors of the ground and excited states have opposite signs. c) Sequence of laser pulses and generated cavity output single-photons.

We propose a scheme, illustrated in Fig. 2.1, involving a four-level atom trapped in a one-mode high-finesse optical cavity. The two ground states 1 and 2 and two upper states 3 and 4 of the atom are Zeeman sublevels (Fig. 2.1b), which are split by a magnetic field acting perpendicular to the cavity axis. The atom is initially prepared in one of the ground states, for instance, in state 1 of magnetic quantum number $m = 0$, and interacts in turns with a sequence of two pumping fields as shown in Fig.2.1a. At first, a coherent σ^+ polarized field of Rabi frequency Ω_1 applied between ground state 1 and excited state 4 transfers the atom to ground state 2 while creating a cavity-mode Stokes-photon. Then, after a programmable delay time τ_d, which is larger as compared to the pump pulse duration T, the σ^- polarized pump pulse Ω_2 generates the anti-Stokes photon at the $3 \rightarrow 1$ transition and transfers the atom back to ground state 1. The Stokes and anti-Stokes photons have identical frequencies, so that the cavity is coherently coupled to the atom on both transitions $4 \rightarrow 2$ and $3 \rightarrow 1$ with the coupling constants g_1 and g_2, respectively, resulting in the generation of linearly polarized cavity-photons in both cases. The laser fields are tuned to the two-photon resonance, while the one-photon detunings are very large compared to the cavity damping rate k and the

Larmor and Rabi frequencies: $\Delta_i \gg k, \Delta_B^{(g,e)}, g_i, \Omega_i, i = 1, 2$, where $\Delta_B^{(g,e)} = g_L^{(g,e)}\mu_B B$ is Zeeman splitting of atomic levels in the magnetic field B with $g_L^{(g,e)}$ the Landé factor of the ground and excited states and μ_B Bohr magneton. This condition makes the system robust against the spontaneous loss from upper levels and dephasing effects induced by other excited states. More importantly, in the off-resonant case the Raman process with effective atom-photon coupling $G_i = g_i\Omega_i/\Delta_i, i = 1, 2$, can be made much slower than the cavity field decay: $G_i \ll k$. This ensures that a generated photon leaves the cavity long before the next cavity-photon is emitted and, hence, no entanglement between the photons will be created, if we also take into account that the coherence between atomic ground states is always zero. Therefore, we can construct identical wavepackets for outgoing photons independently from each other, as they are entirely determined by the temporal shape of the corresponding pump pulse. A remarkable feature of our scheme is that, despite the smallness of $G_{1,2}$, it is able to produce cavity photons with near-unit efficiency, as discussed in more detail below.

Despite of its simplicity, the four-level scheme is realized, for example, in the atom of lithium isotope ^{6}Li (or ^{40}Ca$^+$) with the ground states $2S_{1/2}(F = 1/2, m_F = \mp 1/2)$ and excited states $2P_{1/2}(F' = 1/2, m_{F'} = \mp 1/2)$ as the states 1,2 and 3,4 in our scheme, respectively. The central drawback of this scheme is that the spontaneous decay of upper states into the ground state $2S_{1/2}(F = 3/2)$ constitutes a loss channel that moves the system outside the considered level configuration. However, we show that even in this case, for reasonable values of parameters, the atom can generate about 70 identical SP pulses before falling into the ground $F = 3/2$ state. To restore the generation a repumping field must be applied to transfer the atom into the initial state. For continuous generation of SP, a closed system can be used employing cycling transitions, for example, of the D_2 line in the ^{87}Rb atom with $5S_{1/2}(F = 2)$ and $5P_{3/2}(F' = 3)$ as the ground and excited states. In this case, the only limitation is the atom lifetime in cavities, which amounts to at most one minute [38]. When analyzing this system all Zeeman sublevels participating in the interaction with the laser pulses must be taken into account. However, we show in the next section, that owing to the fact that no coherence is created between the Zeeman sublevels the results of four-level

scheme is easily generalized to this complicated case. In this sense the four-level atom serves as a generic scheme for multilevel atoms.

Firstly we consider a simple case of three-level atom interacting with a pump pulse in the Schrödinger picture, then we develop theory of the full process in Heisenberg picture. The Schrödinger picture gives an easier, more intuitive way of understanding, while the Heisenberg picture gives complete quantum behavior of the atom-cavity QED system.

2.2   Basic equations

2.2.1   Two-level atom-cavity interaction. Basic mathematical tools

To explain the basics of the atom-cavity interaction, firstly we discuss and derive basic equations for the simplest case of two-level atom placed in a cavity QED. The schematic diagram of the two-level atom placed in a cavity is depicted in Fig. 2.2. We assume an imperfect cavity with one of the mirrors partially transparent, while the other one is completely reflective. Initially the atom is in the ground state 1 and the cavity mode is empty, which prevents any interaction between the atom and the cavity. One can excite the atom into state 2, applying transversally to the cavity a classical pump field of frequency ω_p, which is resonant with the atomic transition $1 \rightarrow 2$, i.e. $\omega_p = \omega_{21}$. The cavity is also tuned to resonance with the atomic transition, so that $\omega_c = \omega_{21}$. The Hamiltonian of the atom-cavity-laser field-bath system in
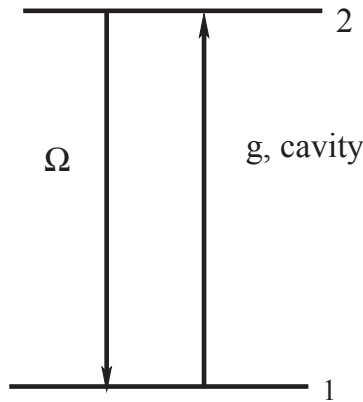

Figure 2.2: Two-level atomic system

the rotating wave approximation (RWA) and in the interaction representation with respect to the atom and cavity is given by

$$H(t) = H_{\mathrm{B}} + H_{\mathrm{S}} + H_{\mathrm{CB}}, \tag{2.1}$$

$$H_{\mathrm{B}} = \hbar \int_{-\infty}^{\infty} d\omega\, \omega\, b_\omega^\dagger b_\omega, \tag{2.2}$$

$$H_{\mathrm{S}}(t) = -\hbar\Omega\sigma_{21} - \hbar g a \sigma_{21} + h.c., \tag{2.3}$$

$$H_{\mathrm{CB}} = i\hbar \int_{-\infty}^{\infty} d\omega\, \gamma(\omega)[b_\omega^\dagger a - a^\dagger b_\omega], \tag{2.4}$$

where $H_{\mathrm{S}}(\mathrm{t})$ is the atom-cavity-laser field interaction Hamiltonian in the RWA, the b_ω is the boson annihilation operator for the bath, $\gamma(\omega)$ is the cavity-bath coupling constant, satisfying the commutation relation

$$[b_\omega, b_{\omega'}^\dagger] = \delta(\omega - \omega') \tag{2.5}$$

The cavity field is described by annihilation and creation operators a and $a^\dagger$, while $\sigma_{ij} = |i\rangle\langle j|$ are the atomic operators, $g = \mu_{12}\sqrt{\omega_c/2\hbar\mathcal{E}_0 V}$ is the atom-cavity coupling constant with V cavity volume, μ_{ij} the dipole matrix element of the $i \to j$ transition, Ω is the Rabi frequency of the pump field. Our aim is to obtain the shape of the generated photons, going out from the cavity. For that at first we derive the quantum Langevin equation, the input-output relation, as well as we describe the technique of adiabatic elimination of cavity variables from the master equations for atom-cavity combined system. For an arbitrary system operator A with the Hamiltonian (2.1-2.4) the Heisenberg picture leads to time dependent operators $A(t) = U^\dagger(t,t_0)A(t_0)U(t,t_0)$ with $U(t,t_0)$ the propagator such that $\psi(t) = U(t,t_0)\psi(t_0)$, where $\psi(t)$ is the solution of time-dependent Schrödinger equation $i\hbar d\psi/dt = H(t)\psi(t)$. In this picture the time-dependent operator $A(t)$ has the same commutation relation as the initial one $A(t_0)$ and obeys the Heisenberg equation

$$\dot{A}(t) = -\frac{i}{\hbar}[A(t), \tilde{H}(t)], \tag{2.6}$$

with $\tilde{H}(t) = U^\dagger(t,t_0)H(t)U(t,t_0)$. We use here a notation for which the operators $A(t) \equiv A$ are time independent in the Shrödinger picture, but the Hamiltonian can be time dependent. When H is time independent, one has $U(t,t_0) = e^{-i\hbar H(t-t_0)}$ and $\tilde{H} = H$. In (2.1) H_{B} and

H_{CB} are generally time independent, but not H_{S}. Eq. (2.6) leads to

$$\dot{b}_\omega(t) = -i\omega b_\omega(t) + \gamma(\omega)a(t), \tag{2.7}$$

$$\dot{a}(t) = -\frac{i}{\hbar}[a(t), \tilde{H}_{\mathrm{S}}(t)] - \int d\omega \gamma(\omega) b_\omega(t). \tag{2.8}$$

Integrating (2.7) we get

$$b_\omega(t) = b_\omega(t_0)e^{-i\omega(t-t_0)} + \gamma(\omega)\int_{t_0}^t e^{-i\omega(t-t')}a(t')dt', \tag{2.9}$$

which substituted into (2.8) gives

$$\dot{a}(t) = -\frac{i}{\hbar}[a(t), H_{\mathrm{S}}(t)] - \int d\omega \gamma^2(\omega)\int_{t_0}^t dt' e^{-i\omega(t-t')}a(t') - \int d\omega \gamma(\omega)e^{-i\omega(t-t_0)}b_\omega(t_0), \tag{2.10}$$

where $b_\omega(t_0) \equiv b_\omega$ is the value of $b_\omega(t)$ at the initial time $t = t_0$ and obeys the same commutation relation as $b_\omega(t)$. We introduce the first Markov approximation, we suppose the coupling constant $\gamma(\omega)$ is independent of frequency:

$$\gamma(\omega) = \sqrt{\kappa/2\pi}. \tag{2.11}$$

At the next step we define an input field by

$$a_{\mathrm{in}}(t) = \frac{1}{\sqrt{2\pi}}\int d\omega e^{-i\omega(t-t_0)}b_\omega(t_0). \tag{2.12}$$

The corresponding quantum field is determined as [109]

$$\hat{\mathcal{E}}_{\mathrm{in}}(z,t) = i\int d\omega \Big(\frac{\hbar\omega}{4\pi\varepsilon_0 Ac}\Big)b_\omega(t_0)e^{-i\omega(t-t_0-z/c)}, \tag{2.13}$$

and the beam propagates in the direction of cavity axis and A is cavity cross-section area. Using (2.12) and the following definition and property of Dirac delta function

$$\frac{1}{2\pi}\int d\omega e^{i\omega(t-t')} = \delta(t-t') \tag{2.14}$$

$$\int_{t_0}^t c(t')\delta(t-t')dt' = \frac{1}{2}c(t), \quad (t > t_0) \tag{2.15}$$

we derive the quantum Langevin equation

$$\dot{a}(t) = -\frac{i}{\hbar}[a(t), H_{\mathrm{S}}] - \frac{\kappa}{2}a(t) - \sqrt{\kappa}a_{\mathrm{in}}(t), \tag{2.16}$$

25

This gives the dynamics of the cavity field. The term depending on a_{in} in (2.16) is the noise terms and it describes the cavity damping. This interpretation is valid if the state of the complete dressed system initially factorizes (at time $t = t_0$). For a single-ended cavity, the bath is simply the radiation field outside the mirror and the operator a_{in} must be ascribed to the incoming part of this external field.

If now we consider $t_1 > t$, we can integrate (2.7) to have

$$b_\omega(t) = e^{-i\omega(t-t_1)} b_\omega(t_1) - \gamma(\omega) \int_t^{t_1} e^{-i\omega(t-t')} a(t') dt', \tag{2.17}$$

substituting this into (2.8), repeating the previous steps and denoting

$$a_{\text{out}}(t) = \frac{1}{\sqrt{2\pi}} \int d\omega e^{-i\omega(t-t_1)} b_\omega(t_1). \tag{2.18}$$

we obtain

$$\dot{a}(t) = -\frac{i}{\hbar}[a(t), H_{\text{S}}] + \frac{\kappa}{2} a(t) - \sqrt{\kappa} a_{\text{out}}(t), \tag{2.19}$$

which is associated to the output quantum field

$$\hat{\mathcal{E}}_{\text{out}}(z, t) = i \int d\omega \Big(\frac{\hbar\omega}{4\pi\varepsilon_0 Ac}\Big)^{1/2} b_\omega(t_1) e^{-i\omega(t-t_1-z/c)}. \tag{2.20}$$

From the definition of the operators $a_{\text{in}}(t)$ and $a_{\text{out}}(t)$ and with Eq.(2.7), we obtain the following expressions

$$b(t) = \frac{1}{\sqrt{2\pi}} \int d\omega b_\omega = a_{\text{in}}(t) + \frac{\sqrt{\kappa}}{2} a(t),$$
$$b(t) = \frac{1}{\sqrt{2\pi}} \int d\omega b_\omega = a_{\text{out}}(t) - \frac{\sqrt{\kappa}}{2} a(t),$$

whose combination leads to an identity, called input-output formulation

$$a_{\text{out}}(t) - a_{\text{in}}(t) = \sqrt{\kappa} a(t), \tag{2.21}$$

which connects the cavity operator $a(t)$ with the incoming cavity field $a_{\text{in}}(t)$ and field going out through the cavity mirror $a_{\text{out}}(t)$. Note that the operators $a_{\text{in}}(t), a_{\text{out}}(t)$ satisfy the commutation relations $[a_{\text{out}}(t), a_{\text{out}}^\dagger(t')] = [a_{\text{in}}(t), a_{\text{in}}^\dagger(t')] = \delta(t - t')$, which follows from their definitions (2.12, 2.18) and (2.5).

Our aim is to find the mean flux of the output photons [109]

$$\frac{dn_{out}(t)}{dt} = \langle a_{\text{out}}^\dagger(t) a_{\text{out}}(t) \rangle \tag{2.22}$$

which describes the outgoing SP wavepacket. Here $n_{\text{out}}(t)$ is the mean photon number of the field going out through the cavity mirror. For the case of vacuum input $\langle a_{\text{in}}^\dagger(t) a_{\text{in}}(t) \rangle = 0$, the flux simply becomes

$$\frac{dn_{out}(t)}{dt} = \kappa \langle a^\dagger(t) a(t) \rangle \tag{2.23}$$

We remark that at this stage we have not used any information concerning atomic system and the cavity operator a. Considering the bad cavity case $\kappa \gg g$, i.e. the case when the generated photons leave the cavity immediately without further interaction with the atom, we simplify the above equation taking $\dot{a} \simeq 0$

$$a(t) = \frac{2}{\kappa}(ig\sigma_{12}(t) - \sqrt{\kappa}a_{\text{in}}(t)). \tag{2.24}$$

The latter along with the input-output relation (2.21) results to

$$\langle a_{\text{out}}(t)^\dagger a_{\text{out}}(t) \rangle = \frac{4g^2}{\kappa}\langle \sigma_{22}(t) \rangle, \tag{2.25}$$

Thus, in the bad-cavity case, we have established a direct relation between the flux of the outgoing photons and the population of excited state of the atom. The latter can be found from the combined atom-cavity system master equation for the density matrix ρ written in the Schrödinger picture as

$$\frac{d\rho}{dt} = -\frac{i}{\hbar}[H, \rho] + \kappa L[a]\rho, \tag{2.26}$$

with

$$L[\hat{O}]\rho = \hat{O}\rho\hat{O}^\dagger - \frac{1}{2}(\hat{O}^\dagger\hat{O}\rho + \rho\hat{O}^\dagger\hat{O}), \tag{2.27}$$

for any operator $\hat{O}$. We use a Lindblad master equation that is equivalent to the model (2.1)-(2.4) which describes the loss of the photon in the bath written explicitly [112]. We have taken into account that the dominant loss associated with the cavity results from the leakage of photons through the mirrors at a rate κ (spontaneous emission from the upper state

has been emitted for simplification). Note, in (2.26) enters only the atom-cavity interaction Hamiltonian (2.3).

Now we make a transformation defined by

$$\sigma(t) = e^{-\mathcal{L}t}\rho(t). \tag{2.28}$$

where $\mathcal{L}\rho = \kappa L[a]\rho$ and (2.28) further will be necessary in order to eliminate the cavity mode operators from the the master equation of four-level atomic system. Substituting this into (2.26) we obtain

$$\frac{d\sigma}{dt} = -\frac{i}{\hbar}(e^{-\mathcal{L}t}H_{\mathrm{S}}e^{\mathcal{L}t}\sigma(t) - e^{-\mathcal{L}t}\rho(t)H_{\mathrm{S}}). \tag{2.29}$$

Taking into account the definition of operator $\mathcal{L}$, we have

$$\{\mathcal{L}(\rho H_{\mathrm{S}})\}^{\dagger} = \{\frac{\kappa}{2}(2a\rho H_{\mathrm{S}}a^{\dagger} - a^{\dagger}a\rho H_{\mathrm{S}} - \rho H a^{\dagger}a)\}^{\dagger}$$

$$= \frac{\kappa}{2}(2aH_{\mathrm{S}}\rho a^{\dagger} - H_{\mathrm{S}}\rho a^{\dagger}a - a^{\dagger}aH_{\mathrm{S}}\rho) = \mathcal{L}(H_{\mathrm{S}}\rho) \tag{2.30}$$

therefore we obtain

$$\frac{d\sigma}{dt} = -\frac{i}{\hbar}[H_{\sigma}, \sigma], \tag{2.31}$$

where

$$H_{\sigma}(t) = e^{-\mathcal{L}t}H_{\mathrm{S}}e^{\mathcal{L}t}. \tag{2.32}$$

The transformation (2.28) can be thus interpreted as an interaction representation with respect to the leakage of the photons. Note that Eq. (2.31) involves only the cavity-atom interaction. We formally integrate Eq. (2.31) and substitute it back into (2.31)

$$\frac{d\sigma}{dt} = -\frac{1}{\hbar^2}\int_0^t dt'[H_{\sigma}(t), [H_{\sigma}(t'), \rho(t')]]. \tag{2.33}$$

The following calculation corresponds to a second order approximation with respect to a weak perturbation g. However, to obtain this expression we haven't made any assumption yet. Supposing that the interaction g is weak ($g \ll \kappa$), we make the Born-Markov approximation which leads to

$$\frac{d\rho_a}{dt} = -\frac{1}{\hbar^2}Tr_c\left(\int_0^t dt'[H_{\sigma}(t), [H_{\sigma}(t'), \rho_a(t)\rho_c(0)]]\right), \tag{2.34}$$
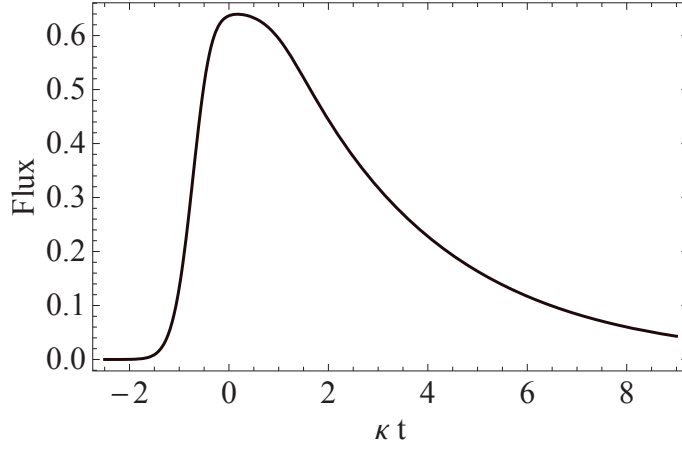
28

Figure 2.3: Flux of the outgoing photons for $gT = 0.1, \Omega T = 5, \kappa T = 6$

where ρ_a is the atomic density operator, while $\rho_c(0)$ is the cavity density matrix at the initial time $t = t_0$. Clearly, if $\hat{O}$ is any atomic operator we can calculate its average if we have the knowledge of ρ_a alone, and not of full atom-cavity $\rho(t)$ density operator:

$$\langle \hat{O} \rangle = Tr_{a \otimes c}[\hat{O}\rho(t)] = Tr_c\{\hat{O}Tr_a[\rho(t)]\} = Tr_c[\hat{O}\rho_a(t)]. \tag{2.35}$$

On using (2.32) and (2.3), Eq. (2.34) reduces to (see Appendix 2.A)

$$\frac{d\rho_a}{dt} = \frac{2\Omega^2}{\kappa}L[\sigma_{21}]\rho_a + 2\frac{\Omega^2 + g^2}{\kappa}L[\sigma_{12}]\rho_a. \tag{2.36}$$

From this we eventually find for the atomic variables

$$\langle \dot{\sigma}_{11}(t) \rangle = 2\frac{\Omega^2 + g^2}{\kappa}\langle \sigma_{22}(t) \rangle - 2\frac{\Omega^2}{\kappa}\langle \sigma_{11}(t) \rangle, \tag{2.37a}$$

$$\langle \dot{\sigma}_{22}(t) \rangle = -2\frac{\Omega^2 + g^2}{\kappa}\langle \sigma_{22}(t) \rangle + 2\frac{\Omega^2}{\kappa}\langle \sigma_{11}(t) \rangle, \tag{2.37b}$$

subjected to initial conditions $\langle \sigma_{11}(-\infty) \rangle = 1, \langle \sigma_{22}(-\infty) \rangle = \langle \sigma_{21}(-\infty) \rangle = 0$. This, along with (2.25) finally gives the flux of outgoing photons

$$\frac{dn_{out}}{dt} = \frac{8g^2}{\kappa}\int_{-\infty}^{t}d\tau\frac{\Omega^2(\tau)}{\kappa}\exp\left\{-\int_{-\tau}^{t}2\frac{\Omega^2(t') + g^2}{\kappa}dt'\right\} \tag{2.38}$$

As one can see from the above expression, the flux of the outgoing photons, which defines the shape of outgoing photons' wavepacket, depends on the classical driving field in the integral form. The flux is shown in Fig. 2.3 for the parameters $gT = 0.1, \Omega T = 5, \kappa T = 6$, where T is the driving Gaussian shaped field duration. As a remark, a SP pulse is generated if the

29

excited atom goes back to its initial ground state stimulated by the cavity field. If the area of the pump field is large enough, the atom can be excited again and more than one photon can be generated. Hence, the drawback of two-level atom as a source of SP photons is that to control the generation of SP pulses, one needs to use a pump pulse with precise area.

2.2.2 Four-level atom. Heisenberg picture

We now describe the full four-level atom, placed in a cavity in a Heisenberg picture. The laser fields propagate perpendicular to the cavity axis and are given by

$$E_j(t) = \mathcal{E}_j f_j^{1/2}(t) \exp(-i\omega_j t), \; j = 1, 2. \tag{2.39}$$

where $f_1(t) = \sum_{l=1}^{N} f_1^l(t)$ and $f_2(t) = \sum_{l=1}^{N} f_2^l(t - \tau_d)$ represent the sum of N well-separated by delay time τ_d temporal modes with profiles $f_1^l(t)$ and $f_2^l(t - \tau_d)$ for the lth mode in the pump series 1 and 2, respectively. $\mathcal{E}_j$ is the peak amplitude of the field j.

In our consideration we take into account the spontaneous decay of the atom from upper levels 3 and 4 into the ground states 1 and 2, as well as to the states outside form the configuration of Fig. 2.1. Therefore, the total Hamiltonian has the form

$$H_{\text{total}} = H_{\text{S}} + H_{\text{R}} + V, \tag{2.40}$$

where H_{S} is the system Hamiltonian and describes the atom coupled to laser pulses and cavity mode field as

$$H_{\text{S}} = \hbar\Delta_1\sigma_{44} + \hbar\Delta_2\sigma_{33} - \hbar\Omega_1\sigma_{41} - \hbar\Omega_2\sigma_{32} + \hbar g a\sigma_{42} + \hbar g a\sigma_{31} + h.c. \tag{2.41}$$

The peak Rabi frequencies of the laser fields are given by $\Omega_1 = \mu_{41}\mathcal{E}_1/\hbar, \Omega_2 = \mu_{32}\mathcal{E}_2/\hbar$ with μ_{ij} the dipole matrix element of the $i \to j$ transition. The detunings of the pump fields from the corresponding transitions are given by $\Delta_1 = \omega_{42} - \omega_1$ and $\Delta_2 = \omega_{31} - \omega_2$. The H_{R} represents the modes of electromagnetic field as a reservoir modes interacting with the atom on the transition $3 \to l$ and $4 \to l, l = 1, 2,$ outside states. In RWA this interaction is given by

$$V(t) = \hbar\sum_l \sum_j [g_{3l}^{(j)}b_j(\omega_j)\sigma_{3l}\exp(i\Delta_{3l}^{(j)}t) + g_{4l}^{(j)}b_j(\omega_j)\sigma_{4l}\exp(i\Delta_{4l}^{(j)}t)], \tag{2.42}$$

with $g_{3l}^{(j)}$ and $g_{4l}^{(j)}$ the coupling constants, $b_j(\omega_j)$ the annihilation operator of j-th mode and $\Delta_{3l}^{(j)} = \omega_{3l} - \omega_j$, $\Delta_{4l}^{(j)} = \omega_{4l} - \omega_j$. The system evolution is described by the master equation for the whole density matrix ρ

$$\frac{d\rho}{dt} = -\frac{i}{\hbar}[H_{\text{total}}, \rho] + \frac{d\rho_c}{dt}|_{rel} \tag{2.43}$$

where the last right-hand side (rhs) term $\frac{d\rho_c}{dt}|_{rel} = \kappa L[a]\rho$ accounts for the cavity decay (see Eq. (2.27)). The reduced density operator for the system is defined as

$$\rho_S = Tr_R[\rho(t)]. \tag{2.44}$$

We assume that initially the system and reservoir are uncorrelated, so that $\rho(0) = \rho_S(0) \otimes \rho_R$, where ρ_R is the denisty operator for the reservoir.

In far off-resonant case, when $\Delta_{1,2} \gg \Omega_{1,2}, g_{1,2,R}$, one can adiabatically eliminate the upper atomic states 3 and 4. Further, assuming that the coupling with reservoir is weak we may calculate this interaction in the second order in V. The both procedures are described in the Appendix 2.B. As a result the Hamiltonian (2.41) of the system is transformed to

$$H_S = \hbar[G_1 f_1^{1/2}(t)\sigma_{21} + G_2 f_2^{1/2}(t)\sigma_{12}]a^\dagger + h.c., \tag{2.45}$$

while the master equation for the density operator of the system becomes

$$\frac{d\rho_S(t)}{dt} = -\frac{i}{\hbar}[H_S, \rho_S(t)] + \frac{d\rho_S}{dt}|_{rel}, \tag{2.46}$$

where

$$\frac{d\rho_S}{dt}|_{rel} = \frac{d\rho_c}{dt}|_{rel} + \Gamma_1(t)L[\sigma_{21}]\rho + \Gamma_2(t)L[\sigma_{12}]\rho - (\Gamma_{1,\text{out}}\sigma_{11} + \Gamma_{2,\text{out}}\sigma_{22})\rho \tag{2.47}$$

and Γ_1, $\Gamma_{1,\text{out}}$ are defined by Eq. (2.B11) and similarly

$$\Gamma_2(t) = \frac{\Omega_2^2}{\Delta_2^2} f_2(t)\gamma_{31}, \Gamma_{2,\text{out}}(t) = \frac{\Omega_2^2}{\Delta_2^2} f_2(t)\gamma_{3,\text{out}}. \tag{2.48}$$

The first term in the rhs of Eq. (2.47) represents the cavity output coupling, the second and third terms describe the optical pumping to ground states 2 and 1 from the states 1 and 2,

31

respectively, and give rise to noise of corresponding rates, the last two terms describe the decay of the upper states outside the considered scheme.

To obtain the flux of the output going photons (2.23), we derive equations of motion for the cavity mode operators with the Hamiltonian (2.45)

$$\dot{a} = -iG_1 f_1^{1/2}(t)\sigma_{21} - iG_2 f_2^{1/2}(t)\sigma_{12} - (\kappa/2)a - \sqrt{\kappa}a_{\text{in}}(t) \tag{2.49}$$

In the bad-cavity limit $\kappa \gg G_{1,2}$, we adiabatically eliminate the cavity mode $a(t)$ yielding

$$a = -\frac{2i}{\kappa}[G_1 f_1^{1/2}(t)\sigma_{21} + G_2 f_2^{1/2}(t)\sigma_{12}] - \frac{2}{\sqrt{\kappa}}a_{\text{in}}(t). \tag{2.50}$$

Thus, to obtain the flux we need to know the dynamics of atomic operators. For that, similarly to the technique described in Appendix 2.A, for the atomic variables we obtain

$$\frac{d\rho_a}{dt} = \frac{\alpha_1(t)}{2}L[\sigma_{21}]\rho_a + \frac{\alpha_2(t)}{2}L[\sigma_{12}]\rho_a + \frac{d\rho_a}{dt}|_{rel}, \tag{2.51}$$

where ρ_a is the atomic density operator, $\frac{d\rho_a}{dt}|_{rel} = \frac{d\rho_S}{dt}|_{rel} - \frac{d\rho_c}{dt}|_{rel}$ and

$$\alpha_i(t) = 4G_i^2 f_i(t)/\kappa = \alpha_i f_i(t), i = 1, 2. \tag{2.52}$$

From Eq.(2.51) we eventually have the following equations for the atomic operators

$$\langle\dot{\sigma}_{ii}(t)\rangle = -[\alpha_i(t) + \Gamma_i(t) + \Gamma_{i,\text{out}}(t)]\langle\sigma_{ii}(t)\rangle + [\alpha_j(t) + \Gamma_j(t)]\langle\sigma_{jj}(t)\rangle \tag{2.53a}$$

$$\langle\dot{\sigma}_{21}(t)\rangle = -\frac{1}{2}\sum_{i=1}^{2}[\alpha_i(t) + \Gamma_i(t)]\langle\sigma_{21}(t)\rangle, \qquad i, j = 1, 2; j \neq i \tag{2.53b}$$

which are subjected to initial conditions $\langle\sigma_{11}(-\infty)\rangle = 1, \langle\sigma_{22}(-\infty)\rangle = \langle\sigma_{21}(-\infty)\rangle = 0$. Eqs (2.53) are easily solved analytically and for $\langle\sigma_{22}\rangle$ we obtain

$$\langle\sigma_{22}\rangle = \int_{-\infty}^{t} d\tau[\alpha_1(\tau) + \Gamma_1(\tau)] \cdot$$
$$\exp\left(-\int_{\tau}^{t} dt'[\alpha_2(t') + \Gamma_2(t') + \alpha_1(t') + \Gamma_1(t')]\right), \tag{2.54}$$

if we suppose $\langle\sigma_{11} + \sigma_{22}\rangle = 1$.

We first discuss some properties of Eqs. (2.53). It is seen that state 1 (and similarly state 2) is populated in two ways: (i) via cavity photon generation with the rate $\alpha_{2(1)}(t)$ and (ii) by

optical pumping of rate $\Gamma_{2(1)}(t)$, that gives for the signal-to-noise ratio $R_{sn} = 4g_{1(2)}^2/(\kappa\gamma_{42(31)})$, which must be quite large: $R_{sn} \gg 1$. The second observation is that the overall population of the atom after a total of n pulses of two laser sequences for $\alpha_i T \gg 1$ decreases as

$$\langle\sigma_{11}(t) + \sigma_{22}(t)\rangle\big|_{t\geq(n-1)\tau_d+T} = (1 - n\Gamma_{\text{out}}/\alpha) \tag{2.55}$$

Here it is assumed that $\Gamma_{1\text{out}} = \Gamma_{2\text{out}} = \Gamma_{\text{out}}, \alpha_1 = \alpha_2 = \alpha$. Thus, the population leakage is negligibly small until $n\Gamma_{\text{out}}/\alpha < 1$. Further, the ground state coherence is always zero: $\sigma_{21}(t) = 0$, as expected due to the spontaneous nature of Raman transitions.

From the explicit expression of the flux calculated from Eq.(2.22) using (2.21, 2.50, 2.53, 2.54) for one pump pulse and considering $\Gamma_{\text{out}} = 0$ we have

$$\frac{dn_{\text{out}}(t)}{dt} = \kappa n_{\text{cav}}(t) = \kappa\langle a(t)a^\dagger(t)\rangle = \alpha_1(t)e^{-\int_{-\infty}^t \alpha_1(t')dt'} \tag{2.56}$$

Thus, we conclude that the waveform of the emitted single-photon is simply related to the shape of the pump pulse and, thereby, is much easier controlled as compared to schemes proposed so far in literature,where this dependence is in integral form [23, 110, 111]. From this equation one finds $n_{\text{out}}(t) = 1 - \exp\big(-\int_{-\infty}^t \alpha_1(t')dt'\big)$ showing that our system is able to produce photons with near-unit efficiency, if

$$\alpha_i T \gg 1. \tag{2.57}$$

In general, for any number of pump subpulses Eq. (2.56) is replaced by

$$\frac{dn_{\text{out}}(t)}{dt} = \alpha_1(t)F(-\infty, t) + \int_{-\infty}^t dt'(\alpha_1(t)\alpha_2(t') + \alpha_1(t')\alpha_2(t))F(t', t), \tag{2.58}$$

where $F(t', t) = \exp(-\int_{t'}^t d\tau(\alpha_1(\tau) + \alpha_2(\tau)))$.

In Fig. 2.4 the calculated flux and total number of output photons, as well as the populations of atomic ground states are shown for the case, when each laser sequence contains four Gaussian-shaped subpulses with duration $T = 1\mu$s corresponding to linewidth 1MHz. The atom is initially in the ground state 1. We present the results for cavity photon generation with wavelength $\lambda \sim 671$nm on the D1 line transition $2P_{1/2}(F' = 1/2) \rightarrow 2S_{1/2}(F = 1/2)$ in the ^{6}Li atom obtained with the following parameters: $\Omega_{1,2} = 2\pi \times 10MHz= 0.1\Delta(\Delta_1 \simeq$
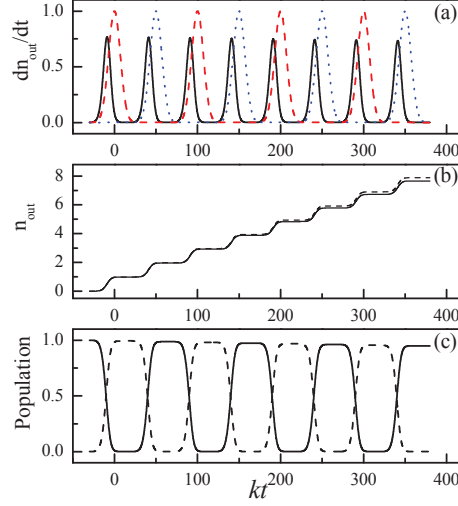
Figure 2.4: Flux (a), total number of output field photons (b) and population of atomic ground states 1 (solid) and 2 (dashed)(c) as a function of time (in units of inverse cavity decay κ^{-1}), in the case, when 4 pulses of each laser beam are applied with delay time $\tau_d = 3\mu s$. For the rest of parameters see the text.

$\Delta_2 = \Delta$), $(g_{1,2}, k, \gamma_{\mathrm{sp}})/2\pi = (10, 3, 5.87)$MHz and $\gamma_{3,\mathrm{out}} = \gamma_{4,\mathrm{out}} \sim \gamma_{sp}$, γ_{sp} being the natural linewidth of Li atom. A magnetic field of 10G produces the Zeeman splitting $\Delta_B/2\pi$ = 7MHz. These parameters are within experimental reach and ensure the fulfillment of all necessary conditions indicated above. The results demonstrate two important features of the scheme. The photons are generated deterministically at the leading edge of each pump pulse with identical duration $T_{\mathrm{cav}} \sim T/2$ and time-symmetric wavepackets. The efficiency of one photon generation by each pump pulse is close to 100% (see Fig. 2.4b). As one can see in Fig. 2.4(a,c), the peak values of the generated SP pulses and of the atomic populations display a slight decrease in time caused by population losses through the channel $2P_{1/2}(F' = 1/2) \rightarrow 2S_{1/2}(F = 3/2)$. Just because of this fact the total number of emitted photons does not reach its maximum value 8 (Fig. 2.4b, solid line). Nevertheless, from Eq. (2.55) it follows that about $n_{\mathrm{out}} \sim \alpha/\Gamma_{\mathrm{out}} \simeq R_{\mathrm{sn}} \simeq 70$ cavity photons are generated before the losses become significant. For comparison, n_{out} is shown also for the lossless case of $\Gamma_{\mathrm{out}} = 0$ (Fig. 2.4b, dashed line).

34

2.3 Continuous generation of SP pulses from alkali atoms

The continuous generation of SP pulses of identical polarization is possible on the cycling transitions of alkali atoms with $F', F \neq 0$. As an example we consider the transition $5S_{1/2}(F = 2) \to 5P_{3/2}(F' = 3)$ in ^{87}Rb atom where the state $5P_{3/2}(F' = 3)$ is well isolated from other hyperfine levels. Using the fact that Zeeman coherence is always 0, the results of the previous section are easily generalized to this case leading to an expression for the photon flux

$$\frac{dn_{\text{out}}(t)}{dt} = f_1(t) \sum_{m_F=-F}^{F-1} \alpha_{1,m_F} \langle \sigma_{m_F}(t) \rangle + f_2(t) \sum_{m_F=-F+1}^{F} \alpha_{2,m_F} \langle \sigma_{m_F}(t) \rangle \tag{2.59}$$

where $\sigma_{m_F}(t)$ is the population of the ground Zeeman sublevel $|F, m_F\rangle$, while α_{1,m_F} and α_{2,m_F} are the probabilities of two-photon transitions $|F, m_F\rangle \to |F, m_F + 1\rangle$ and $|F, m_F\rangle \to |F, m_F - 1\rangle$ with absorbing one laser photon from the σ^+ and σ^- pump pulses and emitting one cavity photon, respectively. They have the same form as the probabilities $\alpha_{1,2}$ defined in Eq.(2.52) for the four-level system. The equation for the Zeeman sublevel populations takes the form

$$
\begin{aligned}
\langle \dot{\sigma}_{m_F}(t) \rangle &= A^{(1)}_{m_F-1}(t) \langle \sigma_{m_F-1}(t) \rangle + A^{(2)}_{m_F+1}(t) \langle \sigma_{m_F+1}(t) \rangle \\
&\quad - [A^{(1)}_{m_F}(t) + A^{(2)}_{m_F}(t) + \Gamma^{(1)}_{m_F,m_F+2}(t) + \Gamma^{(2)}_{m_F,m_F-2}(t)] \langle \sigma_{m_F}(t) \rangle \\
&\quad + \Gamma^{(1)}_{m_F-2,m_F}(t) \langle \sigma_{m_F-2}(t) \rangle + \Gamma^{(2)}_{m_F+2,m_F}(t) \langle \sigma_{m_F+2}(t) \rangle
\end{aligned}
\tag{2.60}
$$

where

$$A^{(1)}_{m_F}(t) = f_1(t)\alpha_{1,m_F} + \Gamma^{(1)}_{m_F,m_F+1}(t) \tag{2.61}$$

$$A^{(2)}_{m_F}(t) = f_2(t)\alpha_{2,m_F} + \Gamma^{(2)}_{m_F,m_F-1}(t) \tag{2.62}$$

The expression (2.60) includes all OP rates, where $\Gamma^{(1)}_{m_F,m_F+1}(t)$ and $\Gamma^{(1)}_{m_F,m_F+2}(t)$ describe the OP from $|F, m_F\rangle$ into the states $|F, m_F + 1\rangle$ and $|F, m_F + 2\rangle$, respectively, induced by the Ω_1 pump pulse and similarly $\Gamma^{(2)}_{m_F,m_F-1}(t)$ and $\Gamma^{(2)}_{m_F,m_F-2}(t)$ represent the OP caused by Ω_2 pulse.
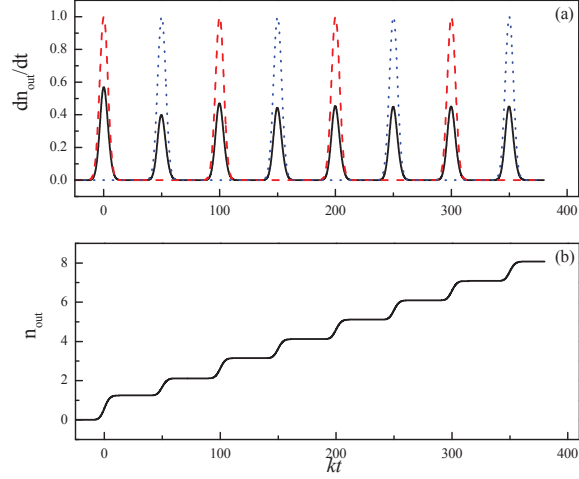
Figure 2.5: Flux (a) and total number (b) of output cavity photons versus the time (in units of k^{-1}) generated on the cycling transition $5S_{1/2}(F = 2) \rightarrow 5P_{3/2}(F' = 3)$ in ^{87}Rb atom. The atom is initially in the state $|F, -F\rangle$. The laser subpulses have a duration $T = 0.5\mu s$ and the same delay time as in Fig.2.4.

The first term in rhs of Eq.(2.59) describes the generation of cavity photons by the Ω_1 field initialized from the Zeeman sublevels $-F \leq m_F \leq F - 1$. Similarly, the flux of output photons generated by Ω_2 from corresponding Zeeman levels is determined by the second term in Eq.(2.59). A remarkable feature of multilevel Zeeman systems is that more than one cavity photon per laser pulse can be emitted. This is achieved for sufficiently high laser power, when the atomic population prepared initially, for example, in the state $|F, -F\rangle$ is completely transferred to the extreme right state $|F, F\rangle$, ensuring the maximal number of output photons $n_{\text{out}} = 2F$. This property can be used to produce Fock states with a given number of photons. Thus, to guarantee single-photon emission in our scheme, the laser power has to be appropriately chosen in contrast to the case of four-level atom, where the condition (2.57) simply imposes a minimum laser intensity.

Figure 2.5 presents the time dependence of the flux and the total number of output photons generated on the transition $5S_{1/2}(F = 2) \rightarrow 5P_{3/2}(F' = 3)$ in ^{87}Rb atom in the case of four Gaussian-shaped laser subpulses. To provide the single-photon generation, the duration and intensity of laser subpulses are taken two times smaller compared to that used

in previous section. Two important features are readily seen. First, Fig. 2.5a shows that the first few SP pulses are different from the next ones. This is due to the asymmetry of the initial conditions. As a consequence, the number of initially generated output photons (Fig.2.5b) per pump pulse is not constant. However, after the first few photons, a stable generation of identical SP pulses occurs (from $kt \geq 100$). Secondly, in contrast to Fig. 2.4, the SP pulses are generated at the center of each pump pulse with identical duration $T_{\text{cav}} \sim T$ and time-symmetric wavepackets. The efficiency of one photon generation by each pump pulse is again close to 100%, as it is seen from Fig.2.5b.

2.4 Schrödinger picture

Now let us discuss the generation of single-photon pulse in the Schrödinger picture in order to have a better understanding of the process. For simplicity instead of considering four-level atom we consider three level atom placed in a cavity QED with atomic levels 1,2,4 shown in Fig.2.1a. We suppose the atom interacts with a classical field Ω_1. As a result, a photon at the cavity mode on the transition $4 \rightarrow 2$ is generated, which then escapes through the transparent mirror of the cavity with a rate κ. The laser field propagating perpendicular to the cavity axis is given simply by

$$E_1(t) = \mathcal{E}_1 \exp(-i\omega_1 t). \tag{2.63}$$

here $\mathcal{E}_1$ is the peak amplitude of the first pump field. The Hamiltonian of the system in the RWA is given by

$$H = \hbar\Delta_1\sigma_{44} + \hbar\delta\sigma_{22} - \hbar\Omega_1\sigma_{41} - \hbar g_1 a\sigma_{42} + h.c., \tag{2.64}$$

with σ_{ij} and $a(a^\dagger)$ the atomic and cavity mode operators, respectively. The Rabi frequency of the laser field is given by $\Omega_1 = \mu_{42}\mathcal{E}_1/\hbar$ with μ_{ij} the dipole matrix element of the $i \rightarrow j$ transition. $\Delta_1 = \omega_{41} - \omega_p$ is the one-photon detuning of the pump field and $\delta = \omega_{41} - \omega_p - \omega_{42} + \omega_c$ is the two-photon detuning. The state of the atom-cavity system is given by the

state function

$$|\psi(t)\rangle = C_1(t)|1,0,0\rangle + C_4(t)|4,0,0\rangle + C_2(t)|2,1,0\rangle + C_{out}(t)|2,0,1\rangle, \qquad (2.65)$$

where the notation $|l,m,n\rangle$ shows that the atom is in state l, with m photons in the cavity mode and with n photons escaped outside the cavity through the transparent mirror. This state function satisfies the Schrödinger equation $\dot{C}_i(t) = -\frac{i}{\hbar}\sum_k\langle i|H|k\rangle C_k(t)$, which leads to the equations for the atomic state amplitudes

$$\dot{C}_1(t) = i\Omega_1 C_4(t), \qquad (2.66a)$$

$$\dot{C}_2(t) = -i(\delta - i\kappa)C_2 + ig_1 C_4(t), \qquad (2.66b)$$

$$\dot{C}_4(t) = -i(\Delta_1 - i\gamma)C_4 + i\Omega_1 C_1(t) + ig_1 C_2, \qquad (2.66c)$$

with the initial conditions

$$C_1(0) = 1, \quad C_{j\neq 0}(0) = 0. \qquad (2.67)$$

In (2.66) we have taken into account the cavity decay and the spontaneous decay with the rate γ of the upper excited state 4. In far off-resonant case, we can adiabatically eliminate the upper atomic state 4 and the effective Hamiltonian takes the form

$$H_{eff} = -\begin{pmatrix} S + i\Gamma & G_1 \\ G_1 & i\kappa \end{pmatrix}, \qquad (2.68)$$

where $S = \Omega_1^2/\Delta_1$ is the Stark shift of the level 1, $\Gamma = \Omega_1^2\gamma/\Delta_1^2$, $G_1 = g_1\Omega_1/\Delta_1$ is the effective atom-cavity coupling. To obtain (2.68) we supposed the detuning is much larger than the atom decay $\Delta_1 \gg \gamma$ and the cavity decay is larger than all relaxations in the system $\kappa \gg g_1^2\gamma/\Delta_1$, also we considered the Stark shift of the level 4 is canceled by two-photon detuning $\delta = g_1^2/\Delta_1$. Using the effective Hamiltonian (2.68) the equations for atomic amplitudes take the form

$$\dot{C}_1(t) = i(S + i\Gamma)C_1 + iG_1 C_2, \qquad (2.69a)$$

$$\dot{C}_2(t) = -\kappa C_2 + iG_1 C_1(t). \qquad (2.69b)$$

We consider the case when the effective atom-cavity coupling is much smaller than the cavity decay rate $G_i \ll \kappa$ which ensures that the created photon escapes the cavity long before the atom interacts with the second coupling field. In this limit taking into account initial conditions (2.67) we have

$$C_2(t) = i\frac{G_1(t)}{\kappa}e^{-\int_0^t d\tau(\Gamma + \frac{G_1^2(\tau)}{\kappa} - iS(\tau))}. \tag{2.70}$$

In the experiments usually the flux of the output photons (i.e. the mean output photon number) is measured which is defined by $n_{out} = |C_{out}|^2$. However, since the state $|2,1,0\rangle$ decays to the state $|2,0,1\rangle$ with rate κ, we have

$$n_{out}(t) = \kappa|C_2|^2 = \frac{G_1^2(t)}{\kappa}Re\left\{e^{-2\int_0^t d\tau(\Gamma + \frac{G_1^2(\tau)}{\kappa} - iS(\tau))}\right\}, \tag{2.71}$$

which is similar to the expression (2.56) obtained using the Schrödinger equation.

2.5 Photon correlations

The probability of a joint detection of two photons produced in the train is given by the intensity correlation function

$$G^{(2)}(t,\tau) = \langle a_{\text{out}}^\dagger(t)a_{\text{out}}^\dagger(t+\tau)a_{\text{out}}(t+\tau)a_{\text{out}}(t)\rangle \tag{2.72}$$

where τ is the time delay between the two photon detections. By applying the quantum regression theorem [112, 113] and using the input-output relation (2.21), the second-order temporal correlation function $G^{(2)}(t,\tau)$ is reduced to

$$G^{(2)}(t,\tau) = \kappa[\alpha_1(t+\tau)Z_1(t,\tau) + \alpha_2(t+\tau)Z_2(t,\tau)] \tag{2.73}$$

where $Z_i(t,\tau) = \langle a^\dagger(t)\sigma_{ii}(t+\tau)a(t)\rangle, i = 1,2$, as a function of τ, obey the following equations

$$
\begin{aligned}
\frac{dZ_i(t,\tau)}{dt} &= -\big[\alpha_i(t+\tau) + \Gamma_i(t+\tau) + \Gamma_{i,\text{out}}(t+\tau)\big]Z_i(t,\tau) \\
&+ \big[\alpha_j(t+\tau) + \Gamma_j(t+\tau)\big]Z_j(t,\tau), \quad i,j = 1,2, i \neq j
\end{aligned} \tag{2.74}
$$

with initial values $Z_1(t,0) = \alpha_2(t)\langle\sigma_{22}(t)\rangle/\kappa$ and $Z_2(t,0) = \alpha_1(t)\langle\sigma_{11}(t)\rangle/\kappa$. Since we are interested in the total probability of a joint detection as a function of the time delay τ, we
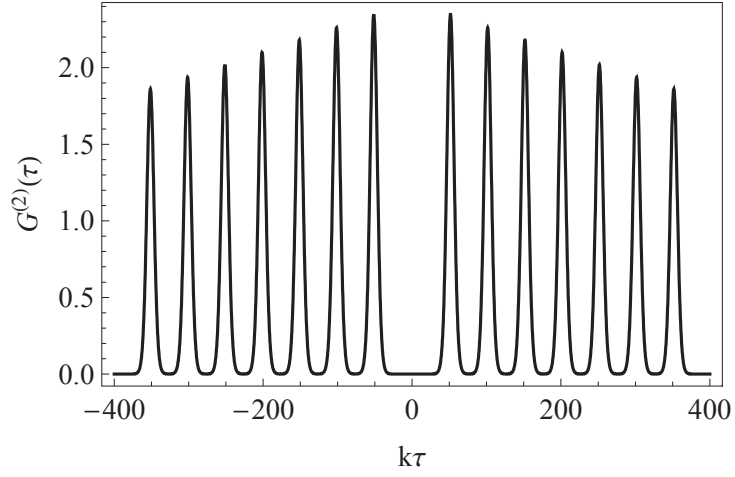
Figure 2.6: Intensity correlation integrated over the single-photon train as a function of time delay τ between the two photon detections. The parameters are the same as in Fig. 2.4

have to integrate Eq.(2.73) over time t. The results of numerical calculations for $G^{(2)}(\tau) = \int_{-\infty}^{\infty} G^{(2)}(t, \tau)dt$ in the case of four-level atom are shown in Fig. 2.6. The temporal structure of $G^{2)}(\tau)$ reveals the characteristics of a pulsed source of light: the absence of a peak at delay time $\tau = 0$ is evidence of the single-photon nature of the source, and the individual peaks are separated by the pump pulses' delay. The decrease in the peak amplitude of the probability of joint detection for increasing delay time results from having a finite train of 8 emitted photons.

Appendix 2.A: Adiabatic elimination of cavity variables

In this Appendix we derive Eq. (2.36) from Eq. (2.34). From the latter we obtain the following

$$
\begin{aligned}
\frac{d\rho_a}{dt} &= -\frac{1}{\hbar^2\kappa}Tr_c \int_0^t dt' \Big(e^{-\mathcal{L}t}H(t)e^{\mathcal{L}t}e^{-\mathcal{L}t'}H(t')e^{\mathcal{L}t'}\rho_a(t)\rho_c(0) \\
&\quad - e^{-\mathcal{L}t}H(t)e^{\mathcal{L}t}\rho_a(t)\rho_c(0)e^{-\mathcal{L}t'}H(t')e^{\mathcal{L}t'} \\
&\quad - e^{-\mathcal{L}t}H(t')e^{\mathcal{L}t'}\rho_a(t)\rho_c(0)e^{-\mathcal{L}t}H(t')e^{\mathcal{L}t} \\
&\quad + \rho_a(t)\rho_c(0)e^{-\mathcal{L}t'}H(t')e^{\mathcal{L}t'}e^{-\mathcal{L}t}H(t)e^{\mathcal{L}t}\Big),
\end{aligned} \tag{2.A1}
$$

Using the explicit form of atom-cavity interaction Hamiltonian (2.3) for the first term of the rhs of (2.A1) we have

$$
\begin{aligned}
(I) &= Tr_c \int_0^t dt' e^{-\mathcal{L}t}(\Omega(t)\sigma_{21}(t) - ga(t)\sigma_{21}(t) + h.c.)e^{\mathcal{L}t}e^{-\mathcal{L}t'}(\Omega(t')\sigma_{21}(t') \\
&\quad - ga(t')\sigma_{21}(t') + h.c.)e^{\mathcal{L}t'}\rho_a(t)\rho_c(0).
\end{aligned}
$$

Taking into account the fact that $\sigma_{ij}(t)$ is slowly varying as compared to $\exp(\mathcal{L}t)$ we suppose $\sigma_{ij}(t) \sim \sigma_{ij}(t')$ and the above equation reduces to

$$
(I) = -\frac{1}{k}\big(\Omega^2(\sigma_{21}\sigma_{12}\rho_a + \sigma_{12}\sigma_{21}\rho_a) + g^2\sigma_{21}\sigma_{12}\rho_a\big). \tag{2.A2}
$$

Similarly for the other terms we obtain

$$
\begin{aligned}
(II) &= (III) = \frac{1}{k}\big(\Omega^2(\sigma_{21}\rho_a\sigma_{12} + \sigma_{12}\rho_a\sigma_{21}) + g^2\sigma_{12}\rho_a\sigma_{21}\big) \\
(IV) &= -\frac{1}{k}\big(\Omega^2(\sigma_{21}\sigma_{12}\rho_a + \sigma_{12}\sigma_{21}) + g^2\sigma_{21}\sigma_{12}\rho_a\big)
\end{aligned}
$$

The sum of latter with (2.A2) finally gives

$$
\frac{d\rho_a}{dt} = \frac{2\Omega^2}{\kappa}L[\sigma_{21}]\rho_a + 2\frac{\Omega^2 + g^2}{\kappa}L[\sigma_{12}]\rho_a, \tag{2.A3}
$$

what we wanted to show.

Appendix 2.B

For simplicity we consider here the elimination of atomic upper level 4 assuming $\Omega_2(t) = 0$. We use the equations for atomic operators

$$\dot{\sigma}_{ij}(t) = \frac{i}{\hbar}[H_{\text{total}}(t), \sigma_{ij}(t)], \tag{2.B1}$$

Inserting Eq. (2.40) into (2.B1) and taking into account that $\Delta_{1,2}^{-1}$ are much smaller as compared to all characteristic times we obtain, e.g. for σ_{41} the solution

$$\sigma_{41} = \frac{1}{\Delta_1}\left[\Omega_1(\sigma_{11} - \sigma_{44}) + g_1 a\sigma_{12} + \sum_l \sum_j g_{4,l}^{(j)} b_j(\omega_j)\sigma_{1l} \exp(i\Delta_{4l}^{(j)}t)\right] \tag{2.B2}$$

Substituting (2.B2) and similar solutions for the rest of atomic operators σ_{4j} into (2.41) we find

$$H_S = \hbar\frac{\Omega_1(t)g_1}{\Delta_1}\sigma_{12}a + h.c., \tag{2.B3}$$

$$V = \frac{\hbar}{\Delta_1}\sum_l \sum_j \left(\Omega_1(t)g_{4l}^{(j)}\sigma_{1l} - g_1 g_{4l}^{(j)}\sigma_{2l}\right)b_j \exp(i\Delta_{4l}^{(j)}t) + h.c., \tag{2.B4}$$

Integrating Eq. (2.43) and for a while ignoring the cavity decay term $\kappa L[a]\rho$ we perform the trace over the reservoir variables with Hamiltonians (2.B3) and (2.B4) and we find

$$\rho_S(t) = \rho_S(0) - \frac{i}{\hbar}\int_0^t dt'[H_S, \rho_S(t')] - \frac{i}{\hbar}\int_0^t dt' Tr_R([V(t'), \rho(t')] \tag{2.B5}$$

We now assume $V(t)$ is such that

$$Tr_R(V(t)\rho_R(t)) = 0. \tag{2.B6}$$

Iterating (2.B5) we have

$$\rho_S(t) = \rho_S(0) - \frac{i}{\hbar}\int_0^t dt'[H_S, \rho_S(t')] +$$

$$+ \sum_{n=1}^{\infty}\left(\frac{-i}{\hbar}\right)^n \int_0^t dt_1 \int_0^{t_1} dt_2 ... \int_0^{t_{n-1}} dt_n Tr_R\{[V_{t1}, [V_{t2}, ..., [V_{tn}, \rho_R \otimes \rho_S(0)]]]\}. \tag{2.B7}$$

If the interaction with reservoir is weak we may keep in rhs of (2.B7) only the lowest (second) order perturbation term. In this case it is easy to see that Eq. (2.B7) is the solution of the equation

$$\frac{d\rho_S}{dt} = -\frac{i}{\hbar}[H_S, \rho_S(t)] - \frac{1}{\hbar^2}Tr_R\left(\int_0^t dt_1[V(t), [V(t_1), \rho_R \otimes \rho_S(t)]]\right). \tag{2.B8}$$

Substituting (2.B4) into (2.B8) we find that the correlation between the reservoir operators $\langle b_i b_j \rangle_R$, $\langle b_i^\dagger b_j \rangle_R$, $\langle b_i b_j^\dagger \rangle_R$, $\langle b_i^\dagger b_j^\dagger \rangle_R$ are required. However, for a thermal bath at zero temperature, when the number of initial thermal photons is zero, only the correlation function $\langle b_i b_j^\dagger \rangle_R \neq 0$. Then the corresponding integral

$$I = \int_0^t dt_1 \sum_{l,m} \sum_{i,j} g_{4l}^{(i)} g_{4m}^{*(j)} \langle b_i b_j^\dagger \rangle_R \exp(i\Delta_{4l}^{(i)}(t-t_1)) \exp(-i\Delta_{4m}^{(j)}(t-t_1)) = \frac{\gamma_{4l}}{2}\delta_{lm}$$

is evaluated by a standard way [132] and eventually we obtain the following master equation for the density operator of the system

$$\frac{d\rho_S}{dt}\Big|_{rel} = -\frac{i}{\hbar}[H_\mathrm{S}, \rho_S(t)] + \sum_{l \neq 1} \Gamma_{1l}(t) L[\sigma_{l1}]\rho_S \tag{2.B9}$$

with

$$\Gamma_{1l}(t) = \frac{\Omega_1^2}{\Delta_1^2} f_1(t)\gamma_{4l}, \tag{2.B10}$$

the optical pumping rate to $l = 2$ and outside states from the ground state 1 induced by the Ω_1 pump field. In Eq. (2.B9) we have emitted the decay term Γ_{11} for $l = 1$, as the latter returns the atom to the starting state 1 and does not change the population of the system.

The relaxation terms in (2.B9) with $l \neq 2$ can be written in a more practical form by noting that for the mean values of atomic operators $\langle \sigma_{ij} \rangle$, $i, j = 1, 2$ they act equivalent to the operator $\Gamma_{1l}\sigma_{11}\rho_S$. Thus, Eq. (2.B9) takes the form

$$\frac{d\rho_S}{dt}\Big|_{rel} = -\frac{i}{\hbar}[H_\mathrm{S}, \rho_S(t)] + \Gamma_1(t) L[\sigma_{21}]\rho_S - \Gamma_{1,\mathrm{out}}(t)\sigma_{11}\rho_S,$$

where

$$\Gamma_1(t) \equiv \Gamma_{12}(t) = \frac{\Omega_1^2}{\Delta_1^2} f_1(t)\gamma_{42}$$

$$\Gamma_{1,\mathrm{out}}(t) = \sum_{l \neq 1,2} \Gamma_{1l}(t) = \frac{\Omega_1^2}{\Delta_1^2} f_1(t)\gamma_{4,\mathrm{out}}, \tag{2.B11}$$

where $\gamma_{4,\mathrm{out}} = \sum_{l \neq 1,2} \Gamma_{4l}$. $\Gamma_1(t)$ describes the the optical pumping to ground state 2 from the state 1 and $\Gamma_{1,\mathrm{out}}(t)$ accounts the decay out of the system.

Finally, combining these results and adding the similar terms for the decay of the state 3, when $\Omega_2(t) \neq 0$, we obtain the Hamiltonian H_S and an equation for the density operator of the system in the forms given in the text by Eqs. (2.45), (2.46).

2.6   Summary

Summarizing, we have proposed a robust and realistic source of indistinguishable single-photons with identical frequency and polarization generated on demand in a well-defined spatio-temporal mode from a coupled double-Raman atom-cavity system. We have considered two cases of four-level system (^{6}Li or ^{40}Ca$^+$) and atoms with many Zeeman sublevels and have shown that in the first case the number of generated SP pulses is limited by the decay of atomic states outside of the system, while in the second one the continuous SP generation is achievable, e.g. in ^{87}Rb atoms. The high efficiency and simplicity of the scheme, free from such complications as repumping process and environmental dephasing, makes the generation of many SP identical pulses feasible. The removal of the repumping field is a principal task, because its usage strongly restricts the process: the repetition rate of emitting photons is limited by the acting time of the repumping field. Unlike this, our mechanism allows to freely change the repetition rate of the single-photon pulses up to zero, because even in this case non-entangled single-photons are generated. We have shown the ability of our scheme to produce a sequence of narrow-band SP pulses with a delay determined only by the pump repetition rate. Such controlled scheme may pave the way to single-photon-based quantum information applications, such as deterministic all-optical quantum computation and quantum communication.

Chapter 3

Quantum frequency conversion in cold atoms

In a present chapter we propose and discuss a method that enables efficient frequency conversion of quantum information based on strong parametric coupling between two single-photon pulses propagating in a slow-light atomic medium at different group velocities. We show that an incoming single-photon state is efficiently converted into another optical mode in a lossless and shape-conserving manner. The persistence of initial quantum coherence and entanglement within frequency conversion is also demonstrated. We first illustrate this result for the case of small frequency difference of converted photons, and then discuss the modified scheme for conversion of photon wavelengths in different spectral ranges. Generation of a narrow-band single-photon frequency-entangled state is discussed as well [134, 138].

3.1 Parametric interaction between two single-photon pulses

We consider an ensemble of cold atoms with level configuration depicted in Fig.3.1. Two quantum fields

$$E_{1,2}(z,t) = \sqrt{\frac{\hbar\omega_{1,2}}{2\varepsilon_0 V}}\hat{\mathcal{E}}_{1,2}(z,t)\exp[i(k_{1,2}z - \omega_{1,2}t)] + h.c.$$

co-propagate along the z axis and interact with the atoms on the transitions $0 \to 1$ and $0 \to 2$, respectively, while the upper electric-dipole forbidden transition $1 \to 2$ is driven by a classical and constant field with real Rabi frequency Ω, and V is the quantization volume taken to be equal to the interaction volume. The electric fields are expressed in terms of the operators $\hat{\mathcal{E}}_i(z,t)$ obeying the commutation relations (see Appendix 3.A)

$$[\hat{\mathcal{E}}_i(z,t), \hat{\mathcal{E}}_j^\dagger(z,t')] = \frac{L}{c}\delta_{ij}\delta(t-t'), \tag{3.1}$$

with L the length of the medium, which is described using atomic operators $\hat{\sigma}_{\alpha\beta}(z,t) = \frac{1}{N_z}\sum_{i=1}^{N_z} |$ $\alpha \rangle_i \langle \beta |$ averaged over the volume containing many atoms $N_z = \frac{N}{L}dz \gg 1$ around position z, where N is the total number of atoms. Note, that the commutator for the electric field is given at different times but equal space coordinates. In general, this can only be correct for a free field, as a two-time commutator would depend on the solution of the field dynamics. However, in the case of linear interaction between the fields, when the field amplitudes depend on their initial values only linearly, the commutation relation for quantum field operators is, obviously, the same as in the free space.
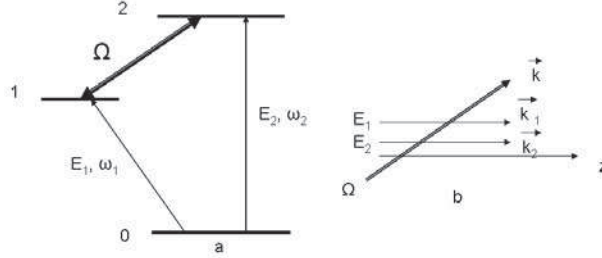

Figure 3.1: (a) Level scheme of atoms interacting with quantum fields $E_{1,2}$ and classical driving field of Rabi frequency Ω. (b) Geometry of fields propagation.

In the rotating wave picture the interaction Hamiltonian is given by

$$H = -\hbar\frac{N}{L}\int_0^L dz[g_1\hat{\mathcal{E}}_1\hat{\sigma}_{10}e^{ik_1z} + g_2\hat{\mathcal{E}}_2\hat{\sigma}_{20}e^{ik_2z} + \Omega\hat{\sigma}_{21}e^{ik_\parallel z} + h.c.] \tag{3.2}$$

Here $k_\parallel = \vec{k}_d\hat{e}_z$ is the projection of the wave-vector of the driving field on the z axis, $g_\alpha = \mu_{\alpha 0}\sqrt{\omega_i/(2\hbar\varepsilon_0 V)}$ is the atom-field coupling constant with $\mu_{\alpha\beta}$ being the dipole matrix element

of the atomic transition $\alpha \to \beta$. We assume that the process is running at low temperature in order to avoid the Doppler broadening, which in a cold atomic sample is smaller than all relaxation rates, and consider the case of exactly resonant interaction with all fields. Then, using the slowly varying envelope approximation, the propagation equations for the quantum field operators take the form:

$$\left(\frac{\partial}{\partial z} + \frac{1}{c} \frac{\partial}{\partial t} \right) \hat{\mathcal{E}}_1(z,t) = ig_1 \frac{N}{c} \hat{\sigma}_{01} e^{-ik_1 z} + \hat{F}_1 \tag{3.3}$$

$$\left(\frac{\partial}{\partial z} + \frac{1}{c} \frac{\partial}{\partial t} \right) \hat{\mathcal{E}}_2(z,t) = ig_2 \frac{N}{c} \hat{\sigma}_{02} e^{-ik_2 z} + \hat{F}_2 \tag{3.4}$$

where $\hat{F}_i(z,t)$ are the commutator preserving Langevin operators, whose explicit form is given below. In the weak-field (single-photon) limit, the equations for atomic coherence $\hat{\rho}_{0i} = \hat{\sigma}_{0i} e^{-ik_i z}, i = 1, 2$ and $\hat{\rho}_{12} = \hat{\sigma}_{12} e^{-i(k_2 - k_1)z}$ are treated perturbatively in $\hat{\mathcal{E}}_{1,2}$. In the first order only $\langle \hat{\sigma}_{00} \rangle \simeq 1$ is different from zero and for these equations we obtain:

$$\frac{\partial}{\partial t} \hat{\rho}_{01} = -\Gamma_1 \hat{\rho}_{01} + ig_1 \hat{\mathcal{E}}_1 \hat{\sigma}_{00} + i\Omega \hat{\rho}_{02} e^{i\triangle kz} - ig_2 \hat{\mathcal{E}}_2 \hat{\rho}_{21} \tag{3.5}$$

$$\frac{\partial}{\partial t} \hat{\rho}_{02} = -\Gamma_2 \hat{\rho}_{02} + ig_2 \hat{\mathcal{E}}_2 \hat{\sigma}_{00} + i\Omega \hat{\rho}_{01} e^{-i\triangle kz} - ig_1 \hat{\mathcal{E}}_1 \hat{\rho}_{12} \tag{3.6}$$

$$\frac{\partial}{\partial t} \hat{\rho}_{12} = -\Gamma_{12} \hat{\rho}_{12} - ig_1 \hat{\mathcal{E}}_1^* \hat{\rho}_{02} + ig_2 \hat{\mathcal{E}}_2 \hat{\rho}_{10} \tag{3.7}$$

Here $\Delta k = k_2 - k_1 - k_\parallel$ is the wave-vector mismatch, $\Gamma_{1,2}$ and Γ_{12} are the transverse relaxation rates involving, apart from natural decay rates $\gamma_{1,2}$ of the excited states 1 and 2, the dephasing rates in corresponding transitions. The latter are caused by atomic collisions and escape of atoms from the laser beam. However, in the ensemble of cold atoms the both effects are negligibly small compared to $\gamma_{1,2}$, so that $\Gamma_{1,2} = \gamma_{1,2}/2$ and $\Gamma_{12} = (\gamma_1 + \gamma_2)/2$. We emphasize that γ_i is a sum of the partial decay rate of i-th upper level to the ground state 0 and the rate of population leak from the i-th level towards the states outside of the system.

Further, we assume that the phase-matching condition $\Delta k = 0$ is fulfilled in the medium. Then, the solution to Eqs.(3.5-3.7) to the first order in $\hat{\mathcal{E}}_{1,2}$ is readily found to be

$$\hat{\rho}_{01} = i\frac{\Gamma}{D} g_1 \hat{\mathcal{E}}_1 + i\frac{\Omega^2 - \Gamma^2}{D^2} g_1 \frac{\partial}{\partial t} \hat{\mathcal{E}}_1 - \frac{\Omega}{D} g_2 \hat{\mathcal{E}}_2 + \frac{2\Gamma\Omega}{D^2} g_2 \frac{\partial}{\partial t} \hat{\mathcal{E}}_2, \tag{3.8}$$

$$\hat{\rho}_{02} = \hat{\rho}_{01}(1 \leftrightarrow 2), \quad D = \Omega^2 + \Gamma^2. \tag{3.9}$$

where, for simplicity, the optical decay rates are taken to be the same: $\Gamma_1 = \Gamma_2 = \Gamma$. The first terms in rhs of Eqs.(3.8, 3.9) are responsible for linear absorption of quantum fields and define the field absorption coefficients $\kappa_i = g_i^2 \Gamma N / c\Omega^2$ upon substituting these expressions into Eqs.(3.3, 3.4). The second terms in rhs of Eqs.(3.8, 3.9) represent the dispersion contribution to the group velocities of the pulses, while the two rest terms describe the parametric interaction between the fields.

To implement the QFC scheme in a dense atomic medium, several conditions must be satisfied. First, the photon absorption must be strongly reduced

$$\kappa_i L \ll 1 \tag{3.10}$$

The limit of this is readily achieved, if the condition of electromagnetically induced transparency (EIT, ref. [10]) $\Omega \gg \Gamma_{1,2}$ is satisfied for both transitions coupled to the weak-fields. Note that the three-level configurations 0-2-1 and 0-1-2 form the Λ- and ladder EIT-systems with the decoherence time Γ_1^{-1} and Γ_2^{-1}, respectively. Second, the initial spectrum of quantum fields should be contained within the EIT window $\Delta\omega_{EIT} = \Omega^2/(\Gamma\sqrt{\alpha})$ [57], resulting in little pulse distortion from absorption, i.e.

$$\Delta\omega_{EIT} T \geq 1 \tag{3.11}$$

where T is the initial pulse width, $\alpha = \mathcal{N}\sigma L$ is the optical depth, $\sigma = \frac{3}{4\pi}\lambda^2$ is the resonant absorption cross-section, and $\mathcal{N}$ is the atomic number density. It is also desirable that the pulse broadening should be minimal. The source of the latter is the various orders of dispersion, beginning from the group-velocity dispersion proportional to the second time derivative of the fields $\frac{\partial^2}{\partial t^2}\hat{\mathcal{E}}_i(z,t)$. The change in pulse width due to this term after propagating through the medium can be roughly estimated by treating the weak fields for a time classically and ignoring the parametric contribution to broadening. Then, for an initial Gaussian pulse $\mathcal{E}_1(0,t) = \mathcal{E}_0 exp(-\frac{2t^2}{T^2})$, the simple calculations yield

$$T_i(L) = T\sqrt{1 + \frac{16L}{v_i T^2 \Omega}}$$

with $v_i = c\Omega^2/g_i^2 N \ll c$ being the pulse group velocity. It is seen that the spreading of the quantum pulses caused by the group-velocity dispersion can be neglected, if

$$\frac{16\tau_i}{T^2\Omega} \leq 1 \tag{3.12}$$

where $\tau_i = L/v_i$ is the pulse propagation time and, in fact, the pulse delay relative to the pulse which travels the same distance in vacuum. It is worth noting that upon satisfying the condition (3.12), the pulse broadening due to next orders of dispersion is more suppressed.

The noise operators $F_{1,2}$ in Eqs.(3.12,3.13) have the properties [114]

$$\langle F_i(z,t)\rangle = \langle F_i(z,t)F_i(z,t')\rangle = \langle F_i(z,t)F_j(z,t')\rangle = 0$$

$$\langle F_i(z,t)F_j^\dagger(z,t')\rangle = 2\frac{\kappa_i}{c}\delta_{ij}\delta(t-t')$$

showing that in the absence of photon losses the noise operators $\hat{F}_i$ give no contribution. Then, in this limit the simple propagation equations for the field operators are obtained:

$$\left(\frac{\partial}{\partial z} + \frac{1}{v_1}\frac{\partial}{\partial t}\right)\hat{\mathcal{E}}_1(z,t) = -i\beta\hat{\mathcal{E}}_2 \tag{3.13}$$

$$\left(\frac{\partial}{\partial z} + \frac{1}{v_2}\frac{\partial}{\partial t}\right)\hat{\mathcal{E}}_2(z,t) = -i\beta\hat{\mathcal{E}}_1 \tag{3.14}$$

where $\beta = g_1 g_2 N/c\Omega$ is the coupling constant of parametric interaction between the quantum fields and decreases with increase of coupling field intensity. In Appendix 3.A we show that these equations preserve the commutation relations (3.1).

The formal solution of Eqs.(3.13,3.14) in the region $0 \leqslant z \leqslant L$ is given by

$$\hat{\mathcal{E}}_i(z,t) = \hat{\mathcal{E}}_i(0,\ t-z/v_i) + \int_0^z dx\{\hat{\mathcal{E}}_i(0,\ t-z/v_j - \frac{\Delta v_{ji}}{v_i v_j}x)$$

$$\times\ \frac{\partial J_0(\psi)}{\partial z} - i\beta\ \hat{\mathcal{E}}_j(0,\ t-z/v_i - \frac{\Delta v_{ij}}{v_i v_j}x)\ J_0(\psi)\} \tag{3.15}$$

where $i,j = 1,2$ and $j \neq i$. The Bessel function $J_0(\psi)$ depends on z via $\psi = 2\beta\sqrt{x(z-x)}$, $\Delta v_{ij} = v_i - v_j$ is the difference of group velocities.

In the limit of equal group velocities $v_2 = v_1 = v$ the Eqs. (3.15) are reduced to a simple form

$$\hat{\mathcal{E}}_i(z,t) = \hat{\mathcal{E}}_i(0,\tau)\cos(\beta z) - i\hat{\mathcal{E}}_j(0,\tau)\sin(\beta z) \tag{3.16}$$

where $\tau = t - z/v$, $j \neq i$. Note, however, that this case is practically never realized, since the atom-field coupling constants g_1 and g_2 are defined by the partial decay rates of upper atomic 1 and 2 levels into the ground state 0, which are different even if the total decay rates are the same $\gamma_1 = \gamma_2$, as is the case, for example, in a V-type atoms with hyperfine-level structure.

3.2 Quantum efficiency of conversion

Our aim is to show that the proposed scheme is suitable for converting individual photons at one frequency to another frequency while preserving initial quantum coherence that results in a generation of frequency-entangled single-photon state. To this end we analyze the evolution of the input state $\mid \psi_{in} \rangle = \mid 1_1 \rangle \otimes \mid 0_2 \rangle$ consisting of a single-photon wave packet at ω_1 frequency, while ω_2 field is in the vacuum state. The similar results are clearly obtained in the case of one input photon at ω_2 frequency. We assume that initially the ω_1 pulse is localized around $z = 0$ with a given temporal profile $f_1(t)$:

$$\langle 0 \mid \hat{\mathcal{E}}_1(0,t) \mid \psi_{in} \rangle = \langle 0 \mid \hat{\mathcal{E}}_1(0,t) \mid 1_1 \rangle = f_1(t) \tag{3.17}$$

In free space, $\hat{\mathcal{E}}_1(z,t) = \hat{\mathcal{E}}_1(0, t - z/c)$ and we have

$$\langle 0 \mid \hat{\mathcal{E}}_1(0, t - z/c) \mid 1_1 \rangle = f_1(t - z/c). \tag{3.18}$$

The intensities of the fields at any distance in the region $0 \leqslant z \leqslant L$ are given by

$$\langle I_i(z,t) \rangle = \mid \langle 0 \mid \hat{\mathcal{E}}_i(z,t) \mid \psi_{in} \rangle \mid^2 \tag{3.19}$$

The quantum efficiency (QE) is determined as the ratio $n_2(L)/n_1(0)$, where $n_i(z) = \langle \psi_{in} \mid \hat{n}_i(z) \mid \psi_{in} \rangle$ are the mean photon numbers and $\hat{n}_i(z)$ are the dimensionless operators for number of photons that pass each point on the z axis in the whole time

$$\hat{n}_i(z) = \frac{c}{L} \int dt \hat{\mathcal{E}}_i^\dagger(z,t) \hat{\mathcal{E}}_i(z,t) \tag{3.20}$$

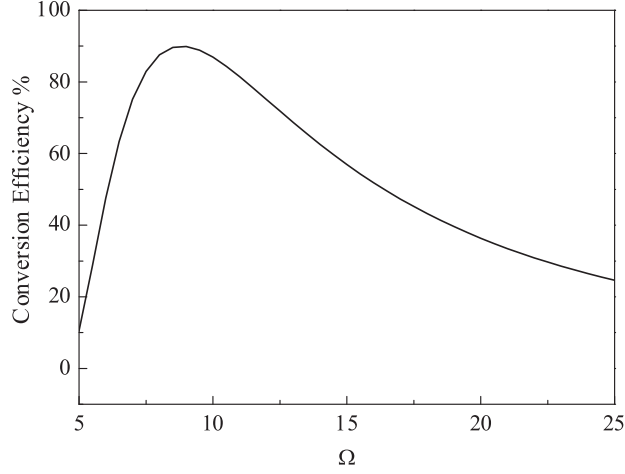Using Eqs.(3.15, 3.17-3.20) and recalling that $\langle 0 \mid \hat{\mathcal{E}}_2(0,t) \mid \psi_{in} \rangle = 0$, we calculate n_i

Figure 3.2: Quantum efficiency of optical field conversion from $\lambda_1 = 795$nm into $\lambda_2 = 780$nm in ^{87}Rb as a function of driving field Rabi frequency Ω (given in units of Γ_2) for the medium length $L = 100\mu$m. For the rest of parameters see the text.

numerically and show in Fig.3.2 the QE as a function of driving field Rabi frequency Ω in the case of a Gaussian input pulse $f(t) = C\exp[-2t^2/T^2]$, which is normalized as $\frac{c}{L}\int |$ $f_1(t)|^2 dt = 1$ indicating that the number of impinged photons is one. The atomic sample is chosen to be ^{87}Rb vapor with the ground state $5S_{1/2}(F_g = 2)$ and exited states $5P_{1/2}(F_e = 1)$, $5P_{3/2}(F_e = 1)$ as the atomic states 0 and $1, 2$ in Fig.3.1, respectively. For calculations we used the following parameters: light wavelength of quantum fields $\lambda_1 = 795$ nm and $\lambda_2 = 780$ nm, $\Gamma = \Gamma_2 = 2\Gamma_1 = 2\pi \times 3$ MHz, atomic density $\mathcal{N} \sim 10^{13}$cm^{-3} in a trap of length $L \sim 100$ μm, and the input pulse duration $T \simeq 20$ ns, for which we have $v_1 \sim 1.25 \cdot 10^4$m/s, $v_2 \sim 0.5v_1$, and $\kappa_i L < 0.1$. All of these parameters appear to be within experimental reach, including the initial single-photon wave packets with a pulse length of several tens of nanoseconds [34, 63], as well as high power narrow-band cw THz radiation at a frequency ~ 7 THz [115] resonant to the fine splitting $\omega(5P_{3/2} - 5P_{1/2})$ in rubidium.

It is worth noting that in most cases of alkali atoms the spectral separation between $D2$ and $D1$ lines lies in the operation range of tunable terahertz silicon and quantum cascade lasers [117, 116] that may give novel important applications of THz radiation such as implementation of QFC in atomic ensembles.
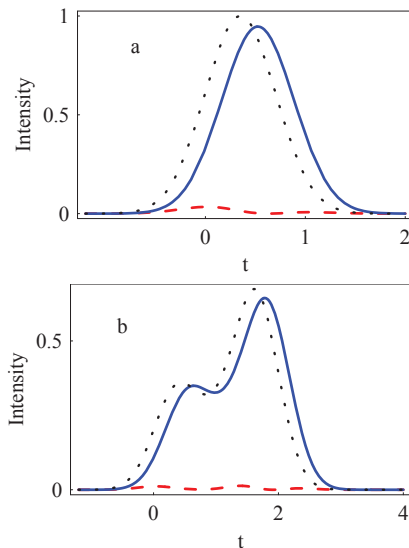
Figure 3.3: Output shapes of λ_1 (dashed line) and λ_2 (solid line) modes in the cases of Gaussian (a) and double-hump (b) input λ_1 pulses for $\Omega = 8\Gamma$ and other parameters as in Fig.3.2. The dotted line displays the λ_1 pulse propagating in the medium with $\beta = 0$. The time is given in units of T.

In Fig.3.2 we do not show the region of small values of Ω, where the solution Eq.(7) is not valid. It is seen that the QE reaches its maximum $\sim 90\%$ at $\Omega \sim 8\Gamma$, which is very close to the corresponding value of Ω following from Eq.(3.16) for equal group velocities. To demonstrate the shape-conserving character of frequency conversion in our scheme we present in Fig.3.3 the results for two different shapes of initial ω_1 pulse. Fig.3.3a shows the case of Gaussian shaped input pulse having a duration T, while in Fig.3.3b the latter is taken as two superimposed Gaussian pulses of the same duration T. It is seen that in both cases the generated ω_2 mode reproduces almost identically the initial form of the input ω_1 pulse, which is evidently a direct consequence of linear relationship between quantum fields in Eqs.(3.13) and (3.14).

At other values of Ω the incoming ω_1 field is converted into ω_2 mode not completely, but different amount of mode conversion is attainable, thus enabling redistribution of quantum information between the two quantum fields. By adjusting the driving field intensity, a single-photon state entangled over the two optical modes ω_1 and ω_2 with the given intensities can

be generated. In particular, such a state with equal intensities of the modes is created for two values of $\Omega \sim 6\Gamma$ and $\Omega \sim 18\Gamma$ (Fig.3.4), which, however, are different in their physical content. The higher values of Ω correspond to a large group velocities of the pulses, while the parametric coupling is reduced. As a result, during propagation in the medium the ω_1 field has time to be converted into ω_2 mode only partially and, owing to $v_2 < v_1$, the ω_2 pulse is slightly delayed with respect to the signal ω_1 pulse that is just observed in Fig.3.4 (left column). On the contrary, at small values of Ω the pulses travel slower, while the parametric coupling is enhanced. Consequently, first the ω_1 field is almost completely converted into the ω_2 pulse at small distances (nearly 60 μm), and then the latter is partially transformed back into the ω_1 photon at the end (100μm) of the medium. This time the newly generated ω_1 pulse is clearly behind the ω_2 pulse (Fig.3.4, right column) with a delay which is longer than in the previous case. By these any input optical mode is split into two optical modes of different frequencies in a controllable way preserving at the same time the total number of photons, which is determined in each mode by the areas of the corresponding peaks. In the absence of losses, the conservation law for photon numbers follows from Eqs.(3.13) and (3.14) as

$$\frac{\partial}{\partial z}(n_1(z) + n_2(z)) = 0 \tag{3.21}$$

with taking into account that $\langle 0 \mid \hat{\mathcal{E}}_i(z, t \to \pm\infty) \mid \psi_{in}\rangle = 0$. At the input of the medium $n_1(0)=1$ and $n_2(0)=0$, so that from Eq.(3.21) one has $n_1(z) + n_2(z)=1$.

So far we considered the pulses with a duration comparable to the lifetime of atomic 1 and 2 levels. However, the conditions (3.10-3.12) do not limit critically the pulse length provided that the spectral bandwidth of quantum fields is still negligible compared to the separation between the upper atomic levels. These conditions can be easily satisfied also for ultrashort pulses, if low atomic densities (lower by several orders of magnitude) are used, thus making our scheme able for efficient frequency conversion in this case as well, which is a permanent need in quantum communication tasks.

Thus, by combining the clear properties of parametric interaction between the photons
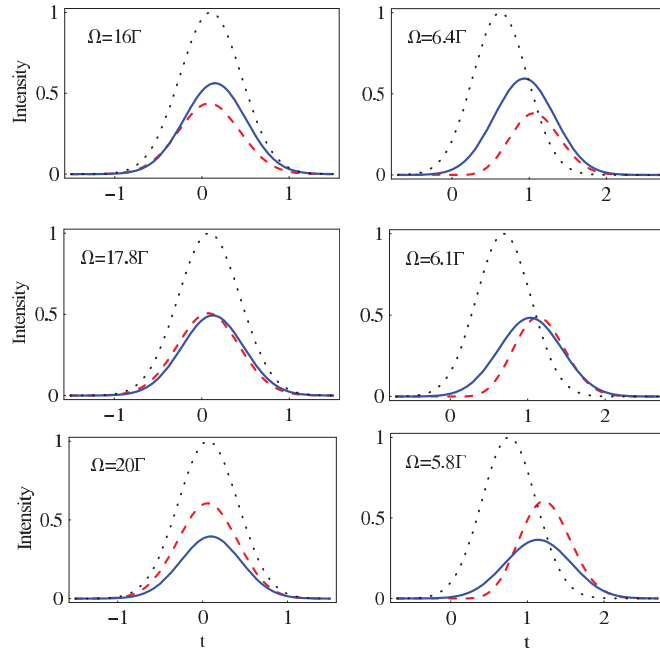
Figure 3.4: The same as in Fig.3.3a, but for different values of Ω.

with that the converted light is within the narrow atomic resonant width, one can significantly expand the ability to distribute the quantum states of narrowband spectra. Above we have demonstrated this possibility in the case of small frequency difference of converted photons that can be used, in particular, for addressable excitation of registers of quantum computers, which may be trapped ions or atoms, atomic ensembles, quantum dots etc. At the same time, there is considerable interest in exploring similar mechanisms that enable coherent conversion of photons with much larger difference in wavelengths. Such a mechanism would enable quantum information to be passed over long distances by telecom fibers, which impose the infrared (IR) wavelengths, and then to be mapped into the states of atoms, which interact resonantly with quantum fields at visible frequencies. Within our approach, the required frequency conversion is easily realized by slightly modifying the interaction configuration in Fig.3.1 and applying a second classical field on the transition $0 \rightarrow 3$ with the Rabi frequency Ω_0 (Fig.3.5a). The details of this analysis are in the next section.

3.3 Qubit transfer between photons at telecom and visible wavelengths

We consider an ensemble of cold atoms interacting with two quantum fields on the transitions $3 \to 2$ and $0 \to 1$ (Fig.3.5a), while the transitions $1 \to 2$ and $0 \to 3$ are driven by two classical and constant fields with real Rabi frequencies Ω and Ω_0, respectively. The classical fields create parametric coupling between two weak fields, while the Ω field provides EIT conditions for both quantum fields. We suppose $\Omega_0 \gg \gamma_3$, with γ_3 the decay rate of the state $\mid 3\rangle$, so that the bare atomic states $\mid 0\rangle$ and $\mid 3\rangle$ are split into a doublet of dressed states $\mid \pm\rangle = (\mid 0\rangle \pm \mid 3\rangle)/\sqrt{2}$, which are well separated by $2\Omega_0$ Fig.3.1b. If now the condition $\Delta = \omega_{10} - \omega_1 = \omega_{32} - \omega_2 = \Omega_0$ for the detunings of the quantum fields is fulfilled, where ω_1 and ω_2 are the carrier frequencies of the fields $\hat{\mathcal{E}}_1$ and $\hat{\mathcal{E}}_2$, respectively, then the quantum fields are in the exact resonance with the transitions $\mid +\rangle \to \mid 1\rangle$ and $\mid +\rangle \to \mid 3\rangle$ and their conversion into each other occurs with the same or higher efficiency as in the previous case of three-level atom [134]. Two-photon ladder type transition in the Rb atom has been considered also in [118], which involves three classical fields for two-photon excitation of the atom and creation of EIT conditions for signal and idler photons. So, this scheme is different from our system. Since $\Delta = \Omega_0$, then taking into account that in this case the excitation of the atoms from
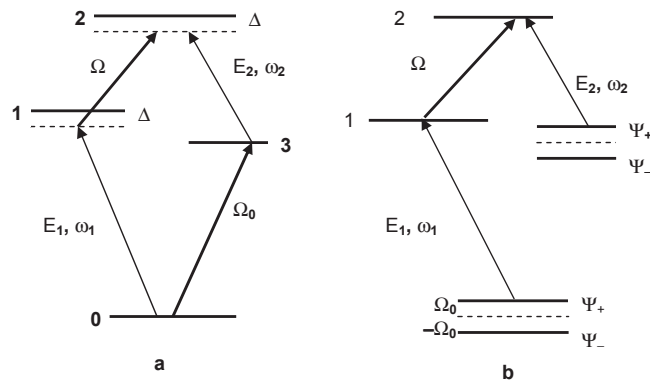

Figure 3.5: Modified scheme for conversion of quantum fields E_1 and E_2 with essentially different wavelengths in the basis of bare (a) and dressed (b) atomic states.

Ψ_- can be neglected, as it is strongly suppressed by the factor of $(\Gamma_3/\Omega_0)^2$, the interaction scheme is reduced to Fig.3.5b, where Ψ_+ serves as the ground state (correspondingly, for alternative choose $\Delta = -\Omega_0$, the ground state of modified system is Ψ_-), thus making this scheme identical to that of Fig.3.1. In RWA the Hamiltonian of the system in the interaction picture is given by

$$
\begin{aligned}
H \;=\; & \hbar \frac{N}{L} \int\limits_0^L dz \big(\Delta \hat{\sigma}_{11} + \Delta \hat{\sigma}_{22} - g_1 \hat{\mathcal{E}}_1 \hat{\sigma}_{10} e^{ik_1 z} \\
& - g_2 \hat{\mathcal{E}}_2 \hat{\sigma}_{23} e^{ik_2 z} - \Omega_0 \hat{\sigma}_{30} e^{ik_0 z} - \Omega \hat{\sigma}_{21} e^{ikz} + h.c. \big).
\end{aligned}
\tag{3.22}
$$

Here $k, k_0 = \vec{k}\hat{e}_z, \vec{k}_0\hat{e}_z$ are the projections of the wave-vectors of the driving fields on the z axis. Using the slowly varying envelope approximation, the propagation equations for the quantum field operators take the form

$$
\left(\frac{\partial}{\partial z} + \frac{1}{c} \frac{\partial}{\partial t} \right) \hat{\mathcal{E}}_1(z,t) \;=\; ig_1 \frac{N}{c} \hat{\sigma}_{01} e^{-ik_1 z} + \hat{F}_1,
\tag{3.23}
$$

$$
\left(\frac{\partial}{\partial z} + \frac{1}{c} \frac{\partial}{\partial t} \right) \hat{\mathcal{E}}_2(z,t) \;=\; ig_2 \frac{N}{c} \hat{\sigma}_{32} e^{-ik_2 z} + \hat{F}_2,
\tag{3.24}
$$

where $\hat{F}_i(z,t)$ are the commutator preserving Langevin operators. We obtain the atomic coherences from the equation

$$
\frac{d\hat{\sigma}_{ij}}{dt} = \frac{i}{\hbar} [H, \hat{\sigma}_{ij}] + \frac{d\hat{\sigma}_{ij}}{dt} \Big|_{rel},
\tag{3.25}
$$

where the last term accounts for all the relaxations. We pass from the bare atomic states $|\phi\rangle = \{|0\rangle, |1\rangle, |2\rangle, |3\rangle\}$ to the dressed ones $|\psi\rangle = S^\dagger U^\dagger \phi = \{|-\rangle, |1\rangle, |2\rangle, |+\rangle\}$ with

$$
S = \begin{pmatrix} \cos\theta & 0 & 0 & -\sin\theta \\ 0 & 1 & 0 & 0 \\ 0 & 0 & 1 & 0 \\ \sin\theta & 0 & 0 & \cos\theta \end{pmatrix}, U = \begin{pmatrix} 1 & 0 & 0 & 0 \\ 0 & 1 & 0 & 0 \\ 0 & 0 & 1 & 0 \\ 0 & 0 & 0 & e^{ik_0 z} \end{pmatrix},
\tag{3.26}
$$

where $\tan 2\theta = 2\Omega_0/\Delta_0$. The transformation U is applied in order all the atoms to experience the same S transformation on the propagation line. In the dressed state and for $\Delta_0 = \omega_{30} - \omega_0 = 0$ the Hamiltonian of the system in the dressed states basis $\tilde{H} = S^\dagger(U^\dagger H U)S$

takes the form

$$\tilde{H} = \hbar\frac{N}{L}\int\limits_0^L dz\big[\Delta\hat{\sigma}_{11} + \Delta\hat{\sigma}_{22} - \Omega_0(\hat{\sigma}_{--} - \hat{\sigma}_{++}) - \Omega\hat{\sigma}_{21}e^{ikz}$$

$$- \frac{g_1\hat{\mathcal{E}}_1}{\sqrt{2}}e^{ik_1z}(\hat{\sigma}_{1-} - \hat{\sigma}_{1+}) - \frac{g_2\hat{\mathcal{E}}_2}{\sqrt{2}}e^{i(k_2+k_0)z}(\hat{\sigma}_{2-} + \hat{\sigma}_{2+})\big] + h.c. \qquad (3.27)$$

Then the atomic coherences $\hat{\sigma}_{01}$ and $\hat{\sigma}_{32}$ are defined by $\hat{\sigma}_{\pm 1,2}$ as

$$\hat{\sigma}_{01} = (\hat{\sigma}_{-1} - \hat{\sigma}_{+1})/\sqrt{2}, \qquad (3.28)$$

$$\hat{\sigma}_{32} = (\hat{\sigma}_{-2} + \hat{\sigma}_{+2})/\sqrt{2}. \qquad (3.29)$$

In the weak-field limit the equations for atomic coherences $\hat{\sigma}_{\pm 1} = \hat{\rho}_{\pm 1}e^{ik_1z}, \hat{\sigma}_{\pm 2} = \hat{\rho}_{\pm 2}e^{i(k_2+k_0)z}$ are treated perturbatively in $\hat{\mathcal{E}}_{1,2}$ and have the form

$$\dot{\hat{\rho}}_{-1,2} = -i(\Delta + \Omega_0 - i\Gamma_{1,2+})\hat{\rho}_{-1,2} - \frac{\Gamma_3}{2}\hat{\rho}_{+1,2}$$

$$+ i\frac{g_{1,2}\hat{\mathcal{E}}_{1,2}}{\sqrt{2}}\hat{\sigma}_{--} + i\Omega\hat{\rho}_{-2,1}, \qquad (3.30)$$

$$\dot{\hat{\rho}}_{+1,2} = -i(\Delta - \Omega_0 - i\Gamma_{1,2+})\hat{\rho}_{+1,2} - \frac{\Gamma_3}{2}\hat{\rho}_{-1,2}$$

$$\mp i\frac{g_{1,2}\hat{\mathcal{E}}_{1,2}}{\sqrt{2}}\hat{\sigma}_{++} + i\Omega\hat{\rho}_{+2,1}, \qquad (3.31)$$

where $\Gamma_{1,2+} = \Gamma_{1,2} + \Gamma_3/2$, $\Gamma_{1,2}$ are the transverse relaxation rates, which in the case of cold atoms are simply $\Gamma_{1,2} = \gamma_{1,2}/2$, with $\gamma_{1,2}$ the natural decay rates of the excited states 1 and 2. Here the phase matching condition $\triangle k = k_1 + k - k_2 - k_0 = 0$ is supposed to be fulfilled.

It is seen from (3.30), (3.31) that for $\Delta = \Omega_0$ the polarizations $\hat{\rho}_{-1,2}$ are strongly suppressed compared to $\hat{\rho}_{+1,2}$ and can be neglected. The solution for $\hat{\rho}_{+1,2}$ are easily found from (3.31) in the first order of $\hat{\mathcal{E}}_{1,2}$ and and with $\langle\hat{\sigma}_{--}\rangle = \langle\hat{\sigma}_{++}\rangle = 1/2$ have the form

$$\hat{\rho}_{+1} = i\frac{\Gamma_{1+}}{2\sqrt{2}D^2}g_1\hat{\mathcal{E}}_1 + i\frac{\Omega^2 + \Gamma_{1+}^2}{2\sqrt{2}D^4}g_1\frac{\partial\hat{\mathcal{E}}_1}{\partial t}$$

$$- \frac{\Omega}{2\sqrt{2}D^2}g_2\hat{\mathcal{E}}_2 - \frac{(\Gamma_{1+} + \Gamma_{2+})\Omega}{2\sqrt{2}D^4}g_2\frac{\partial\hat{\mathcal{E}}_2}{\partial t}, \qquad (3.32)$$

$$\hat{\rho}_{+2} = -i\frac{\Gamma_{2+}}{2\sqrt{2}D^2}g_2\hat{\mathcal{E}}_2 - i\frac{\Omega^2 + \Gamma_{2+}^2}{2\sqrt{2}D^4}g_2\frac{\partial\hat{\mathcal{E}}_2}{\partial t}$$

$$+ \frac{\Omega}{2\sqrt{2}D^2}g_1\hat{\mathcal{E}}_1 + \frac{(\Gamma_{1+} + \Gamma_{2+})\Omega}{2\sqrt{2}D^4}g_1\frac{\partial\hat{\mathcal{E}}_1}{\partial t}, \qquad (3.33)$$

$$D^2 = \Omega^2 + \Gamma_{1+}\Gamma_{2+},$$

which is similar to Eqs. (3.8, 3.9). The first terms in rhs of Eqs.(3.32), (3.33) are responsible for linear absorption of quantum fields and define the field absorption coefficients $\kappa_i = g_i^2 \Gamma N / 4c\Omega^2$ ($\Gamma \sim \Gamma_{1,2}$), upon substituting these expressions into Eqs.(3.23), (3.24). The second terms represent the dispersion contribution to the group velocities v_i of the pulses leading to $v_i = 4c\Omega^2 / g_i^2 N \ll c$. The two rest terms describing the parametric interaction between the fields, are strongly suppressed by the factor $\Omega^2 T / \Gamma \gg 1$, and are neglected below.

Since in the absence of photon losses the noise operators $\hat{F}_i$ give no contribution (see the previous section), they are neglected and finally we obtain

$$\left(\frac{\partial}{\partial z} + \frac{1}{v_j} \frac{\partial}{\partial t} \right) \hat{\mathcal{E}}_j(z, t) = i\beta \hat{\mathcal{E}}_k , \quad j, k = 1, 2, \tag{3.34}$$

where $\beta = g_1 g_2 N / 4c\Omega$ is the parametric coupling between the quantum fields. For numerical estimations we choose a sample of ^{87}Rb vapor with the states $5S_{1/2}, 5P_{3/2}, 4D_{3/2}$, and $5P_{1/2}$ being the atomic states 0, 1, 2 and 3, respectively. In this case the quantum fields' wavelengths are $\lambda_1 \sim 780$nm, $\lambda_2 \sim 1.47\mu$ m and $g_2/g_1 \sim 0.96$ this provides the quantum fields $\hat{\mathcal{E}}_{1,2}$ to have almost equal group velocities on the corresponding transitions $v_1 = v_2 = v$, which leads to a simple solution of equations (3.34) in a form

$$\hat{\mathcal{E}}_i(z, t) = \hat{\mathcal{E}}_i(0, \tau) \cos(\beta z) + i\hat{\mathcal{E}}_j(0, \tau) \sin(\beta z), \tag{3.35}$$

where $i, j = 1, 2$ and $i \neq j$.

The quantum efficiency η of the process is determined as the ratio of the mean photon numbers $\eta = n_2(L)/n_1(0)$, where $n_i(z) = \langle \psi_{in} \mid \hat{n}_i(z) \mid \psi_{in} \rangle$. Hence the quantum efficiency of conversion an input single-photon at frequency ω_1 into a single output photon at frequency ω_2 is easily found from (3.20), (3.35) to be

$$\eta = \sin^2 \beta L. \tag{3.36}$$

The efficiency of the process reaches 100% when $\beta L = \pi/2$. This is the case, e.g. if we take $L = 100\mu$m, $\Omega = 8\Gamma, \Gamma = 2\pi \times 3$ MHz, $\mathcal{N} = 10^{13}$ cm^{-3}. It can be easily checked that

all conditions for efficient FC mentioned above are fulfilled with $T \sim 20$ns. The Doppler broadening can be neglected, if $ku \sim \Gamma$, where u is the mean thermal velocity of the Rb atoms. From this condition the temperature of Rb vapor is obtained to be $T \sim 0.03$K. These parameters appear to be within experimental reach, including the initial single-photon wave packets with a pulse length of several tens of nanoseconds [34, 63] and the Rb vapor temperature at the mentioned densities [119, 120]. From (3.34) and (3.36) it is evident that the shape of the photon pulse is conserved during the FC process.

3.4 Generation of frequency-entangled single-photon state

Now we discuss the quantum properties of output single-photon state. We describe it in terms of quantized wave packets at the frequencies ω_1 and ω_2 containing the mean photon numbers $n_i(L) = \frac{c}{L} \int dt \mid \Phi_i(L,t) \mid^2$, where $\Phi_i(L,t) = \langle 0 \mid \hat{\mathcal{E}}_i(L,t) \mid \psi_{in} \rangle$ are the wave functions of the modes. Using Eq.(3.20) and the commutation relations (3.1) we obtain the output single-photon state as the eigenstate of total photon number operator

$$(\hat{n}_1(L) + \hat{n}_2(L)) \mid \psi_{out} \rangle = \mid \psi_{out} \rangle$$

which yields

$$\mid \psi_{out} \rangle = \frac{c}{L} \int dt [\Phi_1(L,t) \hat{\mathcal{E}}_1^\dagger(L,t) + \Phi_2(L,t) \hat{\mathcal{E}}_2^\dagger(L,t)] \mid 0 \rangle \tag{3.37}$$

Let us introduce the operators of creation of single-photon wave packets at frequencies ω_i associated with mode functions $\Phi_i(L,t)$, where i labels the members of the innumerably infinite set. For $i = 1, 2$ they are given by

$$\hat{c}_{1,2}^\dagger = N_i^{1/2} \int dt \Phi_{1,2}(L,t) \hat{\mathcal{E}}_{1,2}^\dagger(L,t) \tag{3.38}$$

with the normalization constants

$$N_i = \frac{c}{L} \left(\int dt \mid \Phi_1(L,t) \mid^2 \right)^{-1}$$

These operators create the single-particle states in the usual way by acting on the vacuum state $\mid 0 \rangle$

$$\hat{c}_i^\dagger \mid 0 \rangle = \mid 1_i \rangle \tag{3.39}$$

and have the standard boson commutation relations

$$[\hat{c}_i, \hat{c}_j^\dagger] = \delta_{ij} \tag{3.40}$$

following from Eq.(3.1).

Note that this definition of quantized wave packets is only useful, if the mode spectra are much narrower compared to the mode spacing that has been suggested from the very beginning. Now, for the algebra (3.40) we choose the representation of infinite product of all vacua

$$\mid 0\rangle = \prod_i \mid 0_i\rangle = \mid 0_1\rangle \mid 0_2\rangle \prod_{i\neq 1,2} \mid 0_i\rangle. \tag{3.41}$$

However, since in our problem we deal with two frequency modes, while the other modes are not occupied by the photons and, hence, are not taken into account during the measurements, the vacuum may be reduced to $\mid 0\rangle = \mid 0_1\rangle \mid 0_2\rangle$. Then the single-photon state (3.37) can be written as

$$\mid \psi_{out}\rangle = r_1 \hat{c}_1^\dagger \mid 0_1\rangle \mid 0_2\rangle + r_2 \mid 0_1\rangle \hat{c}_2^\dagger \mid 0_2\rangle =$$

$$= r_1 \mid 1_1\rangle \mid 0_2\rangle + r_2 \mid 0_1\rangle \mid 1_2\rangle \tag{3.42}$$

with $r_{1,2} = \sqrt{n_{1,2}(L)}$.

Thus, in general case of $r_{1,2} \neq 0$, the system produces a photonic qubit, i.e., a single-photon state entangled in two distinct frequency modes with the known wave functions $\Phi_{1,2}(L, t)$. The complete conversion of input ω_1 mode depicted in Fig.3.3 corresponds to pure output state $\mid \psi_{out}\rangle = \mid 0_1\rangle \otimes \mid 1_2\rangle$.

Finally, we demonstrate the persistence of initial quantum coherence and entanglement within the QFC in a simple case of input single-photon state entangled in two well-separated temporal modes or time-bins [121](the concept of the single-photon entanglement is discussed in [60])

$$\mid \psi_{in}\rangle = (a \mid 1_1\rangle_t \mid 0_1\rangle_{t+\tau} + b \mid 0_1\rangle_t \mid 1_1\rangle_{t+\tau}) \otimes \mid 0_2\rangle \tag{3.43}$$

where $\mid 0_1\rangle_t$ and $\mid 1_1\rangle_t$ denote Fock states with zero and one ω_1 photon, respectively, at the time t and $\mid a \mid^2 + \mid b \mid^2 = 1$. Suppose that the single-photon wave packets $\mid 1_1\rangle_t$ and $\mid 1_1\rangle_{t+\tau}$

are characterized by temporal profiles $f_0(t)$ and $f_\tau(t)$, respectively, which are not overlapped in time due to large time shift τ. Then, using the Eqs.(3.15) and (3.18), the wave function of output ω_2 mode is readily calculated to be

$$\Phi_2(L, t) = \langle 0 \mid \hat{\mathcal{E}}_2(L, t) \mid \psi_{in} \rangle = a\Phi_{2,0}(L, t) + b\Phi_{2,\tau}(L, t)$$

where

$$\Phi_{2,0(\tau)}(L, t) = -i\beta \int\limits_0^L dx f_{0(\tau)}(X) \ J_0(\psi)$$

with $X = t - L/v_2 - x\Delta v_{21}/v_1 v_2$. Consequently, from Eq.(3.38) the creation operator $c_2^\dagger$ can be represented as a sum of creation operators of the two temporal modes at ω_2 frequency. Following the procedure discussed above the output state in the case of complete conversion ($r_1 = 0$) is eventually found in the form

$$\mid \psi_{out} \rangle = \mid 0_1 \rangle \otimes (a \mid 1_2 \rangle_t \mid 0_2 \rangle_{t+\tau} + b \mid 0_2 \rangle_t \mid 1_2 \rangle_{t+\tau}) \tag{3.44}$$

showing that the initial ω_1 qubit is transformed into another at ω_2 frequency with the same complex amplitudes a and b, thus preserving the original amount of entanglement. Two different methods are available for experimental test of coherence transfer during the frequency conversion. In the first case, following the work [56] the single-photon interference for incoming and outgoing photons can be measured and compared to each other, thus revealing an equal phase periodicity in the two interference patterns in agreement with Eqs.(3.43) and (3.44). The second method [55, 48] is based on photon-pair interference; the input ω_1 photon is first nonclassically correlated with another photon at ω_3, which does not take part in the frequency conversion process. Then, after complete conversion of the ω_1 photon into ω_2 photon, the entanglement will arise between the ω_2 and ω_3 photons and, hence, the strong two-photon interference between the latter will demonstrate the transfer of input qubit at ω_1 frequency into another at $\omega_2 \neq \omega_1$ frequency. To realize this program for narrowband fields, as is the case here, we propose to employ the Duan, Lukin, Cirac, and Zoller (DLCZ) protocol [122, 123] for generation of nonclassically correlated pair of Stokes ω_1- and anti-Stokes ω_3-photons. Note that the key features of DLCZ protocol have been confirmed in

many experiments, including strong quantum correlations between ω_1 and ω_3 fields [124].

Appendix 3.A: Commutation relations for field operators

In this Appendix we derive the commutation relations Eq.(3.1) for traveling-wave electric field operators. In free space $z \leq 0$, the field operators are given by $\hat{\mathcal{E}}_i(z,t) = \sum\limits_{n=0}^{\infty} a_{i,n} e^{-i\omega_n(t-z/c)}$, where $a_{i,n}$ is the annihilation operator for the i-th field discrete mode with a frequency $\omega_i + \omega_n$. These operators satisfy the standard boson commutation relations

$$[a_{i,n}, a_{j,n'}^{\dagger}] = \delta_{ij}\delta_{nn'} \tag{3.A1}$$

In the continuum limit $a_{i,n} \to (\Delta\omega)^{1/2} a_i(\omega)$ and $\sum \to (1/\Delta\omega)\int d\omega$ with $\Delta\omega = 2\pi c/L$, the commutation relations at z=0 are found to be

$$[\hat{\mathcal{E}}_i(0,t), \hat{\mathcal{E}}_j^{\dagger}(0,t')] = \frac{L}{c}\delta_{ij}\delta(t-t') \tag{3.A2}$$

Inside the medium, the commutation relations satisfy the equation

$$\frac{\partial}{\partial z}[\hat{\mathcal{E}}_1(z,t), \hat{\mathcal{E}}_1^{\dagger}(z,t')] = -\frac{1}{v_1}(\frac{\partial}{\partial t} + \frac{\partial}{\partial t'})[\hat{\mathcal{E}}_1(z,t), \hat{\mathcal{E}}_1^{\dagger}(z,t')]$$

$$-i\beta([\hat{\mathcal{E}}_2(z,t), \hat{\mathcal{E}}_1^{\dagger}(z,t')] - [\hat{\mathcal{E}}_1(z,t), \hat{\mathcal{E}}_2^{\dagger}(z,t')]) \tag{3.A3}$$

With the use of Eqs.(3.1) we have

$$[\hat{\mathcal{E}}_2(z,t), \hat{\mathcal{E}}_1^{\dagger}(z,t')] = [\hat{\mathcal{E}}_1(z,t), \hat{\mathcal{E}}_2^{\dagger}(z,t')] = 0$$

Recalling also that $[\hat{\mathcal{E}}_1(z,t), \hat{\mathcal{E}}_1^{\dagger}(z,t')]$ is a function of time difference $t-t'$ and, hence,

$$\left(\frac{\partial}{\partial t} + \frac{\partial}{\partial t'}\right)[\hat{\mathcal{E}}_1(z,t), \hat{\mathcal{E}}_1^{\dagger}(z,t')] = 0$$

we obtain that the commutation relations are spatially invariant and have the form of Eq.(3.1).

3.5 Summary

Summarizing, we have proposed and analyzed a simple scheme of parametric frequency conversion of optical quantum information in atomic ensembles. We have demonstrated remarkable properties of this scheme such as minimal loss and distortion of the pulse shape, the persistence of initial quantum coherence and entanglement that makes it superior against the previous schemes of the QFC in atomic media based on release of stored light state via EIT. Moreover, the narrowband property of single photons and high efficiency of entanglement generation profit the present mechanism to serve as an ideal candidate for frequency conversion and redistribution of optical information in quantum information processing and quantum networking.

Chapter 4

Selective excitation of atoms or molecules and quantum beats in pump-probe experiments

Population transfer to a desired coherent superposition of atomic and molecular states is of an urgent need. In this chapter we propose a mechanism to produce such a superposition by (a) a train of ultrashort laser pulses combined with weak control fields (weak field regime) [135] and (b) strong pump and control fields (strong field regime) [139]. By adjusting the repetition rate of the pump pulses and/or the intensity of the coupling laser, one can suppress a transition, while simultaneously enhancing the desired transitions.

For the first time the complete theory of QBs observed in the intensities of Stokes [136] and ultraviolet fields [137] generated on the basis of HRS and FWM is given. As a first step the theory of quantum beats in a Stokes signal observed in pump-probe experiments upon excitation of four-level atoms with two close upper lying levels by femtosecond laser pulses is developed. Quantum beats arise in the intensity of the Stokes field due to the interference of two atomic wave packets generated by ultrashort pump and probe pulses.

4.1 Shaping coherent excitation by a train of ultrashort weak laser pulses

We consider a system of level configuration shown in Fig. 4.1 interacting with a train of ultrashort femtosecond laser pulses, whose spectrum is wide enough to overlap all the upper states, while a narrow-band weak laser couples, for example, the upper level 1 with an auxiliary state 4. We consider three upper levels for simplicity, but the proposed mechanism can be directly extended to any number of upper-lying levels. By adjusting the repetition rate of the pump pulses with respect to the Rabi frequency Ω_c of the coupling field, this scheme enables one to cancel out the strong transition $0 \to 1$ from the pump field, while enhancing the transitions $0 \to i, i = 2, 3$. To give an insight into the proposed mechanism, let us consider the interaction of the system with two consecutive identical pump pulses in resonance on the transition $0 \to 1$, with a time delay τ_d, which is larger as compared to the pulse duration T. In the low intensity regime, the atomic state amplitudes $C_{1,2,3}$ after the first pump pulse are: $C_j \sim \theta_j = \int \Omega_j(t) e^{i\Delta_j} dt \ll 1, \; j = 1, 2, 3$, with Ω_j the pump Rabi frequencies corresponding to the respective $0 \to j$ transitions [see Eqs. (4.2) and (4.3) for the definition of the fields and the Rabi frequencies]. At the end of the second pulse they take the forms: $C_1 \sim \theta_1 + \theta_1 \cos(\Omega_c \tau_d)$ and $C_{2,3} \sim 2\theta_2$ showing that when the delay time τ_d is such that

$$\Omega_c \tau_d = \pi(1 + 2k), \tag{4.1}$$

with k an integer, the population on the level 1 vanishes, while it increases four times on states 2 and 3: The excitation amplitudes of the two pump pulses add coherently for an appropriate delay [92]. Hereafter we assume that the upper-lying levels are harmonic, such that the condition $\omega_{ij}\tau_d = 2\pi k_{ij}$ applies, with k_{ij} an integer and $\omega_{ij} = \omega_j - \omega_i$ the frequency splitting between the upper levels of energies ω_j. This condition is essential to accumulate population in the upper states from pulse to pulse. Therefore, as long as the pulse delay τ_d remains well smaller than the atomic decoherence time, the second pulse allows the selective

excitation of a superposition of states 2 and 3. Our method does not suffer from a high sensitivity to laser-field instabilities. We show below that the efficiency of the process is preserved even when the condition (4.1) is not well satisfied.
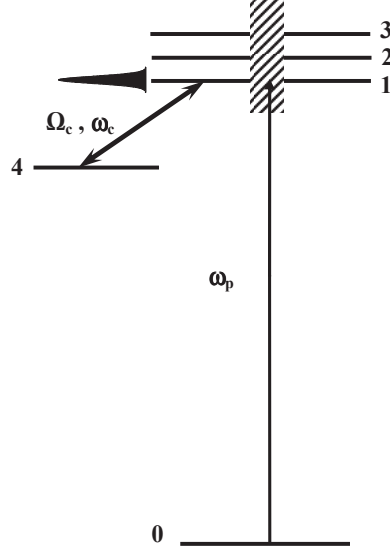

Figure 4.1: Level scheme illustrating the excitation of three upper states by the ultrashort pump laser. A cw coupling field drives the auxiliary transition $1 \rightarrow 4$.

4.1.1 Mechanism of selective excitation

The model

In our scheme (Fig. 4.1), the upper states 1, 2 and 3 are populated via a single photon excitation by a train of m identical and non-overlapping ultrashort laser pulses, whose spectrum is centered on the resonance with the transition $0 \rightarrow 1$ and is wide enough that upon interacting with each pulse, all the states 1, 2 and 3 are excited simultaneously: $T^{-1} \sim \Gamma > \omega_{31}$. Here Γ is the spectral width of the laser fields and ω_{31} is the frequency splitting of the levels 1 and 3. We assume that the narrow-band coupling field is in exact resonance with the transition $1 \rightarrow 4$ with the pulse duration much longer than that of the pump pulses T. In what follows, we neglect the Doppler broadening because it is small as compared to Γ.

The pump $E_p(t)$ and coupling $E_c(t)$ field amplitudes of respective carrier frequencies ω_p

and ω_c are of the form (in complex notation)

$$E_p(t) = \sum_{i=1}^{m} \mathcal{E}_i(t)e^{i\omega_p t}, \quad E_c(t) = \mathcal{E}_c(t)e^{i\omega_c t}, \quad (4.2)$$

with the same shape $f(t)$ for all m pump pulses that determines the time dependence of $\mathcal{E}_i(t) = \mathcal{E}_0 f(t - t_1 - (i-1)\tau_d)$, and the delay τ_d between two consecutive pulses. The interaction of the system with the pump and coupling fields is determined by their Rabi frequencies at the corresponding transitions

$$\Omega_p^{(j)}(t) = \frac{\mu_j}{\hbar}\mathcal{E}_i(t), \quad \Omega_c(t) = \frac{\mu_{14}}{\hbar}\mathcal{E}_c(t), \quad (4.3)$$

where μ_{ij} is the dipole matrix element of the transition $i \to j = 1, 2, 3$ and the notation $\mu_j \equiv \mu_{0j}$. We consider for simplicity a time independent coupling field. Our results generalize for a pulsed coupling field of much longer duration than the pump field. In the rotating wave approximation with respect to the pump field, the Hamiltonian of the system is given by

$$H = -\hbar \sum_{j=1}^{3} \left(\Omega_p^{(j)} \sigma_{j0} - \Delta_j \sigma_{jj} \right) - \hbar\Delta_1 \sigma_{44} - \hbar\Omega_c \sigma_{41} + h.c., \quad (4.4)$$

where $\sigma_{ij} = |i\rangle\langle j|$ are the atomic operators and $\Delta_j = \omega_{j0} - \omega_p$ is two-photon detuning of the pump field from the $0 \to j$, $j = 1, 2, 3$ transition. The state $|\psi(t)\rangle = \sum_i C_i(t)|i\rangle$ of the atom satisfies the Schrödinger equation $\dot{C}_i(t) = -\frac{i}{\hbar}\sum_k \langle i|H|k\rangle C_k(t)$, which leads to the equations for the atomic state amplitudes

$$\dot{C}_0(t) = i \sum_{j=1,2} \Omega_p^{(j)*} C_j(t), \quad (4.5a)$$

$$\dot{C}_1(t) = -i\Delta_1 C_1(t) + i\Omega_p^{(1)} C_0(t) + i\Omega_c C_4(t), \quad (4.5b)$$

$$\dot{C}_{2,3}(t) = -i\Delta_{2,3} C_{2,3}(t) + i\Omega_p^{(2,3)} C_0(t), \quad (4.5c)$$

$$\dot{C}_4(t) = -i\Delta_1 C_4(t) + i\Omega_c^* C_1(t) \quad (4.5d)$$

with the initial conditions

$$C_0(-\infty) = 1, \quad C_{j\neq0}(-\infty) = 0. \quad (4.6)$$

4.1.2 Solution in the impulsive regime

In the general case, Eqs. (4.5) do not provide an analytic solution. However, in the regime of low intensity of the coupling field with respect to the pump fields: $\Omega_c \ll \Omega_p$ and in the impulsive (or sudden) approximation for the ultrashort pump pulse by disregarding the detunings $\Delta_j T \ll 1$ [125], one can determine the solution (see Appendix 4.A). Equations (4.A1)-(4.A5) show the dependence of the state amplitudes after the $(n+1)$-st pulse depending on the amplitudes after the n-th pulse ($n = 1, 2, ...$). For the sequence of two pump pulses right after the interaction with the second pump pulse, Eqs. (4.A1)-(4.A5) lead to

$$C_0(t_2^+) = \cos^2\theta - \frac{1}{\mu^2}\left(\mu_1^2 e^{-i\Delta_1\tau_d}\cos(\Omega_c\tau_d) + \mu_2^2 e^{-i\Delta_2\tau_d} + \mu_3^2 e^{-i\Delta_3\tau_d}\right)\sin^2\theta \qquad (4.7a)$$

$$C_1(t_2^+) = i\frac{\mu_1}{2\mu}\sin 2\theta\left[1 + \frac{1}{\mu^2}\left(\mu_1^2 e^{-i\Delta_1\tau_d}\cos(\Omega_c\tau_d) + \sum_{k=2}^{3}\mu_k^2 e^{-i\Delta_k\tau_d}\right)\right]$$
$$+ \ i\frac{\mu_1}{\mu^3}\sin\theta\left[\left(\sum_{k=2}^{3}\mu_k^2\right)e^{-i\Delta_1\tau_d}\cos(\Omega_c\tau_d) - \left(\sum_{k=2}^{3}\mu_k^2 e^{-i\Delta_k\tau_d}\right)\right] \qquad (4.7b)$$

$$C_2(t_2^+) = i\frac{\mu_2}{2\mu}\sin 2\theta\left[1 + \frac{1}{\mu^2}\left(\mu_1^2 e^{-i\Delta_1\tau_d}\cos(\Omega_c\tau_d) + \sum_{k=2}^{3}\mu_k^2 e^{-i\Delta_k\tau_d}\right)\right]$$
$$+ \ i\frac{\mu_2}{\mu^3}\sin\theta\left\{\mu_1^2\left[e^{-i\Delta_2\tau_d} - e^{-i\Delta_1\tau_d}\cos(\Omega_c\tau_d)\right] + \mu_3^2\left(e^{-i\Delta_2\tau_d} - e^{-i\Delta_3\tau_d}\right)\right\} \qquad (4.7c)$$

$$C_3(t_2^+) = C_{2\leftrightarrow 3}(t_2^+), \qquad (4.7d)$$

$$C_4(t_2^+) = -\frac{\mu_1}{\mu}e^{-i\Delta_1\tau_d}\sin\theta\sin(\Omega_c\tau_d) \qquad (4.7e)$$

with

$$\theta = \frac{\mu}{\hbar}\int \mathcal{E}(t)dt, \quad \mu = \left(\sum_{k=1}^{3}\mu_k^2\right)^{1/2}, \qquad (4.8)$$

and $\int \mathcal{E}(t)dt$ the area of each pump pulse (considered invariant from pulse to pulse). When the upper-lying states 1,2,3 are harmonic such that (i) $\omega_{ij}\tau_d = 2\pi n$, (ii) condition (4.1) is fulfilled, and (iii) the pump pulses are resonant with one of any transitions $0 \to i$, i.e. $\Delta_i = 0$, and implying $\Delta_j\tau_d = 2\pi n_j$ for all j (with n_j an integer) from condition (i), these equations

take the simpler form

$$C_0(t_2^+) = \cos^2\theta - \frac{\mu_2^2 + \mu_3^2 - \mu_1^2}{\mu^2}\sin^2\theta, \tag{4.9a}$$

$$C_1(t_2^+) = 2i\frac{\mu_1}{\mu}\frac{\mu_2^2 + \mu_3^2}{\mu^2}\sin\theta(\cos\theta - 1), \tag{4.9b}$$

$$C_2(t_2^+) = i\frac{\mu_2}{\mu}\Big(\frac{\mu_2^2 + \mu_3^2}{\mu^2}\sin 2\theta + \frac{2\mu_1^2}{\mu^2}\sin\theta\Big), \tag{4.9c}$$

$$C_3(t_2^+) = C_2, (2 \leftrightarrow 3), C_4(t_2^+) = 0. \tag{4.9d}$$

This shows that, in order to cancel out the population transfer to state 1 while increasing the population of states 2 and 3, only the limit of weak pump excitation ($\theta \ll 1$) is suitable since it leads to $\cos\theta - 1 = O(\theta^2)$.

4.1.3 Solution in the perturbative regime

If we consider that each pump pulse is weak: $\Omega_j T \ll 1$, we can perturbatively calculate the solution of Eqs. (4.5) (without invoking explicitly the shortness of the pump pulse). We obtain with correction of order $O(\theta^2)$:

$$C_1(t_{n+1}^+) = i\theta_1 + e^{-i\Delta_1\tau_d}\Big[C_1(t_n^+)\cos(\Omega_c\tau_d) + iC_4(t_n^+)\sin(\Omega_c\tau_d)\Big], \tag{4.10a}$$

$$C_j(t_{n+1}^+) = i\theta_j + e^{-i\Delta_j\tau_d}C_j(t_n^+), \quad j = 2,3 \tag{4.10b}$$

$$C_4(t_{n+1}^+) = e^{-i\Delta_1\tau_d}\Big[iC_1(t_n^+)\sin(\Omega_c\tau_d) + C_4(t_n^+)\cos(\Omega_c\tau_d)\Big] \tag{4.10c}$$

with

$$\theta_j = \frac{\mu_j}{\hbar}\int\mathcal{E}(t)e^{i\Delta_j t}dt \tag{4.11}$$

the Fourier spectral component of the Rabi frequency of the pump pulse at frequency Δ_j. We remark that we recover these equations (4.10) from Eqs. (4.A1)-(4.A5) using $\sin\theta = \theta + O(\theta^3)$ and $\cos\theta = 1 + O(\theta^2)$ except for the phase in the θ_j's that are neglected in the impulsive regime.

⋆ **Selective excitation to a single state [97]**

To excite a single state, say state 1, no control field is required: $\Omega_c = 0$, and the pump needs to be resonant with the target state: $\Delta_1 = 0$. In that case one can determine the

coefficients after n pulses from Eqs. (4.10):

$$C_1(t_n^+) = in\theta_1, \tag{4.12a}$$

$$C_{j=2,3}(t_n^+) = ie^{-i(n-1)\Delta_j\tau_d/2}\frac{\sin(\frac{n}{2}\Delta_j\tau_d)}{\sin(\frac{1}{2}\Delta_j\tau_d)}\theta_j. \tag{4.12b}$$

This shows that population in the target state accumulates linearly as a function of the number of the ultrashort pulses. Population does not coherently accumulate for large n in the other state if one chooses $\Delta_j\tau_d$ *well different from* $2\pi k$, k an integer. This effect is optimal when

$$\Delta_j\tau_d = \pi(1+2k). \tag{4.13}$$

The population transfer to state 1 is closer to 1 when the total area of the pump pulses is 2π. (This value obtained here 2π is due to the definition of the fields (4.2) and the Rabi frequencies (4.3); This corresponds to a "π-pulse" transfer of a single strong field.) The resulting selective excitation is thus very robust with respect to $\Delta_j\tau_d$.

$\star$ Selective excitation to a superposition of states

To excite a superposition of states, one has to impose

$$\Delta_j\tau_d = 2\pi k_j \tag{4.14}$$

with k_j an integer, which leads to

$$C_{j=2,3}(t_n^+) = ie^{-i(n-1)\pi}n\theta_j. \tag{4.15}$$

This condition can be satisfied when the upper-lying states within the bandwidth of a single pulse are harmonic.

We now show that the control field allows to remove the transition to the state to which this control field is resonantly coupled. We choose state 1 to have this feature, i.e. $\Delta_1 = 0$. From Eqs. (4.10), we get after n pulses:

$$C_1(t_n^+) = i\cos\left(\frac{n-1}{2}\Omega_c\tau_d\right)\frac{\sin(\frac{n}{2}\Omega_c\tau_d)}{\sin(\frac{1}{2}\Omega_c\tau_d)}\theta_1, \tag{4.16a}$$

$$C_4(t_n^+) = i\sin\left(\frac{n-1}{2}\Omega_c\tau_d\right)\frac{\sin(\frac{n}{2}\Omega_c\tau_d)}{\sin(\frac{1}{2}\Omega_c\tau_d)}\theta_1. \tag{4.16b}$$
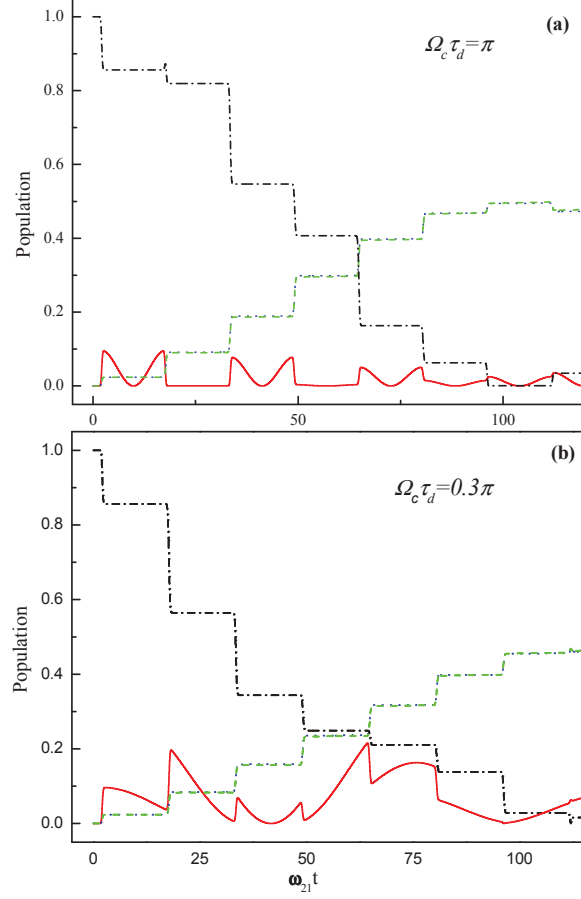
Figure 4.2: Populations of atomic ground state (dash-dotted, black) and upper levels 1 (solid, red), 2 (dotted, blue) and 3 (dashed, green) excited by a train of the pump pulses for $\mu_2 = \mu_3 = 0.5\mu_1, T = 0.3\omega_{21}$ and a) $\Omega_c\tau_d = \pi$; b) $\Omega_c\tau_d = 0.3\pi$.

The populations do not accumulate in states 1 and 4 if one chooses $\Omega_c\tau_d$ *well different from* $2\pi k$, k an integer. This effect is optimal when $\Omega_c\tau_d = \pi(1 + 2k)$ [see condition (4.1)]. The value for $k = 0$ corresponds to a π area, i.e. a "$\pi/2$-pulse", for the control field in this model. We remark that such a cancellation of the transfer to state 1 is thus expected to be robust with respect to a precise area of the control field.

Thus, by choosing the number of the pump-pulses, one can achieve the coherent selective superposition of the levels 2 and 3, while keeping the state 1 almost empty.

In Fig. 4.2a we show the results of numerical integration of Eqs. (4.5) obtained under the conditions mentioned above using Gaussian shape $f(t) = \exp(-t^2/T^2)$ for the pump pulses. Very similar results are obtained, when the condition (4.1) is significantly violated, as shown

in Fig. 4.2b. This demonstrates the robustness of our scheme with respect to the coupling field instabilities as predicted above.
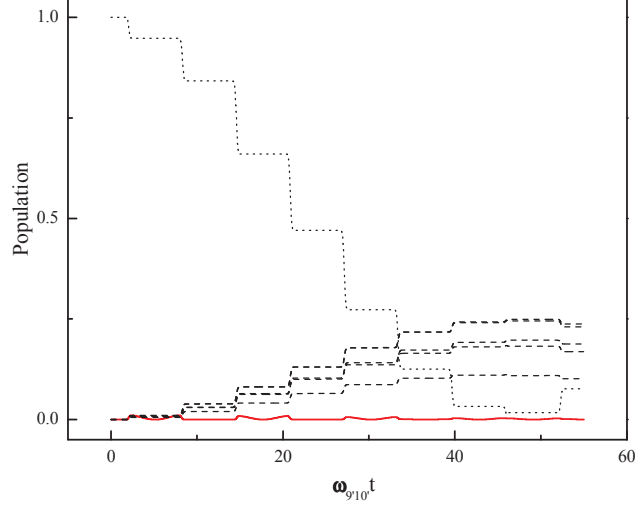

Figure 4.3: Populations of K_2 of the ground state $v'' = 0$ (dotted, black), the upper state $v' = 10$ (solid, red) and the other states $v' = 8, 9, 11, 12, 13$ (dashed lines).

We apply the proposed mechanism in the next subsection to produce a selective coherent superposition of vibrational states in a molecular electronic state.

4.1.4 Application to the potassium dimer

We consider the excitation of the potassium dimer K_2 [126]. The molecule is supposed to be prepared in the ground vibrational state $v'' = 0$ of the electronic state $X^1\Sigma_g^+$. The excited state is chosen to be the first excited electronic state $A^1\Sigma_u^+$ (of lifetime 28ns). For simplicity in the calculations the dependence of the electric dipole moment on internuclear distance is ignored. The pump pulses are assumed to be transform limited of Gaussian envelope $f(t) = \exp(-t^2/T^2)$ with duration $T = 150$fs and peak intensity $I_p^{\max} \sim 10^{11}$ W/cm^2. We assume the pump pulses to be on resonance with the transition $v'' = 0 \rightarrow v' = 10$ ($\omega_L \simeq 11800cm^{-1}$). The excited vibrational levels $v' = 8, 9, ..., 13$ are within the spectrum of the pump field and are expected to be populated. Our main goal is to suppress the strongest transition $v' = 10$ of the upper vibrational levels.
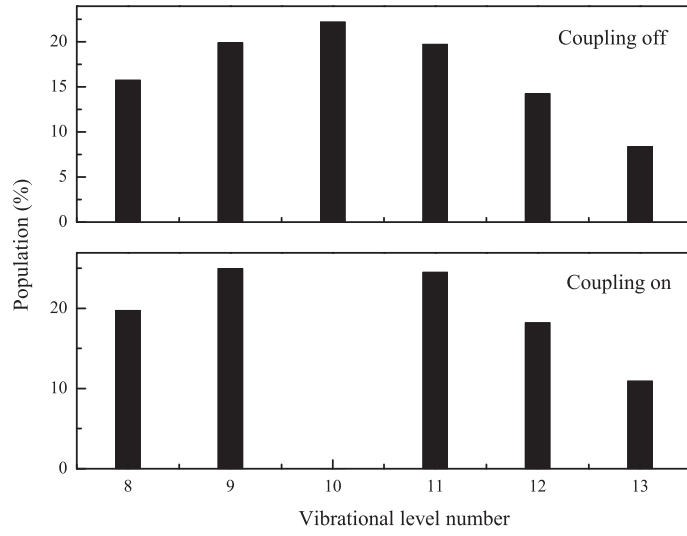
Figure 4.4: Histogram of the vibrational population distribution after excitation without (upper frame) and with (lower frame) the coupling field.
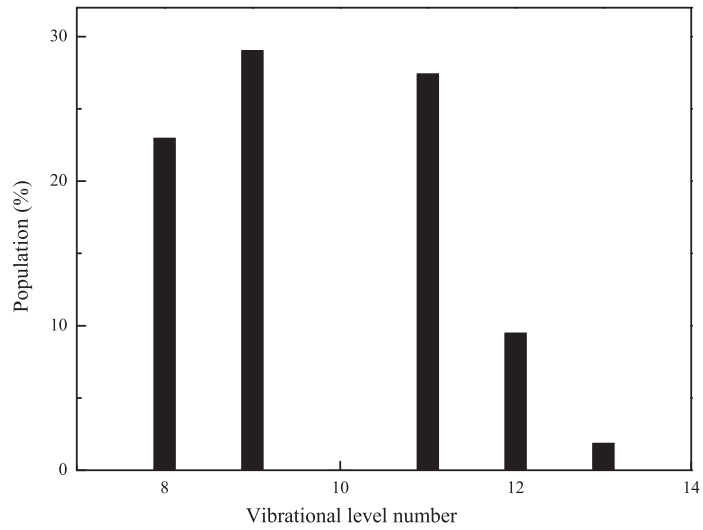

Figure 4.5: Histogram of the vibrational population distribution after excitation by the same pulses used in Fig. 4.4 but of duration 600 fs.

We solve numerically equations for atomic population amplitudes similar to Eq. (4.5), including all the relevant vibrational states of the problem, using the above parameters, and

with the requirement that the conditions (4.1) and $\omega_{9'10'} = 2\pi k \tau_d$ are fulfilled, where $\omega_{9'10'}$ is the frequency splitting of the vibrational states $v' = 9$ and $v' = 10$ of the upper electronic state. For $\omega_{9'10'} = 67.3\text{cm}^{-1}$ the delay time between the subpulses is $\tau_d \simeq 3\text{ps}$. Note, that frequency splitting of the upper lying levels is almost equidistant. The coupling field couples the state $v' = 10$, of largest dipole moment element among the states within the bandwidth of a single pump, with an auxiliary electronic state of the potassium dimer, e.g. $b^3\Pi_u$. Figure
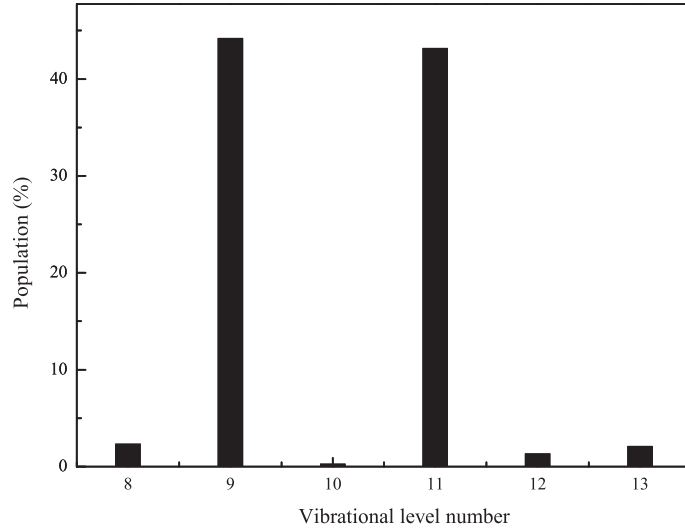

Figure 4.6: Histogram of the vibrational population distribution when the states $v' = 8, 10, 12, 13$ are coupled to auxiliary states by coupling fields.

4.3 shows the dynamics of the populations of the vibrational levels, when it is excited by a train of identical pulses. To calculate the populations we have used the Franck-Condon factors and the corresponding eigenfrequencies, which are well known for vibrational levels of K_2 molecules [126]. The chosen values of the parameters: $\Omega_c \simeq 0.2\omega_{9'10'} \ll \Omega_p^{max} \simeq 0.6\omega_{9'10'}$ and $\theta^2(\infty) \sim 0.15$ provide all the necessary conditions for the analytical analysis made in the previous section to be valid. As it is seen in Fig. 4.3, after the interaction of the molecule with 8 pulses, all the population is distributed between the upper vibrational levels $v' = 8, 9, 11, 12, 13$ (dotted lines), while the level $v' = 10$ (red, solid line) stays almost unpopulated. To have a more complete picture of the process, Fig. 4.4 displays the histogram

of the population distribution in the upper-lying states. In the absence of the coupling field the population is distributed between all upper vibrational states (Fig. 4.4 upper frame). But if the coupling field is on (Fig. 4.4 lower frame), the strongest transition is dramatically suppressed. Adapting the duration of the pulses allows one to modify the shape of the superposition, reducing the population of the upper states, as it is shown in Fig. 4.5. Here the duration of the pump pulses are taken to be four times larger than that of the cases considered previously. To suppress some components of the superposition one can apply other fields coupled to the undesired states from different auxiliary states. As an example in Fig. 4.6 the levels $v' = 8, 10, 12, 13$ are coupled with other molecular states which leads to a coherent superposition of only two states $v' = 9, 11$. Thus, we have shown that the coupling fields allow the decreasing of the populations of the undesired states and the enhancement of the populations of the other states well within the bandwidth of a single pump.

4.2 Selective excitation of atoms and molecules by fs strong laser pulses

Now we discuss a method for selective population transfer in multilevel systems with a model atom with the doublet of neighboring upper states. We suppose the upper levels of the atom are excited by the two-photon interaction with the fs pump pulse, frequency spectrum of which overlaps both the upper states 1 and 2 (Fig.4.7), while a narrow-band powerful laser couples the first upper level with a metastable auxiliary state 3. We assume that the atoms are initially in the ground state 0. The coupling field is strong enough to shift the level 1 out of the spectrum of pump pulse, and therefore it is not populated. Due to large detuning of the coupling field from $3 \rightarrow 2$ transition, the second upper level 2 is populated normally or even more compared to the case, when the coupling field is absent. This method allows one to decouple the strongest transition and enhance the other ones.

In the next subsection, we discuss our mechanism of selective excitation for model atom
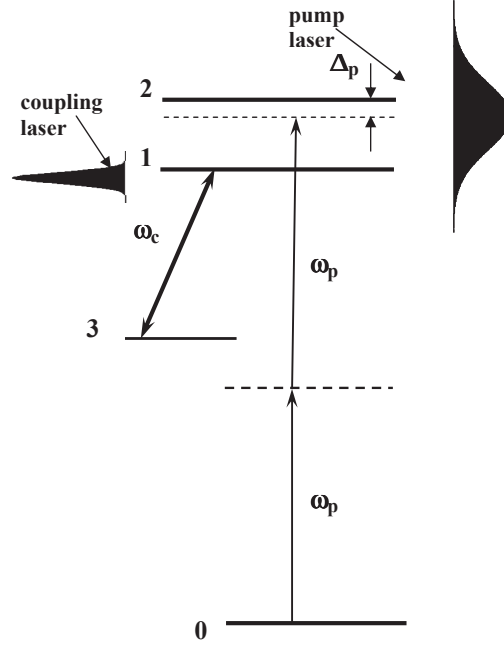
Figure 4.7: Level scheme of model atom illustrating two-photon excitation of two upper eigenstates by ultrashort pump laser and interaction with coupling field on the auxiliary transition $1 \to 3$.

in Fig.4.7 and derive the basic equations of the system. Then we represent graphically the temporal behavior of atomic state populations demonstrating a strong reduction of the population of the state 1, when the coupling field is switched on.

4.2.1 The model of the atom and basic equations

We start from the consideration of two-photon interaction of the atoms depicted in Fig. 4.7 with an ultrashort pump laser pulse, whose spectrum is wide enough to excite both upper levels simultaneously: $T \ll \omega_{2,1}^{-1}$, where T is the duration of the pump field and ω_{21} is the frequency splitting between the states 1 and 2. We neglect the Doppler broadening because it is small as compared to T^{-1}. On the transition $3 \to 1$ the atom interacts resonantly with a narrow-band coupling laser with duration T_c much larger compared to that of the pump pulse: $T_c \gg T$.

The amplitudes of the pump and coupling fields $E_{p,c}(z,t)$, propagating along the z-axis

with wave vectors $k_{p,c}$ and the carrier frequencies $\omega_{p,c} = k_{p,c}c$ are represented in the form

$$E_p(z,t) = \mathcal{E}_p(z,t)\exp[i(k_p z - \omega_p t)], \tag{4.17}$$

$$E_c(z,t) = \mathcal{E}_c(z,t)\exp[i(k_c z - \omega_c t)], \tag{4.18}$$

respectively, where the time dependence of $\mathcal{E}_{p,c}(z,t) = \mathcal{E}_{p,c}(t - z/c)$ determines the pulse shapes. The interaction of the atom with the laser fields is determined by their Rabi frequencies at the corresponding transitions:

$$\Omega_p^{(j)} = \frac{r_j}{\hbar}\mathcal{E}_p^2 \quad (j = 1, 2), \tag{4.19}$$

$$\Omega_c = \frac{\mu_{13}}{\hbar}\mathcal{E}_c, \tag{4.20}$$

where

$$r_j = \sum_n \frac{\mu_{jn}\mu_{n0}}{\hbar(\omega_{n0} - \omega_p)} \tag{4.21}$$

is the matrix element for the two-photon transition $0 \to j$ from the ground state $|0\rangle$ with ω_{ij} the frequency of atomic transition $i \to j$ and μ_{ij} the dipole moment between a pair of states i and j. In the rotating wave approximation, the interaction Hamiltonian of the system is given by

$$H_I = -\hbar e^{2ik_p z}\sum_{j=1,2}\Omega_p^j \sigma_{j0}e^{i\Delta_j t} - \hbar e^{ik_c z}\Omega_c\sigma_{31} + h.c., \tag{4.22}$$

where $\sigma_{ij} = |i\rangle\langle j|$ are the atomic operators and $\Delta_j = \omega_{j0} - 2\omega_p$ is two-photon detuning of pump field from the $0 \to j$ transition, which, however, can be neglected in further calculations thanks to the condition $T\omega_{21} \ll 1$. The state of the atom is described by the wave function

$$\psi(z,t) = \sum_{i=0}^{3} C_i(z,t)|i\rangle, \tag{4.23}$$

where $C_i(z,t)$ is the amplitude of the ith atomic state, satisfying the equation

$$\dot{C}_i(z,t) = -\frac{i}{\hbar}\sum_k H_{ik}C_k(z,t). \tag{4.24}$$

Our purpose is to obtain the population of the states 1 and 2 in the presence of the coupling field and determine the conditions of selective excitation of state 2. In the case
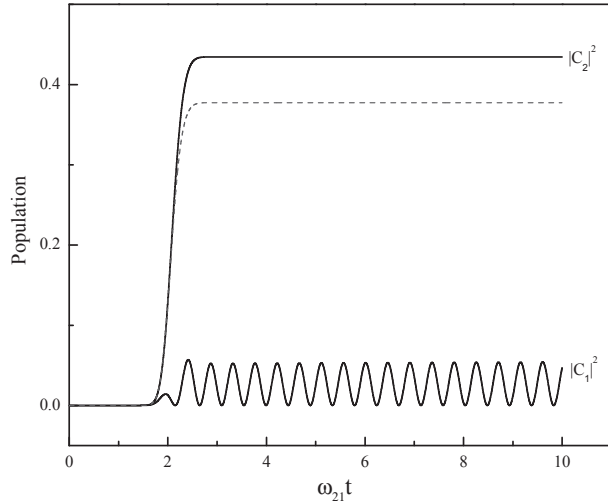
Figure 4.8: Populations of the atomic states 1 and 2 for $\Omega_c = 5\omega_{21}$ and $r_1 = r_2$. In the absence of coupling field, the populations of the states 1 and 2 are equal (dashed gray line).

of ultrashort laser pulses Eq. (4.24) can be solved only numerically that we have carried out for different values of the parameters. An example is shown in Fig.4.8 for the pump field with duration $\omega_{21}T = 0.3$ and for equal dipole moments of the transitions $0 \to 1$ and $0 \to 2$. The Rabi frequencies of coupling and pump pulses is taken to be $\Omega_c = 5\omega_{21}, \Omega_p = \omega_{21}$, respectively. As is seen, the states 1 and 2 are equally populated when the coupling field is off. However, in the presence of coupling field the state 1 is almost unpopulated and characteristic Rabi oscillations arise between the states 1 and 3, while the population of state 2 is weakly enhanced. Thus, by applying a strong coupling field, the effective selective excitation of level 2 is achieved. In addition, for ultrashort laser pulses, as is the case here, this scheme is robust to any relaxation noise. Besides, in order to avoid the effect of the laser phase fluctuations on the creation of atomic coherence between the states 0 and 3, we assume that the pump and coupling lasers are phase-locked. In this case, after the pump pulse passed through the medium, the phase fluctuations of the coupling laser smooth out the oscillations in population of the level 1, but apparently do not affect the excitation of level 2.

An important question arises how this mechanism can be verified experimentally. We discuss this question in the next section.

4.3 Quantum beats in SERS of ultrashort laser pulses

Laser fields having a wide spectrum can simultaneously excite a large number of close-lying upper levels of atoms or molecules, thus forming a coherent superposition of two or more atomic eigenstates, i.e. WPs. They can be observed in a fluorescence signal or in pumpprobe experiments. In these experiments, a first, pump, laser pulse generates a WP in an atom or molecule, which is then observed by a second pulse coming with a certain delay time τ_d. In this case, due to the Ramsey-type interference [100] of the two atomic WPs generated by the pump and probe pulses, periodic change or quantum beats appear in the dependence of the detected signal on τ_d. The frequencies of these beats are proportional to the differences between the energies of atomic or molecular excited states. The QB technique has been applied successfully for the determination of small frequency shifts, in particular, for the measurement of fine and hyperfine splitting of upper lying atomic levels [101].

To study QBs in the Stokes radiation generated in the SERS process, we consider a simple model of a four-level atom with a doublet of the upper levels. The analytical solutions obtained describe qualitatively well the observed features of the effect under discussion.

4.3.1 The model of the atom and basic equations

Let consider the interaction of a four-level atom having the configuration of energy levels shown in Fig.4.9 with two consequent ultrashort laser pulses, whose duration T is much shorter than the inverted frequency splitting ω_{21} between levels 1 and 2: $T \ll \omega_{21}$. Thus, upon the interaction of the atom with each of the pulses, two transitions $0 \rightarrow 1$ and $0 \rightarrow 2$ are excited simultaneously. In what follows, we neglect the Doppler broadening because it is small as compared to T^{-1}.

The field amplitudes of the pump $E_p(z,t)$ and probe $E_{pr}(z,t)$ pulses, propagating along the z-axis with wave vectors $k_p = k_{pr} = k_L$ and the carrier frequency $\omega_p = \omega_{pr} = \omega_L = k_L c$, are represented in the form

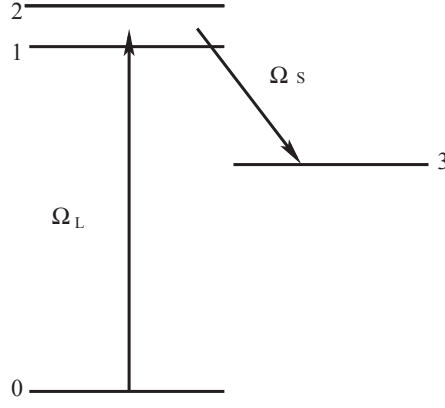$$E_{p,pr}(z,t) = \mathcal{E}_{p,pr}(z,t) \exp[i(k_L z - \omega_L t), \tag{4.25}$$

Figure 4.9: Scheme of the interaction of four-level atom with laser and Stokes fields.

where the time dependence of $\mathcal{E}_{p,pr}(z,t) = \mathcal{E}_{p,pr}(t - z/c)$ is determined by the pulse shapes, while the maximum of the probe field $\mathcal{E}_{pr}(z,t)$ is shifted with respect to that of $\mathcal{E}_p(z,t)$ by the delay time τ_d.

The interaction of the atom with the laser fields is determined by their Rabi frequencies at the corresponding transitions

$$\Omega_{p,pr}^{(j)} = \mu_{0j}\mathcal{E}_{p,pr}(t)/\hbar, \quad j = 1, 2, \tag{4.26}$$

where μ_{nl} is the dipole moment between a pair of states n and l.

The Stokes radiation is generated in the forward direction of propagation of the laser pulse simultaneously at the transitions $1 \rightarrow 3$ and $2 \rightarrow 3$. The total Stokes field can be represented in the form

$$E_S(z,t) = \mathcal{E}_S(z,t)\exp[i(k_S z - \omega_S t), \tag{4.27}$$

with the carrier frequency ω_S and the wave vector $k_z || z$. Its Rabi frequencies for the transitions $1 \rightarrow 3$ and $2 \rightarrow 3$ can be determined as

$$\Omega_S^{(j)}(z,t) = \mathcal{E}_S(z,t)\mu_{i,3}/\hbar, \quad i = 1, 2. \tag{4.28}$$

It should be noted that a contribution can also be made by the stimulated resonance radiation at the frequency of the exact resonance between the transitions $1 \rightarrow 3$ and $2 \rightarrow 3$. However, this contribution is usually small [127] and, in addition, this radiation is always generated with some delay with respect to the laser pulse. The delay is longer than 100ps at an atomic

81

number denisty of $10^{15} - 10^{16}$cm^{-3} and laser power of 10GW, while QBs are observed in a time interval of several picoseconds, so, in the following, we will discuss only SERS.

In a frame rotating with the laser and Stokes field frequencies, the Hamiltonian of the system is given by

$$H = -\hbar\Big\{[\Omega_p^{(1)}(t) + \Omega_{pr}^{(1)}(t)]e^{i\Delta_{L1}t}\sigma_{10} + [\Omega_p^{(2)}(t) + \Omega_{pr}^{(2)}(t)]e^{i\Delta_{L2}t}\sigma_{20}$$

$$-e^{ik_S z}\mathcal{E}_S\sum_{j=1}^{m}\mu_{js}\sigma_{js}e^{i\Delta_j t} - e^{ik_{UV}z}\mu_{sg}\mathcal{E}_{UV}\sigma_{sg} + h.c.\Big\} \tag{4.29}$$

where $\sigma_{ij} = |i\rangle\langle j|$ are the atomic operators and $\Delta_{Lj} = \omega_{j0} - \omega_L, \Delta_{Sj} = \omega_{j3} - \omega_S, j = 1, 2$ are detuning of laser fields from the atomic resonances.

The state of the atom is described by the wave function (4.23) with $C_i(z, t)$ the amplitude of the ith atomic state satisfying the equation (4.24). The Stokes field can be found from the Maxwell equation

$$\left(\frac{\partial}{\partial z} + \frac{1}{c}\frac{\partial}{\partial t}\right)\mathcal{E}_S(z, t) = 2i\pi\frac{\omega_S}{c}\sum_{j=1}^{2}P^j(z, t), \tag{4.30}$$

where the polarization of the medium at the transition $j \to 3, (j = 1, 2)$ is

$$P_j(z, t) = \mu_{j3}NC_j(t)C_3^*(z, t)C_j(t)e^{-i\Delta_{Sj}t}. \tag{4.31}$$

Here N is the atomic number density. Eqs. (4.30) and (4.24) along with Hamiltonian (4.29) describe the evolution of the system in the field of two laser pulses. Our task is to find the intensity of the Stokes field after switching off the probe pulse as a function of the delay time τ_d. In the general case, the equations for the amplitudes C_j have the following form:

$$\dot{C}_0(t) = i\sum_{j=1}^{2}(\Omega_p^{j*} + \Omega_{pr}^{j*})C_j(t)e^{-i\Delta_{Lj}t},$$

$$\dot{C}_j(t) = i(\Omega_p^j + \Omega_{pr}^j)C_0(t)e^{i\Delta_{Lj}t} + i\Omega_S^{(j)}C_3 e^{i\Delta_{Sj}t}, \tag{4.32}$$

$$\dot{C}_3(z, t) = i\sum_{j=1}^{2}\Omega_S^{(j*)}C_j(t)e^{-i\Delta_{Sj}t}.$$

In the region of the atom interaction with the pump pulse, Eqs. (4.32) are solved on the assumption that the atoms were in the ground state $|0\rangle$ before the pump field was turned on; this is, $C_i(-\infty) = 0, i = 1, 2, 3$. We suppose that the Stokes field, although being stimulated,

is not so strong to change markedly the populations of the upper levels 1 and 2 while pump and probe fields are acting. Then taking $\Omega_S^{(j)} = 0$ in Eqs. (4.32), the solution of latter is obtained from (4.A1)-(4.A5) when $\Omega_c = 0$, $C_3 = C_4 = 0$ and $n = 2$, which corresponds to interaction of atoms or molecules with two pump and probe pulses.

$$
\begin{aligned}
C_0(t) &= \cos\theta_p(\infty)\cos\theta_{pr}(t) - \sin\theta_p(\infty)\sin\theta_{pr}(t)\left(\frac{\Omega_{pr}^{(1)2}}{\Omega^2}e^{-i\Delta_{L1}t} + \frac{\Omega_{pr}^{(2)2}}{\Omega^2}e^{-i\Delta_{L2}t}\right) \\
C_j(t) &= i\frac{\Omega_{pr}^{(j)}}{\Omega_{pr}}[\cos\theta_p(\infty)\sin\theta_{pr}(t) + \sin\theta_p(\infty)\cos\theta_{pr}(t) \\
&\quad * \left(\frac{\Omega_{pr}^{(1)2}}{\Omega^2}e^{-i\Delta_{L1}t} + \frac{\Omega_{pr}^{(2)2}}{\Omega^2}e^{-i\Delta_{L2}t}\right)],
\end{aligned}
\tag{4.33}
$$

where $j = 1, 2$, $\theta_{p,pr}(t) = \int_{-\infty}^{t}\Omega_{p,pr}(t')dt'$ are areas of the pump and probe fields, respectively, and $\Omega_{p,pr} = \sqrt{\Omega_{p,pr}^{(1)2} + \Omega_{p,pr}^{(2)2}}$. Here we suppose the pump and probe pulses have different amplitudes, but the same temporal shape, so that $\Omega_p^{(1,2)}/\Omega_p$ and $\Omega_{pr}^{(1,2)}/\Omega_{pr}$ are equal. It's easy to check that $\sum_{j=0}^{2}|C_j|^2 = 1$. This fact is a consequence of the above assumption about the smallness of the Stokes field, whose generation does not change the population of the levels 1 and 2.

Having the solution of the amplitudes for the atomic states, we can find from Eqs. (4.30) and (4.32) the Stokes field generated by the probe pulse. In the wave variables z and $t - z/c$, these equations take the form

$$
\frac{\partial \mathcal{E}_S}{\partial z} = 2i\pi\frac{\omega_S}{c}\sum_{j=1}^{2}\mu_{j3}C_j(\tau)e^{-i\Delta_{Sj}\tau}C_3^*(z,t),
\tag{4.34a}
$$

$$
\frac{\partial C_3}{\partial \tau} = \frac{i}{\hbar}\mathcal{E}_S^*\sum_{j=1}^{2}\mu_{j3}C_j(\tau)e^{-i\Delta_{Sj}\tau},
\tag{4.34b}
$$

where $C_{1,2}(\tau)$ are determined in (4.33). Note that it follows from Eq. (4.34b) with the initial condition $C_3(z, -\infty) = 0$ that the amplitude C_3 is nonzero only in the vicinity $\tau \sim \tau_d$, where the probe field is maximum. Therefore, in what follows, τ can be replaced with τ_d in the exponential factors $e^{-i\Delta_{S1,2}\tau}$. The solution of Eqs.(4.34) with the boundary condition $\mathcal{E}_S(0,\tau) = \mathcal{E}_S(\tau)$ is found in a way similarly to the method described in the Appendix 4.B,

and, for the Stokes field, it has the form

$$\mathcal{E}_S(z,\tau) = \mathcal{E}_S(\tau) + 2zq\sum_{j=1}^{2}\mu_{j3}C_j(\tau)e^{-i\Delta_{Sj}\tau_d}\int_{-\infty}^{\tau}\sum_{j=1}^{2}\mu_{j3}C_j(\tau')e^{-i\Delta_{Sj}\tau_d}I_1(\psi)\psi^{-1}(\tau',\tau)d\tau',$$

(4.35)

where $q = 2\pi\omega_S N/c\hbar$, $I_1(x)$ is the modified first-order Bessel function,

$$\psi(\tau',\tau) = 2\left\{qz\int_{\tau'}^{\tau}\mid\mu_{13}C_1(\tau'')e^{-i\Delta_{S1}\tau_d} + \mu_{23}C_2(\tau'')e^{-i\Delta_{S2}\tau_d}\mid d\tau''\right\}^{1/2}.$$

(4.36)

Since the Stokes radiation is generated from spontaneous noise and/or from quantum fluctu-ations, $\mathcal{E}_S(\tau)$ has the correlation function

$$\frac{c}{2\pi}\langle\mathcal{E}_S(\tau)\mathcal{E}_S^*(\tau')\rangle = \frac{J_{sp}}{\Gamma_s}\delta(\tau - \tau')$$

(4.37)

where J_{sp} is the intensity of the spontaneous noise and Γ_s is the width of the Stokes radiation. For the intensity of the Stokes field taking into account Eq. (4.37), we find

$$J_S(z,\tau) = 4zqJ_{sp}\Gamma_s^{-1}|\mu_{13}C_1(\tau) + \mu_{23}C_2(\tau)e^{i\omega_{21}\tau_d}|^2 + 4z^2q^2J_{sp}\Gamma_s^{-1}|\mu_{13}C_1(\tau)$$

$$+\mu_{23}C_2(\tau)e^{i\omega_{21}\tau_d}|^2\int_{-\infty}^{\tau}d\tau'|\mu_{13}C_1(\tau) + \mu_{23}C_2(\tau)e^{i\omega_{21}\tau_d}|^2 I_1^2(\psi)\psi(\tau',\tau).$$

(4.38)

Here the first term is the contribution of the Raman scattering, which is proportional to the path length. The second term describes the SERS, whose contribution becomes prevalent in the range of high amplification, where $\psi(\tau',\tau) \gg 1$. If this condition is fulfilled, in Eq. (4.38), we can pass to the asymptotic form $I_1^2(x) \to e^{2x}/2\pi x$ and approximate $\psi(\tau',\tau) \sim \psi(-\infty,\tau)$. Then, for the intensity of the Stokes field at the exit from the medium ($z = L$), we have

$$J_S(L,\tau) = LqJ_{sp}\Gamma_s^{-1}|\mu_{13}C_1(\tau) + \mu_{23}C_2(\tau)e^{i\omega_{21}\tau_d}|^2 e^{2\psi(-\infty,\tau)}/2\pi\psi(-\infty,\tau).$$

(4.39)

In the experiment, the Stokes signal is measured,

$$\int_{\tau_d-T/2}^{\tau_d+T/2}J_S(\tau)d\tau \sim J_S(\infty)T.$$

(4.40)

It is taken into account here that the range $\tau \geq \tau_d$ is the major contributor to the integral. The following section presents the numerical calculations of the intensity of the Stokes signal $J_S(\tau)$ as a function of the delay time τ_d.

4.3.2 Results

The pump-probe scheme, along with the detection of the signal of the coherent Stokes radiation, has femtosecond time resolution with an extremely high signal-to-noise ratio due to the exponential amplification of the Stokes intensity, as is seen from Eq. (4.39). It is this that is the qualitative difference between the approach considered and the techniques of QB observation in resonance fluorescence or in a photoionization signal, which do not have exponential amplification. The normalized intensity of the Stokes radiation $J_S/(Lq\Gamma_s^{-1})$ is shown
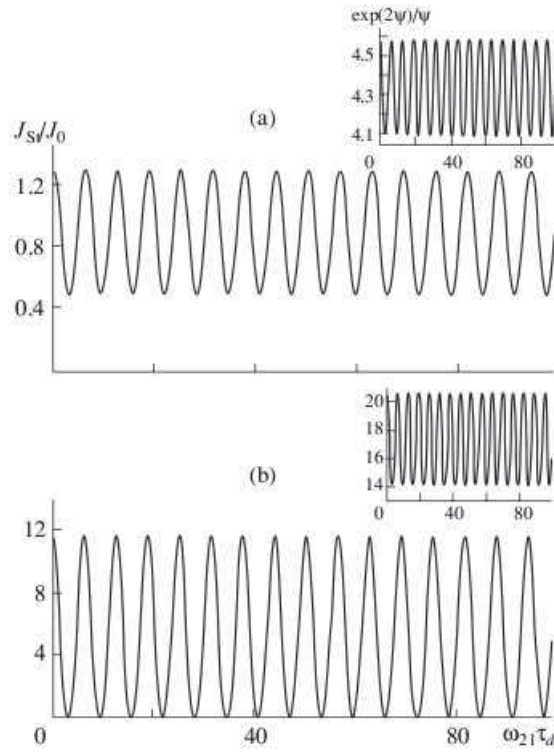
Figure 4.10: Level scheme of atoms illustrating two-photon excitation of a manifold of upper structure containing m atomic eigenstates and generation of the Stokes and UV fields on the basis of hyper-Raman scattering and four-wave mixing, respectively.

in Fig. 4.10 as a function of τ_d for different values of the dipole matrix elements μ_{31} and μ_{32}. Despite the simplicity of the model considered, the results obtained reconstruct qualitatively well the experimentally observed features [105, 106]. First, the QB frequency in the Stokes signal is equal to the frequency difference between the excited levels 1 and 2. Second, the

beat depth achieves 100% if the excited transition dipole moments satisfy the condition

$$\mu_{02}/\mu_{32} = \mu_{01}/\mu_{31} = 1 \qquad (4.41)$$

but it is much smaller if this relation is violated. It is very important that the factor $\exp(2\psi)/\psi$ in Eq. (4.39), being a periodic function with the same frequency ω_{21} (shown in the insets in Fig. 4.10), not only amplifies the signal but also increases the contrast of the oscillations.

4.4 Quantum beats in UV generation by ultrashort laser pulses via four-wave mixing

From practical point of view it is preferable to observe QBs in the intensities of Stokes and UV fields generated on the basis of HRS and FWM [108], respectively. In [107] the QB in the Stokes signal at a wavelength $\lambda \sim 4 \div 8\mu$m was used for detection of the motion of atomic fragments in the dissociation of diatomic molecules. Experiments in this field are in further progress [128, 129], while the theory of quantum beating in HRS and FWM was firstly developed in [136, 137] and is given below.

4.4.1 The model of the atom and equations of motion

We consider two-photon interaction of the atoms having a level configuration shown in Fig. 4.11 with two consecutive ultrashort laser pulses of wide spectrum, which overlap all states in the excited manifold: $\Gamma \geq \omega_{m,1}$, where Γ is the spectral width of the laser fields and $\omega_{m,1}$ is the frequency splitting between the extreme states m and 1. Hence, upon interacting of the atoms with each of the pulses, all the states $j = 1, ...m$ within the manifold are excited simultaneously thus producing an atomic WP, whose properties depend on the laser phase coherence. In what follows, here as well we neglect the Doppler broadening because it is small as compared to Γ.
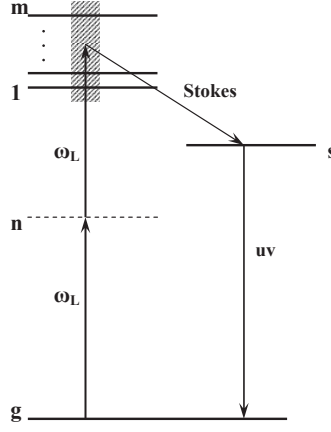
Figure 4.11: Level scheme of atoms illustrating two-photon excitation of a manifold of upper structure containing m atomic eigenstates and generation of the Stokes and UV fields on the basis of hyper-Raman scattering and four-wave mixing, respectively.

The interaction of the atom with the laser fields (4.17) is determined by their Rabi frequencies at the corresponding transitions

$$\Omega_{p,pr}^{(j)} = \frac{r_j}{\hbar} \mathcal{E}_{p,pr}^2,$$
(4.42)

where

$$r_j = \sum_n \frac{\mu_{jn}\mu_{ng}}{\hbar(\omega_{ng} - \omega_L)}$$
(4.43)

is the matrix element for two-photon transition $g \to j$ from the ground state $|g\rangle$ with ω_{nl} the frequency of atomic transition $n \to l$ and μ_{nl} the dipole moment between a pair of states n and l.

The total Stokes field, which is generated simultaneously on the transitions $j \to s$, and UV radiation emitted on the transition $s \to g$ are defined as

$$E_{S,UV}(z,t) = \mathcal{E}_{S,UV}(z,t) \exp[i(k_{S,UV}z - \omega_{S,UV}t),$$

with the carrier frequency ω_S and ω_{UV} and the projection $k_{S,UV} = \vec{k}_{S,UV}\hat{e}_z$ of the wave-vectors $\vec{k}_S$ and $\vec{k}_{UV}$ on the z-axis, respectively.

In a frame rotating with the laser and Stokes field frequencies, the Hamiltonian of the

system is given by

$$H = -\hbar e^{2ik_L z} \sum_{j=1}^{m} (\Omega_p^j + \Omega_{pr}^j) \sigma_{jg} e^{i\Delta_j t} - e^{ik_S z} \mathcal{E}_S \sum_{j=1}^{m} \mu_{js} \sigma_{js} e^{i\Delta_j t} - e^{ik_{UV} z} \mu_{sg} \mathcal{E}_{UV} \sigma_{sg} + h.c. \quad (4.44)$$

where $\Delta_j = \omega_{jg} - 2\omega_L = \omega_{js} - \omega_S$ is two-photon detuning of laser fields from the $g \to j$ transition, as well as the detuning of Stokes field from the $s \to j$ transition. We assume that the spectrum of UV radiation is localized at the exact resonance $\omega_{UV} = \omega_{sg}$. The amplitude $C_i(z,t)$ of the ith atomic state satisfy the equation (4.24).

We neglect the laser field depletion and as in Section 4.3.1 we suppose that the Stokes field is not so strong to change markedly the populations of the excited states. This means that only the amplitude of the Raman state $|s\rangle$ depends on the propagation distance. Then, using the slowly varying envelope approximation, we obtain the following propagation equations for the Stokes and UV field amplitudes

$$\left(\frac{\partial}{\partial z} + \frac{1}{c} \frac{\partial}{\partial t} \right) \mathcal{E}_S(z,t) = 2i\pi \frac{\omega_S}{c} \sum_{j=1}^{m} P_S^{(j)}(z,t) \quad (4.45a)$$

$$\left(\frac{\partial}{\partial z} + \frac{1}{c} \frac{\partial}{\partial t} \right) \mathcal{E}_{UV}(z,t) = 2i\pi \frac{\omega_{UV}}{c} e^{i\Delta k z} P_{UV}(z,t), \quad (4.45b)$$

where the polarizations $P_S^j(z,t)$ at the Stokes transitions $j \to s$ and $P_{UV}(z,t)$ at the UV frequency are given by

$$P_S^j(z,t) = \mu_{js} N C_j(t) \tilde{C}_s^{\ *}(z,t) e^{-i\Delta_j t}, \quad (4.46a)$$

$$P_{UV}(z,t) = \mu_{gs} N \tilde{C}_s(z,t) \tilde{C}_g^{\ *}(t), \quad (4.46b)$$

with $\Delta k = 2k_L - k_S - k_{UV}$ the wave-vector mismatch. Here the propagation phase-factors are included in the ground and Raman state amplitudes by $\tilde{C}_g = C_g e^{2ik_L z}$ and $\tilde{C}_s = C_s e^{ik_S z}$.

Under the adopted approximations we obtain the following equations for atomic state amplitudes

$$\dot{\tilde{C}}_g(t) = i \sum_{j=1}^{m} (\Omega_p^{j*} + \Omega_{pr}^{j*}) C_j(t) e^{-i\Delta_j t} \quad (4.47a)$$

$$\dot{C}_j(t) = i(\Omega_p^j + \Omega_{pr}^j) \tilde{C}_g(t) e^{i\Delta_j t} \quad (4.47b)$$

$$\dot{\tilde{C}}_s(z,t) = \frac{i}{\hbar} \mathcal{E}_S^*(z,t) \sum_{j=1}^{m} \mu_{js} C_j(t) e^{-i\Delta_j t} + \frac{i\mu_{sg}}{\hbar} \mathcal{E}_{UV}(z,t) \tilde{C}_g(t) e^{-i\Delta k z} \quad (4.47c)$$

which are subject to the initial conditions $C_g(-\infty) = 1$ and $C_l(-\infty) = 0$, $l \neq g$.

Equations (4.45)-(4.47) describe the evolution of the system in the field of the two laser pulses. Our task is to find the intensity of UV light as a function of time delay τ_d after switching on the probe pulse.

4.4.2 Solution of the basic equations

Here we obtain the general solution of Eqs.(4.45a),(4.45b) accounting for the phase fluctuations of laser fields. We note complexity of the density matrix approach, which does not provide an analytic solution for the field amplitudes, therefore it is convenient to find first this solution in terms of the atomic state amplitudes and then to express the final expressions through the elements of density matrix, which can then easily be averaged over the laser fluctuations.

In wave variables z and $\tau = t - z/c$ the Eqs.(4.45a),(4.45b) and (4.47c) are reduced to

$$\frac{\partial \mathcal{E}_S}{\partial z} = 2i\pi N \frac{\omega_S}{c} f(\tau) \tilde{C}_s{}^*, \qquad \frac{\partial \mathcal{E}_{UV}}{\partial z} = 2i\pi N \frac{\omega_{UV}}{c} g^*(\tau) \tilde{C}_s \qquad (4.48)$$

$$\dot{\tilde{C}}_s = \frac{i}{\hbar} f(\tau) \mathcal{E}_S^* + \frac{i}{\hbar} g(\tau) \mathcal{E}_{UV} \qquad (4.49)$$

where

$$f(\tau) = \sum_{j=1}^{m} \mu_{js} C_j(\tau) e^{-i\Delta_j \tau}, \qquad g(\tau) = \mu_{sg} \tilde{C}_g(\tau) \qquad (4.50)$$

and the phase matching condition $\Delta k = 2k_L - k_S - k_{UV} = 0$ is assumed to be fulfilled in the medium. The solution of Eqs.(4.48), (4.49) with the boundary condition $\mathcal{E}_S(0, \tau) = \mathcal{E}_S(\tau)$ is found in the Appendix 4.B, which for UV field has the form

$$\mathcal{E}_{UV}(z, \tau) = -qzg^*(\tau) \int_{\tau_d - T/2}^{\tau} d\tau' f(\tau') \mathcal{E}_S^*(\tau') I_1(\psi) \psi^{-1}(\tau', \tau) \qquad (4.51)$$

where $q = 4\pi N \omega_{UV}/c\hbar$, $I_1(x)$ is the modified Bessel function of the first order and

$$\psi(\tau', \tau) = \left(2qz \int_{\tau'}^{\tau} (\frac{\omega_S}{\omega_{UV}} |f|^2 - |g|^2) d\tau'' \right)^{1/2} \qquad (4.52)$$

Note that Eq.(4.51) displays nonvanishing generation of UV light even in the limit $\tau \to \infty$. This is because after the laser pulses have propagated through the medium, a coherent polarization is retained at the frequency ω_{UV}. In practice, however, due to dephasing of the atoms this polarization decays rapidly via fast exponential law ceasing immediately the UV generation. Therefore, the time integration in Eq.(4.51) must be limited to the interval $\tau_d - T/2 \leq \tau \leq \tau_d + T/2$ centered around time τ_d with the length equal to probe pulse duration $T \ll \tau_d$. This relaxation is not incorporated in our calculations, so that we have to introduce the cutoff of upper integration in Eq.(4.51) by hand.

We do not present the solution for Stokes field, which is not relevant here, but we note that it is easily found from the equations (4.B2) and (4.B4).

In the absence of input Stokes signal, the Stokes field is generated from spontaneous noise or quantum fluctuations with a δ correlated amplitude $\mathcal{E}_S(\tau)$

$$\frac{c}{2\pi} \langle \mathcal{E}_S(\tau)\mathcal{E}_S^*(\tau') \rangle = \frac{J_{sp}}{\Gamma_s} \delta(\tau - \tau') \tag{4.53}$$

where $J_{sp}(\omega_S) = \hbar\omega_S^3 \Delta\Omega\Delta\nu_S/2\pi^2 c^2$ is the intensity of spontaneous noise determined as the intensity of a light containing one photon in each mode within the Stokes linewidth $\Delta\nu_S = \Gamma_S/2\pi$ and in a small solid angle $\Delta\Omega$ in the forward direction [108].

Then using Eq.(4.53), for UV intensity we get

$$I_{UV} = q^2 z^2 \frac{J_{sp}}{\Gamma_s} |g(\tau)|^2 \int_{\tau_d - T}^{\tau} d\tau' |f(\tau')|^2 I_1^2(\psi)\psi^{-2}(\tau', \tau) \tag{4.54}$$

Finally, this expression must be averaged over laser phase fluctuations that is easily performed, if one notes that only the amplitudes $C_j(t)$ of the excited atomic states depend on the laser phase through the two-photon Rabi frequencies, as it is seen from Eqs.(4.47). So, we arrive at the final result by replacing everywhere the quantity $|f(\tau)|^2$ by its averaged value $\langle |f(\tau)|^2 \rangle$. In what follows, we will show how the QB arises in the latter thanks to the exponential factors $\exp(-i\Delta_j\tau)$ in Eq. (4.50).

Before proceeding to these calculations, we find it worthwhile to review the solution of Eq.(4.54) for different gain regimes. It is clear that Bessel function $I_1(\psi)$ in the integrand

of Eq.(4.54) is responsible for stimulated gain in UV emission. However, by analyzing the structure of ψ we recognize that the gain is generally possible, only if the condition

$$\omega_S \langle |f(t)|^2 \rangle > \omega_{UV} |g(t)|^2 \qquad (4.55)$$

holds in the most part of laser pulses. Indeed, in alternate case $I_1(\psi)$ is replaced by the ordinary Bessel function $J_1(|\psi|)$, which vanishes as z increases and UV radiation remains at the spontaneous noise level. This is well known effect of self-induced suppression of HRS caused by destructive interference between HRS and FWM [108]. The effect has been confirmed in a number of experiments with alkali vapors [130]. The condition (4.55) restricts the laser intensity from below and increases the UV generation threshold. To overcome this constraint, it is enough usually to use a sufficiently strong pumping. However, in our case this does not always guarantee a substantial gain of Stokes and UV fields, since the condition (4.55) can still be violated periodically in dependence on time delay τ_d. This happens at the values of τ_d, where $\langle |f(t)|^2 \rangle$ reaches its minima (dark fringes) due to interference between the two atomic WPs created by the pump and probe laser pulses. This means that instead of intuitively expected QB patterns that could be observed being originated by only the first term $\langle |f(t)|^2 \rangle$ in the integrand in Eq.(4.51) (see, for example, the discussion in [105]), the real picture is much more complicated. To make this point more transparent, let us recall that in high-gain limit, when $\psi(\tau', \tau) \gg 1$ that corresponds to $\omega_S \langle |f(t)|^2 \rangle \gg \omega_{UV} |g(t)|^2$, $I_1^2(x)$ has an asymptotic form $e^{2x}/2\pi x$. Then we can approximate $\psi(\tau', \tau) \sim \psi(\tau_d - T, \tau) = \psi_d(\tau)$ that yields

$$I_{UV} = \frac{\omega_{UV}^2 N z}{\hbar c \omega_S} \frac{J_{sp}}{\Gamma_s} |g(\tau)|^2 \frac{e^{2\psi_d}}{\psi_d} \qquad (4.56)$$

showing that the factor $e^{2\psi_d}/\psi_d$ being a periodic function of τ_d with the same frequency as $\langle |f(t)|^2 \rangle$ exponentially amplifies the maxima of the fringe function (bright fringes) in QB and, thereby, appreciably increases the visibility of the oscillations. Furthermore, whenever $\langle |f(t)|^2 \rangle$ attains its minima at corresponding values of τ_d, two regimes are realized depending on whether $1 > \psi(\tau', \tau) > 0$ or $\psi(\tau', \tau) < 0$. In the first case $I_1(x)/x \sim 1$ and the UV field experiences albeit small, but nonvanishing gain, while for negative $\psi(\tau', \tau)$ it is emitted
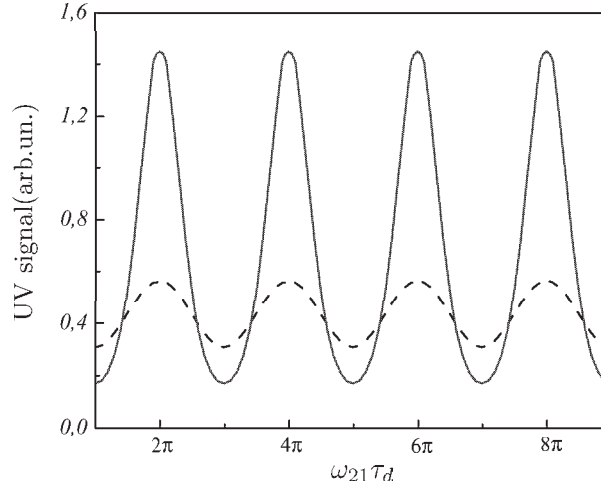
Figure 4.12: The UV signal obtained from Eq.(4.54) as a function of time delay τ_d for a model atoms having two upper eigenstates with the energy difference $\hbar\omega_{21}$ (solid). The parameters are chosen such that at the minima of $|f(t)|^2$ the condition (4.55) is violated, while at the maxima the exponential gain (4.56) takes place. The QB in $|f(t)|^2$ is shown by dashed line.

only spontaneously, as is shown above. Along with Eq.(4.56), this dramatic reduction of UV intensity demonstrates that two interference effects, the destructive one between HRS and FWM and the other between two atomic WPs are superimposed enhancing the contrast of QB practically up to 100%. Fig.4.12 depicts an illustration of this effect for a model atom having two eigenstates in the upper manifold. Which of two regimes is realized depends evidently not only on the laser intensity but more essentially on the ratio of dipole matrix elements of Stokes and UV transitions, as is evident from Eq.(4.55). Despite the complexity of this dependence, it allows us to understand the features of fringe pattern in UV generation at different transitions when the rest of the parameters are the same.

We now return to the calculations of QB in $\langle |f(\tau)|^2 \rangle$ starting from the solution of Eqs.(4.47a),(4.47b). We are interested in this solution for the time after probe pulse switched on. We consider first the Fourier-transform-limited laser pulses with duration $T \sim \Gamma^{-1}$. For this case the solution to Eqs.(4.47a),(4.47b) is easily found in the three steps similar to the method described in Appendix 4.A in the form (4.33) but with notation $\Omega_{p,pr} =$

$\sqrt{\sum_{j=1}^{m} |\Omega_{p,pr}^{j}(t)|^2}$ and $\Delta_{Lj} \equiv \Delta_j$.
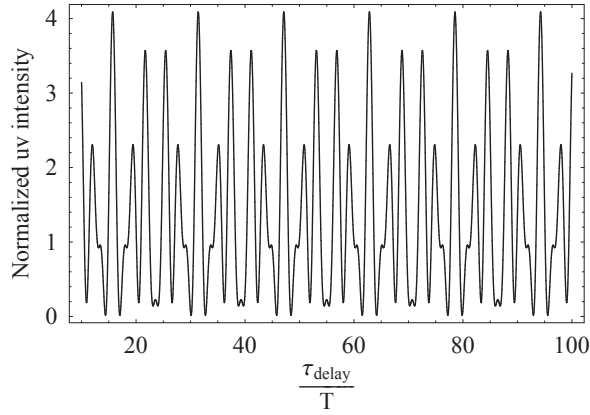

Figure 4.13: The QB in UV signal in the case of two-photon excitation of three upper atomic levels by Fourier-transform-limited laser pulses. All three QB modes are present.

Upon substituting Eq.(4.33) into Eq.(4.54) and taking into account that for $\tau \simeq \tau_d \gg T$ one can replace $\Delta_j\tau$ by $\Delta_j\tau_d$, we conclude that $|f(t)|^2$ contains all possible beating modes with frequencies ω_{kj} that produces a very complicated QB pattern in UV intensity after the time integration in Eq.(4.54). As an example, we show in Fig.4.13 the QB in UV signal in the case of excitation of three upper levels of the atoms that differs substantially from a simple picture reported in the experiment with Rb atoms [105], where four atomic states in the upper manifold get populated by two-photon excitation. This discrepancy emerges from that the laser phase fluctuations, which are typical for ordinary ultrashort lasers, essentially influence the QB washing out the contribution of many beating modes.

To solve the problem with allowing for laser *field fluctuations* we have to employ the density matrix approach instead of using Eq.(4.47), which is no longer applicable. From Eq.(4.50), in terms of the density matrix elements $\rho_{jk} = C_j C_k^*$ averaged over the laser phase fluctuations, $\langle |f(\tau)|^2 \rangle$ is represented as

$$\langle |f(\tau)|^2 \rangle = \sum_{j=1}^{m} \mu_{js}^2 \langle \rho_{jj}(\tau) \rangle + 2Re \sum_{j<k}^{m} \mu_{js}\mu_{ks} \langle \rho_{jk}(\tau) \rangle \exp(i\omega_{kj}\tau) \qquad (4.57)$$

Again, the second term in Eq.(4.57) being proportional to the atomic coherence ρ_{jk} between the upper levels gives rise to QB. The equations for ρ_{jk} are derived from Eqs.(4.47a),(4.47b)

and have the form

$$\dot{\rho}_{jj} = 2Im[(\Omega_p^{j*} + \Omega_{pr}^{j*})\rho_{jg}e^{-i\Delta_j\tau}] \tag{4.58a}$$

$$\dot{\rho}_{jg} = i(\Omega_p^j + \Omega_{pr}^j)e^{i\Delta_j\tau} - i\sum_{k\neq j}^m(\Omega_p^k + \Omega_{pr}^k)\rho_{jk}e^{i\Delta_k\tau}, \tag{4.58b}$$

$$\dot{\rho}_{jk} = i(\Omega_p^j + \Omega_{pr}^j)\rho_{gk}e^{i\Delta_j\tau} - i(\Omega_p^{k*} + \Omega_{pr}^{k*})\rho_{jg}e^{-i\Delta_k\tau}, \tag{4.58c}$$

with $\rho_{jg} = C_j\tilde{C}_g^*$ and $\rho_{jj} \ll \rho_{gg} \sim 1$. We separate the phase ϕ of the pump and probe lasers

$$\mathcal{E}_{p,pr}(z,t) = |\mathcal{E}_{p,pr}(z,t)|e^{i\phi}, \quad \Omega_{p,pr} = G_{p,pr}e^{2i\phi}$$

and transform ρ_{jg} to new variables $\rho_{jg} = \sigma_{jg}e^{2i\phi}$. The phase in an ordinary laser undergoes free diffusion according to the equation of motion [131] $\dot{\phi}(t) = \varphi(t)$, where $\varphi(t)$ is a δ-correlated Langevin-noise operator,

$$\langle\varphi(t)\varphi(t')\rangle = \Gamma\delta(t-t') \tag{4.59}$$

with diffusion coefficient given by the laser linewidth Γ, which is much larger compared to inverse pulse duration: $\Gamma T \gg 1$, as well as it is assumed again that $\Gamma > \omega_{m1}$. Then Eq.(4.58b) is modified to

$$\dot{\sigma}_{jg} = -2i\varphi\sigma_{jg} + i(G_p^j + G_{pr}^j)e^{i\Delta_j\tau} - i\sum_{k\neq j}^m(G_p^k + G_{pr}^k)\rho_{jk}e^{i\Delta_k\tau} \tag{4.60}$$

The mean value of the first term on the right-hand side of this equation can be obtained by its formal integration and substituting the correlation function Eq.(4.59). We obtain

$$i\langle\varphi(\tau)\sigma_{jg}(\tau)\rangle = -2\int_{-\infty}^\tau d\tau'\langle\varphi(\tau)\varphi(\tau')\sigma_{jg}(\tau')\rangle$$

$$\simeq -2\int_{-\infty}^\tau d\tau'\langle\varphi(\tau)\varphi(\tau')\rangle\langle\sigma_{jg}(\tau')\rangle = -\Gamma\langle\sigma_{jg}(\tau)\rangle. \tag{4.61}$$

Thus the equation for $\langle\sigma_{jg}(\tau)\rangle$ is reduced to

$$\langle\dot{\sigma}_{jg}(\tau)\rangle = -2\Gamma\langle\sigma_{jg}(\tau)\rangle + i(G_p^j + G_{pr}^j)e^{i\Delta_j\tau} - i\sum_{k\neq j}^m(G_p^k + G_{pr}^k)\langle\rho_{jk}\rangle e^{i\Delta_k\tau} \tag{4.62}$$

Since $\Gamma T \gg 1$, we can neglect the time derivative on the left-hand side of Eq.(4.62) and obtain

$$\langle\sigma_{jg}(\tau)\rangle = \frac{i}{2\Gamma}[(G_p^j + G_{pr}^j)e^{i\Delta_j\tau} - \sum_{k\neq j}^m(G_p^k + G_{pr}^k)\langle\rho_{jk}\rangle e^{i\Delta_k\tau}] \tag{4.63}$$

94

Substituting $\langle \sigma_{jg}(\tau) \rangle$ into Eq.(4.58), we derive equations for the mean values of the populations $\langle \rho_{jj}(\tau) \rangle$ and atomic coherence $\langle \rho_{jk}(\tau) \rangle$ in the first order of the small parameter $G_{p,pr}/\Gamma$

$$\langle \dot{\rho}_{jj}(\tau) \rangle = \frac{1}{\Gamma}(G_p^j + G_{pr}^j)^2 \tag{4.64}$$

$$\langle \dot{\rho}_{jk}(\tau) \rangle = \frac{1}{\Gamma}(G_p^j + G_{pr}^j)(G_p^k + G_{pr}^k)e^{i\omega_{jk}\tau} \tag{4.65}$$

Equation (4.65) is very important, as it demonstrates that the atomic coherence ρ_{jk} differs from zero only between the upper states j and k, whose frequency splitting satisfies

$$\omega_{jk}T \leq 1. \tag{4.66}$$

In opposite case, the rhs of Eq.(4.65) undergoes rapid exponential oscillations that nullifies $\langle \rho_{jk}(\tau) \rangle$ after integration of Eq.(4.65) over the interaction time with laser pulses. No such suppression could occur in the previous case of Fourier-transform-limited pulses, for which $\omega_{jk}T < \omega_{m1}T < 1$.

Then, the solution for populations $\langle \rho_{jj}(\tau) \rangle$ and nonvanishing atomic coherence $\langle \rho_{jk}(\tau) \rangle$ for $\tau \sim \tau_d \gg T$ is readily found from Eqs.(4.64), (4.65) as

$$\langle \rho_{jj}(\tau) \rangle = \frac{1}{\Gamma}(\eta_{p,jj}(\infty) + \eta_{pr,jj}(\tau)) \tag{4.67}$$

$$\langle \rho_{jk}(\tau) \rangle = \frac{1}{\Gamma}(\eta_{p,jk}(\infty) + \eta_{pr,jk}(\tau)e^{i\omega_{kj}\tau_d}), \tag{4.68}$$

with

$$\eta_{\alpha,jk}(\tau)) = \int_{-\infty}^{\tau} d\tau' G_\alpha^j(\tau') G_\alpha^k(\tau'), \quad \alpha = p, pr. \tag{4.69}$$

and in the exponential term in (4.65) we have replaced τ with τ_d. Upon substituting this solution into Eq.(4.57), we finally obtain

$$\langle |f(\tau)|^2 \rangle = \frac{1}{\Gamma}[\sum_{j=1}^{m}\mu_{js}^2(\eta_{p,jj}(\infty) + \eta_{pr,jj}(\tau))$$
$$+ 2\sum_{j<k}^{m}{}' \mu_{js}\mu_{ks}(\eta_{p,jk}(\infty)\cos(\omega_{kj}\tau_d) + \eta_{pr,jk}(\tau))], \tag{4.70}$$

where the notation $\sum_{j<k}^{m}{}'$ indicates that the summation is running over the states, for which the condition (4.66) is fulfilled and, thereby, in Eq.(4.57) one may replace $\exp(i\omega_{jk}\tau)$ by

$\exp(i\omega_{jk}\tau_d)$. The final step is the time integration in Eq.(4.54), which is performed numerically for the given shapes of laser pulses.

4.4.3   Comparison with experiment

Now, finding the solution (4.70), we are able to calculate with the help of Eq.(4.54) the UV signal for a realistic situation and to compare the results with the existing data. The sample is chosen to be Rb vapor with the ground state $5S_{1/2}$, from which four upper states $9d, 11s, 10d$, and $12s$ are simultaneously excited by broadband laser pulses with light wavelength $\lambda \simeq 620$ nm and linewidth $\Gamma/2\pi c \sim 500$ cm^{-1}. The state $5P_{3/2}$ serves as an intermediate one giving the main contribution to the two-photon excitation, while the UV generation may occur at different $nP \to 5S$ ($n = 7 - 11$) transitions. Note, however, that the $11P \to 5S$ transition is much suited for comparison with the experiment, since precisely in this case the "cleanest" signal has been achieved in Rb vapor [105]. Using the following parameters - pulse duration $T \simeq 100$ fs, peak intensity of Gaussian laser-pulses $I_L \sim 10$GW cm^{-2}, and atomic number density $N \sim 10^{17}$ cm^{-3}, we have calculated the intensity of the UV emission near the $11P_{3/2} \to$
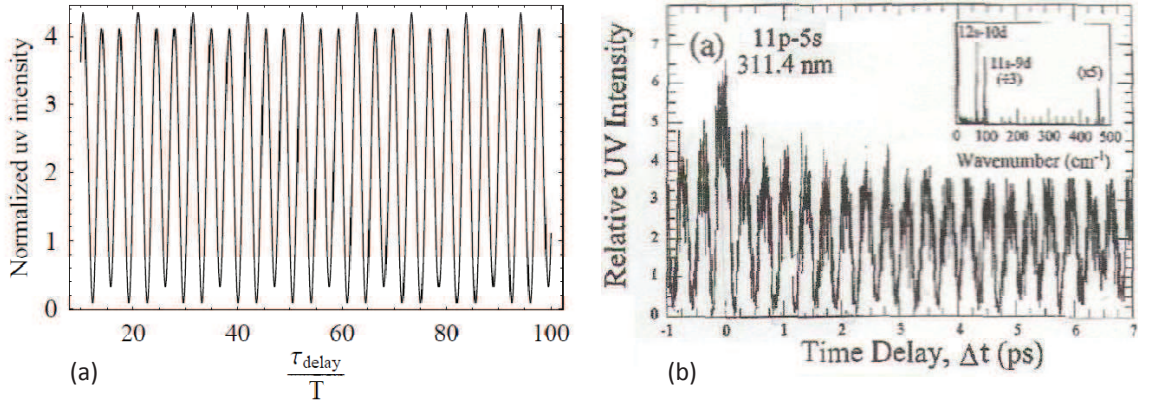

Figure 4.14: (a) Theoretical and (b) experimental [105] curves for UV signal generated near the $11P_{3/2} \to 5S_{1/2}$ line of Rb as a function of the time delay τ_d between the pump and probe laser pulses. In numerical simulations, the parameters of the experiment in Rb vapor [105] have been used (see the text).

$5S_{1/2}$ ($\lambda_{UV} \sim 311$ nm) line as a function of the time delay τ_d between the pump and probe laser pulses depicted in Fig.4.14a. This picture reproduces very well the main features of the observed QB pattern Fig. 4.14b. First, in accordance with our calculations only two beating modes with frequencies $\omega(12s - 10d)/2\pi c \sim 67$ cm^{-1} and $\omega(11s - 9d)/2\pi c = 95$ cm^{-1}, which satisfy the condition (4.66), must be taken into account in Eq.(4.70). This prediction is confirmed by the experiment. Secondly, the oscillations in the UV signal have a periodicity $T_{os} \sim 350$ fs, which coincides with the measured value and corresponds well to the frequency $\omega(11s - 9d)$. It is worth noting that this result demonstrates both the validity and correctness of our theory. The point is that one would intuitively expect that the mode $\omega(12s - 10d)$ must prevail in the QB because the contribution of atomic coherence $\rho_{11s,9d}$ in $\langle|f(\tau)|^2\rangle$ (Eq.(4.70)) is suppressed compared to that of $\rho_{12s,10d}$ by a factor ~ 1.5, which is merely the ratio of the corresponding dipole matrix elements. However, just due to the term $\rho_{11s,9d}$ the minima of $\langle|f(\tau)|^2\rangle$ are reduced so much (note that two contributions, $\rho_{11s,9d}$ and $\rho_{12s,10d}$, have the same sign) that the gain condition (4.55) is violated resulting in vanishing dark fringes with periodicity T_{os} in the UV signal (see Fig.4.14a). Thus, the destructive interference between HRS and FWM not only affects the visibility of the fringe pattern, but also determines the prominent mode in the UV spectrum to be $\omega(11s - 9d)$ instead of $\omega(12s - 10d)$ in full agreement with the experimental observations. Note that the decay time for the coherence of the upper levels due to the dephasing of atoms amounts to tens of picoseconds. So, the QB can be observed, practically, for long delay times $\tau_d \gg T_{os}$.

The next question is the dependence of UV signal on the laser intensity I_L. As numerical calculations show, the parameters used in the experiment [105] are such that even at the maxima of $\langle|f(\tau)|^2\rangle$ the exponential gain (4.56) is unattainable, so that to a good approximation the peak UV intensity can be represented in a simple form: $I_{UV}^{max} \sim \int d\tau'|f(\tau')|^2$ showing, along with Eqs.(4.69),(4.70), its quadratic variation with I_L that has been detected experimentally.

We wish to point out an important role of the plasma being created in the medium by a two-photon resonant three-photon ionization. The quasi-electrostatic field of the plasma can

strongly mix the atomic s and p (or d and p) states that opens new way for UV generation again via FWM, where the plasma field plays the same role as the Stokes field in the previous case. This possibility can be tested experimentally by monitoring the appearance of new modes in Fourier spectrum of the QB corresponding to the $s-p$ or $d-p$ frequency differences. We foresee a new interference effect between the two FWM processes. What way dominates in the UV generation depends evidently on the strength of the plasma field. Moreover, as the latter varies sinusoidally in time with the frequency ω_{pl} of plasma oscillations, we predict a periodical transformation of the QB modes from the $(s-d)$ modes to the $(s-p)$ ones and back. Clearly, due to $\omega_{pl} \ll \omega_{s-d}$ this exchange between the modes will take place in a much larger time scale compared to that of quantum beating.

Another factor influencing the QB properties is the polarization of the laser fields. In our model, it was assumed that both the pump and probe fields have the same polarization. In the case of different polarizations, they excite different magnetic sublevels of the upper states that can significantly change the QB pattern in the UV signal. This dependence on the polarization can be used for selective spectroscopic studies of the upper lying levels, in particular, for the measurement of the oscillator strengths of the corresponding transitions. Of particular interest is the coherent violation of the superposition of the upper states owing to interaction with some control field connecting one of these states with an auxiliary level. In the presence of the control field, the QB, obviously, are strongly modified and even absent under certain conditions, which provides the possibility of controlling the coherent excitation of highly excited atomic and molecular levels and, in other cases, ensuring their selective excitation by femtosecond laser pulses.

4.4.4 Monitoring of selective excitation via QB in UV generation

In this section, we show that the QB technique widely employed in pump-probe experiments can be used as a powerful tool to detect the selective excitation as a model discussing an atom with a doublet of upper levels, described in Section 4.2. The essence of the method

is the following. In the considered scheme, upon two-photon excitation of the atoms by ultrashort pump pulse, the Stokes and UV light are generated on the basis of HRS and FWM, respectively (Fig.4.15). If now this system is probed by a second laser pulse coming after a certain delay time τ_d, then due to the Ramsey-type interference [100] between the two atomic WPs created by the pump and probe pulses, the periodic changes or QB should appear in the τ_d dependence of UV signal in the absence of the coupling laser. However, the interaction of the atoms with the coupling field strongly destroys the WPs that evidently leads to dramatic changes in the QB pattern. Moreover, since this violation is realized in a coherent way by depopulating of the state 1, but not introducing any random relative phase in WP, then the experimental observation of the modified QB will indicate undoubtedly the selective excitation of the second upper level of the atoms, allowing at the same time to measure the ratio of the upper level populations with a high efficiency.
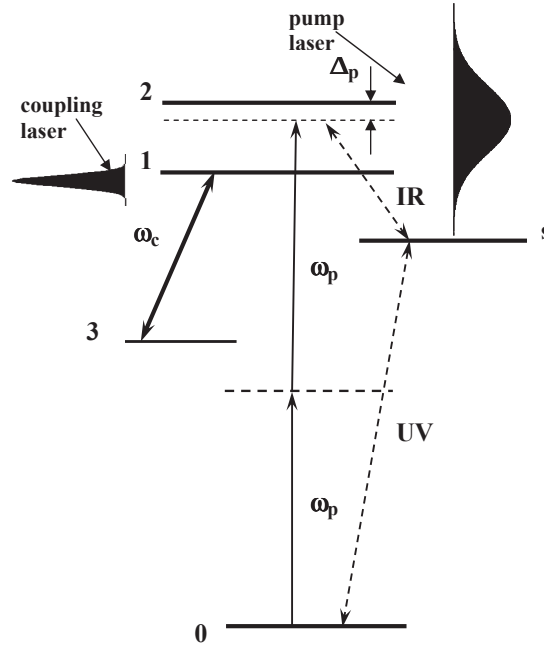

Figure 4.15: Level scheme of atoms illustrating two-photon excitation of doublet of upper atomic eigenstates and interaction with coupling field and generation of the Stokes and UV fields on the basis of hyper-Raman scattering and four-wave mixing, respectively.

For the atom model with two-upper levels Eq.(4.54) is reduced to

$$I_{UV} = q^2 z^2 \frac{J_{sp}}{\Gamma_s} |g(\tau)|^2 \int_{\tau_d - T}^{\tau} d\tau' |f(\tau')|^2 I_1^2(\psi) \psi^{-2}(\tau', \tau), \qquad (4.71)$$

where

$$f(\tau) = \mu_{1s} C_1(\tau) e^{-i\Delta_1 \tau} + \mu_{2s} C_2(\tau) e^{-i\Delta_2 \tau}, \qquad g(\tau) = \mu_{s0} \tilde{C}_0(\tau). \qquad (4.72)$$

The atomic amplitudes are obtained from

$$\dot{C}_0(t) = i \sum_{j=1,2} (\Omega_p^{j*} + \Omega_{pr}^{j*}) C_j(t) e^{-i\Delta_j t}, \qquad (4.73a)$$

$$\dot{C}_1(t) = i(\Omega_p^1 + \Omega_{pr}^1) \tilde{C}_0(t) e^{i\Delta_1 t} + i\Omega_c C_3, \qquad (4.73b)$$

$$\dot{C}_2(t) = i(\Omega_p^2 + \Omega_{pr}^2) \tilde{C}_0(t) e^{i\Delta_2 t}, \qquad (4.73c)$$

$$\dot{C}_3(t) = i\Omega_c^* C_1, \qquad (4.73d)$$

In Fig.4.16 we show the temporal behavior of the atomic state populations, when the pump and probe Gaussian pulses with the same length T, but slightly different intensities, are impinged on the medium at the time moments $\omega_{21} t_p = 2$ and $\omega_{21} t_{pr} = 5$, respectively. The coupling pulse with Rabi frequency $\Omega_c = 5\omega_{21}$ is sufficiently longer such that it can be taken to be constant. We distinguish two cases of equal (Fig.4.16a) and different (Fig.4.16b) matrix elements for the two-photon $0 \to 1$ and $0 \to 2$ transitions. We see that in both cases the probe pulse strengthens the selectivity of the excitation of the atomic upper levels, reducing the population of level 1 and enhancing at the same time the population of level 2. The dashed lines in Fig.4.16 illustrate atomic state populations in the absence of coupling field, which coincide for the states 1 and 2 in the case of equal matrix elements, but the state 1 is four times more populated (Figure 4.16b), than state 2, when the matrix elements of two-photon transitions are different. Nevertheless, when the coupling field is on, the population of the state 1 becomes much smaller than that of the state 2, even if the transition $0 \to 1$ is stronger.

In Fig.4.17 we illustrate the QB in UV intensity in dependence on the delay time τ_d between the pump and probe pulses for different value of the coupling field. As expected, in the absence of the latter, the UV signal experiences regular oscillations with the frequency
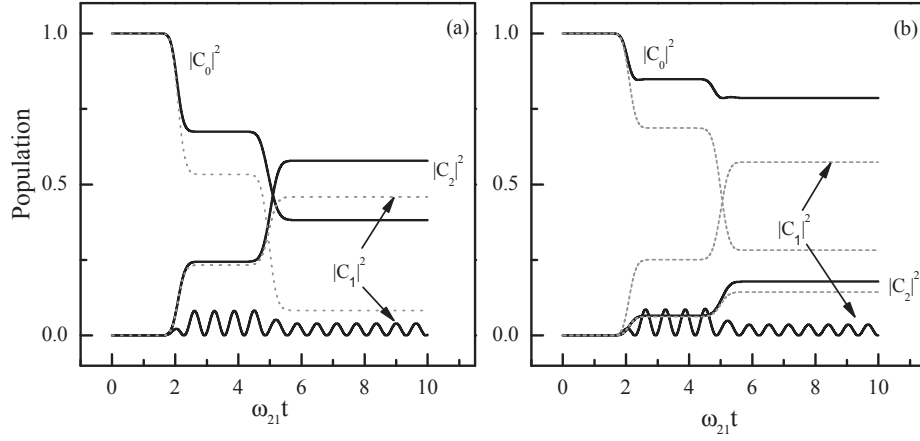
Figure 4.16: Population of the atomic levels 0, 1, 2 in the presence ($\Omega_c = 5\omega_{21}$) and absence of coupling field - solid and dashed lines, the pump and probe pulses are turned on at the moments $\omega_{21}t_p = 2$ and $\omega_{21}t_{pr} = 5$, respectively. $\mathcal{E}_{pr}/\mathcal{E}_p = 0.7, \omega_{21}\tau_d = 3$, (a) $r_2/r_1 = 1$, (b) $r_2/r_1 = 0.5$.
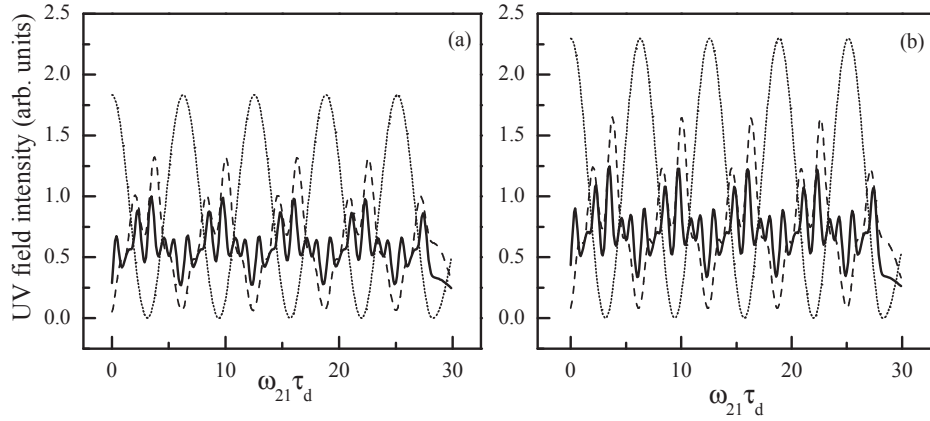

Figure 4.17: Dependence of intensity of UV field on delay time between pump and probe pulses τ_d in arbitrary units. Dotted line - $\Omega_c = 0$, dashed line - $\Omega_c = 3\omega_{21}$, solid line - $\Omega_c = 5\omega_{21}$. $\mathcal{E}_{pr}/\mathcal{E}_p = 0.7$, (a) $r_2/r_1 = 1$, (b) $r_2/r_1 = 0.5$.

ω_{21}. For moderate values of coupling field intensities they are still observed (dashed line in Figure 4.17). With further increase of the coupling field intensity the QB almost disappears that indicates the selective excitation of the state 2. Note that if the state 1 is completely unpopulated, the UV field intensity doesn't depend on the delay time τ_d.

Appendix 4.A: General solution in the impulsive regime

We integrate Eqs. (4.5) over the time of interaction with the nth pump pulse in the impulsive approximation, disregarding the detunings $\Delta_j T \ll 1$ and where to a good approximation the weak Ω_c - terms can be neglected. This yields a simple solution right after the nth pump pulse at time $t = t_n^+$ (considered interacting at $t = t_n$), from the solution right before the pulse at time $t = t_n^-$:

$$
\begin{aligned}
C_0(t_n^+) &= C_0(t_n^-)\cos\theta + i\bar{C}_n^-\sin\theta \\
C_j(t_n^+) &= C_j(t_n^-) + i\frac{\mu_j}{\mu}C_0(t_n^-)\sin\theta + \frac{\mu_j}{\mu}\bar{C}_n^-(\cos\theta - 1), \quad j = 1, 2, 3 \\
C_4(t_n^+) &= C_4(t_n^-),
\end{aligned}
$$

where $\mu = \sqrt{\sum_{k=1}^3 \mu_k^2}$, $\theta = \frac{\mu}{\hbar}\int \mathcal{E}(t)dt$ with $\int \mathcal{E}(t)dt$ the area of each pump pulse (considered invariant from pulse to pulse), and $\bar{C}_n^- = [\sum_{k=1}^3 \mu_k C_k(t_n^-)]/\mu$. After the nth pulse turned off, the amplitudes C_0, C_2 and C_3 evolve freely up to $t \sim t_n + \tau_d$, $\tau_d \gg T$:

$$
\begin{aligned}
C_0(t) &= C_0(t_n^+), \\
C_j(t) &= e^{-i\Delta_j(t-t_n)}C_j(t_n^+), \; j = 2, 3,
\end{aligned}
$$

while $C_1(t)$ and $C_4(t)$, $t_{n+1} > t > t_n$ are found from Eqs. (4.5) with the initial values (4.74a-4.74a) as

$$
\begin{aligned}
C_1(t) &= e^{-i\Delta_1(t-t_n)}\Big\{C_1(t_n^+)\cos\big[\Omega_c(t-t_n)\big] + iC_4(t_n^+)\sin\big[\Omega_c(t-t_n)\big]\Big\}, \\
C_4(t) &= e^{-i\Delta_1(t-t_n)}\Big\{iC_1(t_n^+)\sin\big[\Omega_c(t-t_n)\big] + C_4(t_n^+)\cos\big[\Omega_c(t-t_n)\big]\Big\},
\end{aligned}
$$

We iterate the above procedure for all the ultrashort pump pulses:

$$
\begin{aligned}
C_0(t_{n+1}^+) = C_0(t_n^+)\cos\theta &+ \frac{i}{\mu}\sin\theta\Big\{\mu_1 e^{-i\Delta_1\tau_d}\Big[C_1(t_n^+)\cos(\Omega_c\tau_d) + iC_4(t_n^+)\sin(\Omega_c\tau_d)\Big] \\
&+ \sum_{k=2}^3 \mu_k e^{-i\Delta_k\tau_d}C_k(t_n^+)\Big\},
\end{aligned}
\tag{4.A1}
$$

$$
\begin{aligned}
C_1(t_{n+1}^+) = i\frac{\mu_1}{\mu}C_0(t_n^+)\sin\theta &+ e^{-i\Delta_1\tau_d}\Big[C_1(t_n^+)\cos(\Omega_c\tau_d) + iC_4(t_n^+)\sin(\Omega_c\tau_d)\Big] \\
&* \Big[1 + \frac{\mu_1^2}{\mu^2}(\cos\theta - 1)\Big] + \frac{\mu_1}{\mu}(\cos\theta - 1)\sum_{k=2}^3 \frac{\mu_k}{\mu}e^{-i\Delta_k\tau_d}C_k(t_n^+),
\end{aligned}
\tag{4.A2}
$$

$$C_2(t_{n+1}^+) = i\frac{\mu_2}{\mu}C_0(t_n^+)\sin\theta + e^{-i\Delta_2\tau_d}C_2(t_n^+)\left[1 + \frac{\mu_2^2}{\mu^2}(\cos\theta - 1)\right]$$

$$+ \frac{\mu_2}{\mu}(\cos\theta - 1)\left\{\frac{\mu_1}{\mu}e^{-i\Delta_1\tau_d}\left[C_1(t_n^+)\cos(\Omega_c\tau_d) + iC_4(t_n^+)\sin(\Omega_c\tau_d)\right]\right.$$

$$\left. + \frac{\mu_3}{\mu}e^{-i\Delta_3\tau_d}C_3(t_n^+)\right\}, \tag{4.A3}$$

$$C_3(t_{n+1}^+) = C_{2\leftrightarrow 3}(t_{n+1}^+), \tag{4.A4}$$

$$C_4(t_{n+1}^+) = e^{-i\Delta_1\tau_d}\left[iC_1(t_n^+)\sin(\Omega_c\tau_d) + C_4(t_n^+)\cos(\Omega_c\tau_d)\right]. \tag{4.A5}$$

Which is the general solution of the atomic amplitudes in the impulsive regime.

Appendix 4.B: Solution of Maxwell equations

In this Appendix we obtain the solution to the Eqs.(13-15) with the initial and boundary conditions $\tilde{C}_s(z, -\infty) = 0$, $\mathcal{E}_S(0, \tau) = \mathcal{E}_S(\tau)$, and $\mathcal{E}_{UV}(0, \tau) = 0$. We introduce a new function $U(z, \tau) = \int_0^z \tilde{C}_s(z', \tau)dz'$. Then from Eq.(15) one obtains

$$\frac{\partial^2 U(z, \tau)}{\partial z \partial \tau} = \frac{i}{\hbar}g(\tau)\mathcal{E}_{UV}(z, \tau) + \frac{i}{\hbar}f(\tau)\mathcal{E}_S^*(z, \tau), \tag{4.B1}$$

The Maxwell equations (4.48) are integrated to the form

$$\mathcal{E}_S(z, \tau) = 2i\pi N\frac{\omega_S}{c}f(\tau)U^*(z, \tau) + \mathcal{E}_S(\tau) \tag{4.B2}$$

$$\mathcal{E}_{UV}(z, \tau) = 2i\pi N\frac{\omega_{UV}}{c}g^*(\tau)U(z, \tau) \tag{4.B3}$$

Substitution of these solutions into Eq.(4.B1) yields

$$\frac{\partial^2 U}{\partial z \partial \tau} = \frac{2\pi N}{c\hbar}\left(\omega_S|f|^2 - \omega_{UV}|g|^2\right)U + \frac{i}{\hbar}f(\tau)\mathcal{E}_S^*(\tau)$$

With the initial values $U(z, -\infty) = U(0, \tau) = 0$, this equation has the solution

$$U(z, \tau) = 2z\int_{-\infty}^{\tau} F(\tau')I_1(\psi)\psi^{-1}(\tau', \tau)d\tau' \tag{4.B4}$$

where

$$F(\tau) = \frac{i}{\hbar}f(\tau)\mathcal{E}_S^*(\tau)$$

$$\psi(\tau', \tau) = 2\left(\frac{2\pi N}{c\hbar}z\int_{\tau'}^{\tau}\left(\omega_S|f|^2 - \omega_{UV}|g|^2\right)d\tau''\right)^{1/2} \tag{4.B5}$$

and $I_1(\psi)$ is the modified Bessel function of the first order.

4.5 Summary

We have proposed a mechanism for the coherent excitation of the molecule or atom to a superposition of pre-selected states in in strong-field regime and weak-field regime by a train of fs laser pulses, combined with narrow-band weak laser fields coupling the undesired states well within the bandwidth of a single pulse to auxiliary states. The coupling fields allow the cancellation of specific transitions from the ground state to a set of states i when they induce a coherence between each state i and an auxiliary state (all different). These predictions of selective coherent excitation could be measured experimentally by a sensitive method such as the one developed in [137]. For that we have developed the theory of the QB in Stokes field via SERS and UV generation via FWM in pump-probe experiments. We have presented a detailed analytical study of the system. Comparison of the results with experimental data demonstrated the ability of our theory to reveal the key features of the QB observed in Rb vapor. One conclusion that emerges from this study is that the visibility of beating fringes increases remarkably due to destructive interference between the HRS and FWM, which, in addition, determines the dominant mode of the QB. Another finding is that the laser phase fluctuations strongly limit the number of the QB modes. With assistance of the destructive interference effect, this allows one to create and study the atomic coherence between the selected upper levels of the atoms or molecules that otherwise is very difficult, if not impossible.

Conclusion

In conclusion, we have proposed a robust and realistic source of indistinguishable single-photons with identical frequency and polarization generated on demand in a well-defined spatio-temporal mode from a coupled double-Raman atom-cavity system. We have considered two cases of four-level system (^{6}Li or ^{40}Ca$^+$) and atoms with many Zeeman sublevels and have shown that in the first case the number of generated SP pulses is limited by the decay of atomic states outside of the system, while in the second one the continuous SP generation is achievable, e.g. in ^{87}Rb atoms. The high efficiency and simplicity of the scheme, free from such complications as repumping process and environmental dephasing, makes the generation of many SP identical pulses feasible. We have shown the ability of our scheme to produce a sequence of narrow-band SP pulses with a delay determined only by the pump repetition rate. Such controlled scheme may pave the way to single-photon-based quantum information applications, such as deterministic all-optical quantum computation and quantum communication.

Our scheme allows, as well, to generate Fock states by two different mechanisms. As is mentioned in Sec. III, Fock states containing fixed number of photons can be generated from each pump subpulse if multi-level atoms with ground state $F \geq 1$ are used and laser fields are sufficiently strong. In the second mechanism, the generation of Fock states with programmable number of photons is possible with overlapped weak pump pulses even in the case of four-level systems such as ^{6}Li atoms or ^{40}Ca$^+$ ions. These questions will be addressed in future publications.

We have proposed and analyzed a simple scheme of parametric frequency conversion of optical quantum information in atomic ensembles. We have demonstrated remarkable properties of this scheme such as minimal loss and distortion of the pulse shape and the persistence of initial quantum coherence and entanglement that make it superior against the previous schemes of the QFC in atomic media based on release of stored light state via EIT. Moreover, efficient conversion of the quantum information frequency between different regions of a spectrum of light has been shown. The narrowband property of single photons and high efficiency of entanglement generation profit the present mechanism to serve as an ideal candidate for frequency conversion and redistribution of optical information in quantum information processing and quantum networking.

We have proposed a robust and simple mechanism for the coherent excitation of the molecule or atom to a superposition of pre-selected states by a train of fs laser pulses, combined with narrow-band weak laser fields coupling the undesired states well within the bandwidth of a single pulse to auxiliary states. The coupling fields allow the cancellation of specific transitions from the ground state to a set of states i when they induce a coherence between each state i and an auxiliary state (all different). Selective excitation of atoms or molecules with fs laser pulses in strong-field regime has been discussed as well.

The theory of the QB in UV generation via FWM in pump-probe experiments has been developed. We have presented a detailed analytical study of the system. Comparison of the results with experimental data demonstrated the ability of our theory to reveal the key features of the QB observed in Rb vapor. One conclusion that emerges from this study is that the visibility of beating fringes increases remarkably due to destructive interference between the HRS and FWM, which, in addition, determines the dominant mode of the QB. Another finding is that the laser phase fluctuations strongly limit the number of the QB modes. With assistance of the destructive interference effect, this allows one to create and study the atomic coherence between the selected upper levels of the atoms or molecules that otherwise is very difficult, if not impossible.

Bibliography

[1] M. A. Nielsen, I. L. Chuang, "Quantum computation and quantum information" (Cambridge University Press,2000).

[2] N. Gisin, G. Ribordy, W. Tittel, H. Zbinden, "Quantum cryptography", Rev. Mod. Phys. **74**, 145-195 (2002).

[3] V. Giovannetti, S. Lloyd, L. Maccone, "Quantum-enhanced measurements: beating the standard quantum limit", Science **306**, 1330-1336 (2004).

[4] A. N. Boto, P. Kok, D. S. Abrams, S. L. Braunstein, C. P. Williams, and J. P. Dowling, "Quantum interferometric optical lithography: exploiting entanglement to beat the diffraction limit", Phys. Rev. Lett. **85**, 2733-2743 (2000).

[5] D. Deutsch, "Quantum theory, the Church-Turing principle and the universal quantum computer", Proc. R. Soc. Lond. A **400**, 97-117 (1985).

[6] G. Brassard, S.L. Braunstein, and R.Cleve., "Teleportation as a quantum computation", Physica D, **120**, 43-47, 1998.

[7] C.Monroe, "Quantum information processing with atoms and photons", Nature **416**, 238-246 (2002).

[8] E. Knill, R. Laflamme and G. J. Milburn, "A scheme for efficient quantum computation with linear optics", Nature, **409**, 46-52 (2001).

[9] J.P.Dowling, J. D. Franson, H. Lee, G. J. Milburn, "Towards scalable linear-optical quantum computers", Quantum Inf.Process, **3**, 205-213 (2004).

[10] S. E. Harris and Y. Yamamoto, "Photon switching by quantum interference", Phys.Rev.Lett. **81**, 3611-3614 (1998).

[11] J.-W.Pan, D.Bouwmeester, H.Weinfurter, and A.Zeilinger, "Experimental entanglement swapping: entangling photons that never interacted", Phys.Rev.Lett. **80**, 3891-3894 (1998).

[12] N.Sangouard, C.Simon, J.Min, H.Zbinden, H.de Riedmatten, and N.Gisin, "Long-distance entanglement distribution with single-photon sources", Phys.Rev.A, **76**, 050301(R), 1-4 (2007).

[13] C. K. Hong, Z.Y. Ou, and L.Mandel, "Measurement of subpicosecond time intervals between two photons by interference", Phys. Rev. Lett.**59**, 2044-2046 (1987).

[14] P. P. Rohde and T. C. Ralph, "Frequency and temporal effects in linear optical quantum computing", Phys. Rev. A **71**, 032320, 1-10 (2005).

[15] F.W. Sun, B. H. Liu, Y. X. Gong, Y. F. Huang, Z. Y. Ou,and G. C. Guo, "Stimulated emission of two photons in parametric amplification and its interpretation as multiphoton interference", Europhys. Lett. **82**, 24001, 1-5, (2008).

[16] A. Lamas-Linares, J. C.Howell, and D. Bouwmeester, "Stimulated emission of polarization-entangled photons", Nature **412**, 887-890 (2001).

[17] F.W.Sun, B. H. Liu, Y. X. Gong, Y. F. Huang, Z. Y. Ou, and G. C. Guo,"Stimulated emission as a result of multiphoton interference", Phys. Rev. Lett. **99**, 043601, 1-4 (2007).

[18] A. Lamas-Linares, C. Simon,J. C. Howell, and D. Bouwmeester, "Experimental quantum cloning of single photons", Science **296**, 712-714 (2002).

[19] S. Fasel, N. Gisin,G. Ribordy, V. Scarani, and H. Zbinden, "Quantum cloning with an optical fiber amplifier", Phys. Rev. Lett. **89**, 107901, 1-4 (2002).

[20] F. W. Sun, J. M. Cai, J. S. Xu, G. Chen, B. H. Liu, C. F. Li, Z.W. Zhou, and G. C. Guo, "Experimental measurement of multidimensional entanglement via equivalent symmetric projection", Phys. Rev. A **76**, 052303, 1-5 (2007).

[21] P. Michler, A. Kiraz, C. Becher, W. V. Schoenfeld, P. M.Petroff, L. Zhang, E. Hu, and A. Imamoglu, "A quantum dot single-photon turnstile device", Science **290**, 2282-2285 (2000).

[22] M. Pelton, C. Santori, J. Vuĉković, B. Zhang, G. S.Solomon, J. Plant, and Y. Yamamoto, "Efficient source of single photons: A single quantum dot in a micropost microcavity", Phys. Rev. Lett. **89**, 233602, 1-4 (2002).

[23] J.McKeever, A. Boca, A. D. Boozer, R. Miller, J. R. Buck, A.Kuzmich, and H. J. Kimble, "Deterministic generation of single photons from one atom trapped in a cavity", Science **303**, 1992,2004.

[24] C. K. Law, and J. H. Eberly, "Arbitrary Control of a Quantum Electromagnetic Field", Phys. Rev. Lett., **76**, 1055-1058 (1996).

[25] C. K. Law, and J. H. Eberly, "Deterministic generation of a bit-stream of single-photon pulses", J. Mod. Opt., **44**, 2067-2074 (1997).

[26] J. Kim, O. Benson, H. Kan, and Y. Yamamoto, "A Single-Photon Turnstile Device", Nature, **397**, 500-503 (1999).

[27] C. Kurtsiefer, S. Mayer, P. Zarda, and H. Weinfurter, "Stable Solid-State Source of Single Photons", Phys. Rev. Lett., **85**, 290-293 (2000).

[28] E. Moreau, I. Robert, J. M. Gérard, I. Abram, L. Maniv, and V. Thierry-Mieg, "Single-mode solid-state single photon source based on isolated quantum dots in pillar micro-cavities", Appl. Phys. Lett., **79**, 2865-2867 (2001).

[29] B. Sanders, J. Vuckovic, and P. Grangier, "Single photons on demand", Europhysics News **36**, 56-58 (2005).

[30] B. Lounis and W. E. Moerner, "Single photons on demand from a single molecule at room temperature", Nature **407**, 491-493 (2000).

[31] F. Treussart, R. Alleaume, V. Le Floc'h, L. T. Xiao, J.-M. Courty, and J.-F. Roch, "Direct measurement of the photon statistics of a triggered single photon source", Phys. Rev. Lett. **89**, 093601, 1-4 (2002).

[32] C. Santori, D. Fattal, J. Vuĉković and Y. Yamamoto, "Indistinguishable photons from a single-photon device", Nature **419**, 594-597 (2002).

[33] S. E. Harris, "Electromagnetically induced transparency", Phys. Today **50**, 36-42 (1997).

[34] D. N. Matsukevich, T. Chaneliere, S. D. Jenkins, S.-Y. Lan, T. A. B. Kennedy, and A. Kuzmich, "Deterministic single photons via conditional quantum evolution", Phys. Rev. Lett. **97**, 013601, 1-4 (2006).

[35] S. Chen, Y.-A. Chen, T. Strassel, Z.-S. Yuan, B. Zhao, J. Schmiedmayer and J.-W. Pan, "Deterministic and Storable Single-Photon Source Based on a Quantum Memory", Phys.Rev.Lett. **97**, 173004, 1-4 (2006).

[36] A. Kuhn, M. Hennrich, and G. Rempe, "Deterministic single-photon source for distributed quantum networking", Phys. Rev. Lett. **89**, 067901, 1-4 (2002).

[37] M.Keller, B. Lange, K. Hayasaka, W. Lange, and H. Walther, "Continuous generation of single photons with controlled waveform in an ion-trap cavity system", Nature **431**, 1075-1078 (2004).

[38] M.Hijlkema, B. Weber, H. P. Specht, S. C. Webster, A. Kuhn, and G. Rempe, "A single-photon server with just one atom", Nature Phys. **3**, 253-255 (2007).

[39] T. Wilk, S. C. Webster, H. P. Specht, G. Rempe, and A. Kuhn, "Polarization-controlled single photons", Phys. Rev. Lett. **98**, 063601, 1-4 (2007).

[40] M. W. McCutcheon, J. F. Young, G. W. Rieger, D. Dalacu, S.Frederick, P. J. Poole, and R. L. Williams, "Experimental demonstration of second-order processes in photonic crystal microcavities at submilliwatt excitation powers", Phys. Rev. B **76**,245104, 1-6 (2007).

[41] J. Bravo-Abad, A. Rodriguez, P. Bermel, S. G. Johnson, J. D.Joannopoulos, and M. Soljacic, "Enhanced nonlinear optics in photonic-crystal microcavities", Optics Express **15**, 16161-16176 (2007).

[42] M. Liscidini and L. C. Andreani, "Second-harmonic generation in doubly resonant microcavities with periodic dielectric mirrors", Phys. Rev. E **73**, 016613, 1-11 (2006).

[43] P. Kumar, "Quantum frequency conversion", Opt. Lett. 15, 1476-1478 (1990).

[44] J.Shapiro, "Architectures for long-distance quantum teleportation", New J. Phys., 4, 47.1-47.18 (2002).

[45] M. A. Albota and F. C. Wong, "Efficient single-photon counting at 1.55 mm by means of frequency upconversion", Opt. Lett. **29**, 1449-1451 (2004).

[46] A. P. VanDevender and P. G. Kwiat, "High efficiency single photon detection via frequency up-conversion", J. Mod. Opt. **51**, 1433-1445 (2004).

[47] C. Langrock, E. Diamanti, R. V. Roussev, Y. Yamamoto, M. M. Fejer, and H. Takesue, "Highly efficient single-photon detection at communication wavelengths by use of up-conversion in reverse-proton-exchanged periodically poled LiNbO3 waveguides", Opt. Lett. **30**, 1725-1727 (2005).

[48] S. Tanzilli, W. Tittel, M. Halder, O. Alibart, P. Baldi, N.Gisin, and H. Zbinden, "A photonic quantum information interface", Nature **437**, 116-120 (2005).

[49] H.Pan, E. Wu, H.Dong, and H.Zeng, "Single-photon frequency up-conversion with multimode pumping", Phys.Rev. A **77**, 033815, 1-6 (2008).

[50] R. V. Roussev, C. Langrock, J. R. Kurz, and M. M. Fejer, "Periodically poled lithium niobate waveguide sum-frequency generator for efficient single-photon detection at communication wavelengths", Opt. Lett. **29**, 1518-1520 (2004).

[51] H.-J. Briegel, W. Dur, J. I. Cirac, and P. Zoller, "Quantum repeaters: the role of imperfect local operations in quantum communication", Phys. Rev. Lett. **81**, 5932-5935 (1998).

[52] H. Takesue, "Quantum frequency downconversion experiment", Phys.Rev. A **82**, 013833, 1-5 (2010).

[53] Yu Ding and Z.Y. Ou, "Frequency downconversion for quantum network", Opt. Lett. **35** 25912593 (2010).

[54] W.K.Wootters and W.H.Zurek, "A single quantum cannot be cloned", Nature, **299**, 802-803 (1982).

[55] J. Huang and P. Kumar, "Observation of quantum frequency conversion", Phys. Rev. Lett. **68**, 2153-2156 (1992).

[56] G. Giorgi, P. Mataloni, and F. De Martini, "Frequency hopping in quantum interferometry: efficient up-down conversion for qubits and ebits", Phys. Rev. Lett. **90**, 027902, 1-4 (2003).

[57] M. Fleischhauer and M. D. Lukin, "Dark-State polaritons in electromagnetically induced transparency ", Phys. Rev. Lett. **84**, 5094-5097, (2000); Phys. Rev. A "Quantum memory for photons:dark-state polaritons", **65**, 022314, 1-12 (2002).

[58] A. S. Zibrov, A. B. Matsko, O. Kocharovskaya, Y. V. Rostovtsev, G.R. Welch, and M. O. Scully, "Transporting and time reversing light via atomic coherence", Phys. Rev. Lett. **88**, 103601, 1-4 (2002).

[59] B. Wang, S. Li, H. Wu, H. Chang, H. Wang, and M. Xiao, "Controlled release of stored optical pulses in an atomic ensemble into two separate photonic channels", Phys. Rev. A **72**, 043801, 1-5 (2005).

[60] N. Sisakyan and Yu. Malakyan, "Creation of a photonic time-bin qubit via parametric interaction of photons in a driven resonant medium", Phys. Rev. A **75**, 063831, 1-8 (2007).

[61] C. W. Chou, S. V. Polyakov, A. Kuzmich, and H. J. Kimble,"Single-photon generation from stored excitation in an atomic ensemble ", Phys. Rev. Lett. **92**, 213601, 1-4 (2004).

[62] M. D. Eisaman, A. Andre, F. Massou, M. Fleischhauer, A. S. Zibrov, and M. D. Lukin, "Electromagnetically induced transparency with tunable single-photon pulses", Nature, **438**, 837-841 (2005).

[63] Z.-S. Yuan, Y. A. Chen, S. Chen, B. Zhao, M. Koch, T. Strassel, Y.Zhao, G. J. Zhu, J. Schmiedmayer, and J. W. Pan, "Synchronized independent narrow-band single photons and efficient generation of photonic entanglement ", Phys.Rev. Lett. **98**, 180503, 1-4 (2007).

[64] D. Deutsch, "Quantum computational networks", Proc. R. Soc. A **425**, 73-90 (1989).

[65] R. Raussendorf and H. J. Briegel, "A One-Way Quantum Computer", Phys. Rev. Lett. **86**, 5188-5191, (2001).

[66] M. D. Lukin, M. Fleischhauer, R.Cote, L. M. Duan, D. Jaksch, J. I. Cirac and P. Zoller, "Dipole blockade and quantum information processing in mesoscopic atomic ensembles", Phys.Rev.Lett. **87**, 037901, 1-4 (2001).

[67] E. Urban, T. A. Johnson, T. Henage, L. Isenhower, D. D. Yavuz, T. G. Walker, and M. Saffman, "Observation of Rydberg blockade between two atoms", Nature Phys.**5**, 110-114 (2009).

[68] D. Jaksch, J.I. Cirac, and P. Zoller, S.L.Rolston, R. Cote and M.D. Lukin, "Fast quantum gates for neutral atoms", Phys.Rev.Lett.**85**, 2208-2211 (2000).

[69] C.M. Tesch and R.de Vivie-Riedle, "Quantum computation with vibrationally excited molecules", Phys.Rev.Lett.**89**, 157901, 1-4 (2002).

[70] C. Brif, R. Chakrabarti, H. Rabitz, "Control of quantum phenomena: Past, present and future", New J. Phys. **12**, 075008, 1-68 (2010).

[71] H. Rabitz, R. de Vivie-Riedle, M. Motzkus, and K. L.Kompa, "Whither the future of controlling quantum phenomena?", Science **288**, 824-828 (2000).

[72] S. A. Rice and M. Zhao, "Optical Control of Molecular Dynamics" (Wiley, New York, 2000).

[73] T. C. Weinacht, J. Ahn, and P. H. Bucksbaum, "Controlling the shape of a quantum wave function", Nature, **397**, 233-235 (1999).

[74] J.L. Herek, W.Wohlleben, R.J. Cogdell, D.Zeidler, M.Motzkus, "Quantum control of energy flow in light harvesting", Nature, **417**, 533-535 (2002).

[75] G. Alber, and P. Zoller, "Laser excitation of electronic wave packets in Rydberg atoms", Phys. Rep., **199**, 231-280 (1991).

[76] J. Allen and J.H. Eberly, "Optical resonance and two-level atoms" (Wiley, New York, 1975).

[77] B.W. Shore, "The Theory of Coherent Atomic Excitation" (Wiley, New York, 1990).

[78] M. Holthaus and B. Just, "Generalized π pulses", Phys. Rev. A **49**, 1950-1960 (1994).

[79] L. P. Yatsenko, S. Guérin, and H. R. Jauslin, "Pulse-driven near-resonant quantum adiabatic dynamics: Lifting of quasidegeneracy", Phys. Rev. A **70**, 043402 1-19 (2004).

[80] T.E. Skinner, T.O. Reiss, B. Luy, N. Khaneja, and S. Glaser, "Reducing the duration of broadband excitation pulses using optimal control with limited RF amplitude", J. Magn. Reson. **167**, 68-74 (2004).

[81] L.P. Yatsenko, N.V. Vitanov, B.W. Shore, T. Rickes, and K. Bergmann, "Creation of coherent superpositions using Stark-chirped rapid adiabatic passage", Opt. Commun. 204, 413-423 (2002).

[82] N. Sangouard, S. Guérin, L.P. Yatsenko, and T. Halfmann, "Preparation of coherent superposition in a three-state system by adiabatic passage", Phys. Rev. A **70**, 013415 1-9 (2004).

[83] T. Rickes, J.P. Marangos and T. Halfmann, "Enhancement of third-harmonic generation by Stark-chirped rapid adiabatic passage", Opt. Commun. 227, 133-142 (2003).

[84] V.A. Sautenkov, C.Y. Ye, Y.V. Rostovtsev, G.R. Welch, and M.O. Scully, "Enhancement of field generation via maximal atomic coherence prepared by fast adiabatic passage in Rb vapor", Phys. Rev. A **70**, 033406 1-5 (2004).

[85] M. Oberst, J. Klein and T. Halfmann, "Enhanced four-wave mixing in mercury isotopes, prepared by stark-chirped rapid adiabatic passage", Opt. Commun. **264**, 463-470 (2006).

[86] Y.-X. Yan, E. B. Gamble, Jr., and K. A. Nelson, "Impulsive stimulated scattering: General importance in femtosecond laser pulse interactions with matter, and spectroscopic applications", J. Chem. Phys. **83**, 5391, 1-9 (1985).

[87] A. Nazarkin, G. Korn, M. Wittmann, and T. Elsaesser, "Generation of Multiple Phase-Locked Stokes and Anti-Stokes Components in an Impulsively Excited Raman Medium", Phys. Rev. Lett. **83**, 2560-2563 (1999).

[88] M. Wittmann, A. Nazarkin, G. Korn, "Synthesis of periodic femtosecond pulse trains in the ultraviolet by phase-locked Raman sideband generation", Opt. Lett., **26** 298-300 (2001).

[89] R.A. Bartels, S.Backus, M.M. Murnane, H.C. Kapteyn, "Impulsive stimulated Raman scattering of molecular vibrations using nonlinear pulse shaping", Chemical Physics Letters **374**, 326-333 (2003).

[90] J. Reichert , R. Holzwarth, Th. Udem, T.W. Hänsch, "Measuring the frequency of light with mode-locked lasers", Opt. Commun. **172**, 59-68 (1999).

[91] S.T. Cundiff and J. Ye, "Colloquium: Femtosecond optical frequency combs", Rev. Mod. phys. **75**, 325-342 (2003); "Femtosecond Optical Frequency Comb Technology: Principle, Operation, and Applications", edited by J. Ye and S. T. Cundiff (Springer, New York, 2005).

[92] N. V. Vitanov and P. T. Knight, "Coherent excitation of a two-state system by a train of short pulses", Phys. Rev. A **52**, 2245-2261 (1995).

[93] D. Felinto, C. A. C. Bosco, L. H. Acioli, S. S. Vianna, "Coherent accumulation in two-level atoms excited by a train of ultrashort pulses", Opt. Commun. **215**, 69-73 (2003).

[94] M. Seidl, C. Uiberacker, and W. Jakubetz, "Pulse-train control of multiphoton transitions in enharmonic progressions: Resonance loci and resonance ridges", Chem. Phys. **349**, 296-307 (2008); M. Seidl, M. Etinski, C. Uiberacker, and W. Jakubetz, "Pulse-train control of branching processes: Elimination of background and intruder state population", J. Chem. Phys. **129**, 234305, 1-10 (2008).

[95] D. Felinto, L.H. Acioli, S.S. Vianna, "Accumulative effects in the coherence of three-level atoms excited by femtosecond-laser frequency combs", Phys. Rev. A **70**, 043403, 1-10 (2004).

[96] A. Marian, M. C. Stowe, J. R. Lawall, D. Felinto, and J. Ye, "United Time-Frequency Spectroscopy for Dynamics and Global Structure", Science **306**, 2063-2068 (2004).

[97] L. E. E. de Araujo, "Selective and efficient excitation of diatomic molecules by an ultrashort pulse train", Phys. Rev. A **77**, 033419, 1-6 (2008).

[98] E. A. Shapiro, V. Milner, and M. Shapiro, "Complete transfer of populations from a single state to a preselected superposition of states using piecewise adiabatic passage: Theory", Phys. Rev. A **79**, 023422, 1-7 (2009).

[99] S. Zhdanovich, E. A. Shapiro, J.W. Hepburn, M. Shapiro, V. Milner, "Complete transfer of populations from a single state to a pre-selected superposition of states using Piecewise Adiabatic Passage: Experiment", arXiv: 0909.0984v1, 1-9 (2009).

[100] R. R. Jones, C. S. Raman, D. W. Schumacher, and P. H.Bucksbaum, "Ramsey interference in strongly driven Rydberg systems", Phys. Rev. Lett. **71**, 2575-2578 (1993).

[101] J.A.C. Gallas, G. Leuchs, H. Walther, H. Figger, "Rydberg atoms: high-resolution spectroscopy and radiation interaction-Rydberg molecules", Adv. At. Mol. Phys. **20**, 413-466 (1985).

[102] A. ten Wolde, L. D. Noordam, A. Lagendijk, and H. B. van Linden van den Heuvell, "Observation of radially localized atomic electron wave packets", Phys.Rev. Lett. 61, 2099-2101 (1988).

[103] J. A. Yeazell, M. Mallalieu, J. Parker, and C. R. Stroud, "Classical periodic motion of atomic-electron wave packets", Phys. Rev. A **40**, 5040-5043 (1989).

[104] L. D. Nordam, H. Stapelfeldt, D. I. Duncan, and T. F.Gallagher, "Redistribution of Rydberg states by intense picosecond pulses", Phys. Rev. Lett. **68**, 1496-1499 (1992).

[105] H. C. Tran, P. C. John, J. Gao, and J. G. Eden, "Interaction of atomic wave packets with four-wave mixing: detection of rubidium and potassium wave packets by coherent ultraviolet emission", Opt. Lett. **23**, 70-72 (1998).

[106] D. Felinto, L. H. Acioli, and S. S. Vienna, "Temporal coherent control of a sequential transition in rubidium atoms", Opt. Lett. **25**, 917-919 (2000).

[107] A. A. Senin, H. C. Tran, J. Gao, Z. H. Lu, C. J. Zhu, A. L. Oldenburg, J. R. Allen, J. G. Eden, "Molecular dissociation observed with an atomic wavepacket and parametric four-wave mixing", Chem. Phys. Lett. **381**, 53-59 (2003).

[108] Yu. P. Malakyan, "Hyper-Raman scattering and four-wave parametric interaction in two-photon pumping of metal vapors", Sov.J.Quant.Electron. **15**, 905-1004 (1985).

[109] K. J. Blow, R. Loudon, and S. J. D. Phoenix, "Continuum fields in quantum optics", Phys. Rev. A **42**, 4102-4114 (1990).

[110] A. Kuhn, M. Hennrich, T. Bondo, and G. Rempe, "Controlled generation of single photons from a strongly coupled atom-cavity system", Appl. Phys. B **69**, 373-377 (1999).

[111] P. Lambropoulos and D. Petrosyan, "Fundamentals of Quantum Optics and Quantum Information" (Springer, Berlin 2006).

[112] C. W. Gardiner and P. Zoller, "Quantum Noise" (Springer-Verlag, Berlin 1999).

[113] M. Lax, Fluctuation and Coherence Phenomena and Quantum Optics (Gordon and Breach, New-York 1968).

[114] M. O. Scully, M. S. Zubairy, "Quantum optics" (Cambridge University Press 1997).

[115] H.-W. Hubers, S. G. Pavlov, and V. N. Shastin, "Terahertz lasers based on germanium and silicon", Semicond. Sci. Technol. **20**, 211-221 (2005).

[116] S. G. Pavlov, H.-W. Hbers, M. F. Kimmitt, H. Riemann, and V. N. Shastin, "Frequency tunability of the terahertz silicon laser by a magnetic field", App. Phys. Lett., **89**, 021108, 1-3 (2006).

[117] A. Barkan, F. Kittel, D. M. Mittleman, R. Dengler, P. H. Siegel, G. Scalari, L. Ajili, J. Faist, H. E. Beere, E. H. Linfield, A. G. Davies, D. A. Ritchie, "Linewidth and tuning characteristics of terahertz quantum cascade lasers", Opt. Lett. **29** 575-577 (2004).

[118] T. Chanelière, D. N. Matsukevich, S. D. Jenkins, T. A. B. Kennedy, M. S. Chapman, and A. Kuzmich, "Quantum Telecommunication Based on Atomic Cascade Transitions", Phys. Rev. Lett. **96**, 093604, 1-4 (2006).

[119] W. Ketterle, K. B. Davis, M. A. Joffe, A. Martin, and D. E. Pritchard,"High densities of cold atoms in a dark spontaneous-force optical trap", Phys. Rev. Lett. **70**, 2253-2256 (1993).

[120] R. Onofrio, C. Raman, J. M. Vogels, J. R. Abo-Shaeer, A. P. Chikkatur, and W. Ketterle, "Observation of Superfluid Flow in a Bose-Einstein Condensed Gas", Phys. Rev. Lett. **85**, 2228-2231 (2000).

[121] J. Brendel, N. Gisin, W. Tittel, and H. Zbinden, "Pulsed Energy-Time Entangled Twin-Photon Source for Quantum Communication", Phys. Rev. Lett.**82**, 2594-2597 (1999).

[122] L. M. Duan, M. D. Lukin, J. I.Cirac, and P. Zoller, "Long-distance quantum communication with atomic ensembles and linear optics", Nature **414**, 413-418 (2001).

[123] N. Sisakyan and Yu. Malakyan, "Quantum theory for generation of nonclassical photon pairs by a medium with collective atomic memory", Phys. Rev. A **72**, 043806 1-9 (2005).

[124] A. Kuzmich, W. P. Bowen, A. D. Boozer, A. Boca, C. W. Chou, L.-M. Duan, and H. J. Kimble, "Generation of Nonclassical Photon Pairs for Scalable Quantum Communication with Atomic Ensembles", Nature **423**, 731-734 (2003); Wei Jiang, C. Han, P. Xue, L. M. Duan, and G. C. Guo, "Nonclassical photon pairs generated from a room-temperature atomic ensemble", Phys. Rev. A **69**, 043819 1-5 (2004).

[125] D. Daems, A. Keller, S. Guérin, H. R. Jauslin, and O. Atabek, "Unitary time-dependent superconvergent technique for pulse-driven quantum dynamics", Phys. Rev. A **67**, 052505, 1-9 (2003).

[126] A. M. Lyyra, W.T. Luh, L. Li, H. Wang, and W.C. Stwalley, "The $A^1\Sigma_u^+$ state of the potassium dimer", J. Chem. Phys. **92**, 43, 1-8 (1990).

[127] R. Boyd, M. S. Malcuit, and D. J. Gauthier, "Competition between amplified spontaneous emission and the four-wave-mixing process", Phys. Rev. A **35**, 1648-1658 (1987).

[128] Z. H. Lu, C.-J.Zhu, Zhu, A.A. Senin, J.R. Allen, J. Gao, J.G. Eden, "Production and probing of atomic wavepackets with ultrafast laser pulses: applications to atomic and molecular dynamics", IEEE J. Sel. Top.Quant. Electron. **10**, 159-168 (2004).

[129] C.-J. Zhu, Y. Xiao, A. A. Senin, J. Gao, J. G. Eden, T. S. Varzhapetyan and D. H. Sarkisyan, "Quantum beating in Rb at 18.3 THz (608 cm^1) detected by parametric six-wave mixing and sum-frequency generation in $LiIO_3$", Phys.Rev. A **75**, 053405, 1-5 (2007).

[130] Q. H. F.Vrehen and H. M. Hikspoors, "Parametric generation in cesium vapor by nearly resonant two-photon pumping", Optics Commun. **18**, 113-114 (1976); D.Cotter, D.Hanna, W.Tuttlebee, and M.Yuratich, "Stimulated hyper-Raman emission from sodium vapour", Optics Commun. **22**, 190-194 (1977); M.A.Moore, W. R. Garrett, and M. G. Payne, "Suppression of electronic hyper-Raman emission by four-wave mixing interference", Optics Commun. **68**, 310-316 (1988); M.-H.Lu and Yu mei Liu, "Suppression of stimulated hyper-Raman scattering in lithium vapor", Appl.Phys.B **57**, 167-176 (1993).

[131] W.H.Louisell, Quantum Statistical Properties of Radiation (Wiley, New York, 1973).

[132] D.F. Walls, Gerard J. Milburn, "Quantum optics" (Springer, Berlin, 2008).

Papers included in the thesis

[133] A. Gogyan, S. Guérin, H.-R. Jauslin, and Yu. Malakyan, "Deterministic source of a train of indistinguishable single-photon pulses with single-atom-cavity system", Phys. Rev. A **82**, 023821, 1-6 (2010).

[134] A. L. Gogyan, and Yu. P. Malakyan, "Entanglement-preserving frequency conversion in cold atoms", Phys. Rev. A, **77**, 033822, 1-7 (2008).

[135] A. Gogyan, S. Guérin, and Yu. Malakyan, "Shaping coherent excitation of atoms and molecules by a train of ultrashort laser pulses", Phys. Rev. A, **81**, 033401, 1-7 (2010).

[136] A. L. Gogyan, and Yu. P. Malakyan, "Quantum Beats in Stimulated Electronic Raman Scattering of Ultrashort Laser Pulses", Optics and Spectroscopy, **101**, 751-756 (2006).

[137] A. L. Gogyan, and Yu. P. Malakyan, "Quantum beating in uv radiation generation by ultrashort laser pulses via four-wave mixing", Phys. Rev. A, **78**, 053401, 1-8 (2008).

[138] A. Gogyan, "Qubit transfer between photons at telecom and visible wavelengths in a slow-light atomic medium", Phys. Rev. A, **81**, 024304, 1-4 (2010).

[139] A. Gogyan and Yu. Malakyan, "Selective excitation of atoms and molecules by ultrashort laser pulses", Proc. of SPIE, **7027** 70271L, 1-10 (2008).

Conference thesis and abstracts

[140] A. Gogyan, S. Guérin, H.-R. Jauslin, and Yu. Malakyan, "Deterministic generation of indistinguishable single-photon pulses in the single-atom-cavity QED system", 5-th workshop advances in foundation of quantum mechanics and quantum information and 3-rd IQIS conference, May 23-29, Turin, Italy, Book of abstracts, alph. ordering (2010).

[141] A. Gogyan, "Deterministic generation of indistinguishable single-photon pulses", Control of Quantum Dynamics of Atoms, Molecules and Ensembles by Light Workshop 2010 , Varna, Bulgaria, June 29-July 2, Book of abstracts p.10 (2010).

[142] Yu. Malakyan, A. Gogyan, "Optical control of coherent excitation of atoms and molecules via quantum beating in uv generation", 10th European Conference on Atoms Molecules and Photons, 4-9 July, Salamanca, Spain, P-683 (2010).

[143] Yu. Malakyan, A. Gogyan, S. Guérin, H.-R. Jauslin, "Indistinguishable single-photon pulses from double-raman-single-atom-cavity system", 10th European Conference on Atoms Molecules and Photons, 4-9 July, Salamanca, Spain, P-538 (2010).

[144] A.Gogyan, Journées des Écoles Doctorales Carnot et Pasteur, "Shaping coherent excitation of atoms and molecules by a train of ultrashort laser pulses", May 6-7, Besancon, France, Abstracts, p. C02 (2010).

[145] A.Gogyan, Journées des Écoles Doctorales Carnot et Pasteur, "Deterministic emission of a single-photon in a single-atom-cavity system, May 7-8, Dijon, France, Abstracts, p.40 (2009).

[146] A.Gogyan, S. Guérin, H.-R. Jauslin, and Yu. Malakyan, "Deterministic emission of a single-photon in a single-atom-cavity system", Modern Problems of Optics and Photonics, Abstract Book, August 27-Sept. 2, Yerevan, Armenia, p. 36. (2009).

[147] A. Gogyan and Yu. Malakyan, "Selective excitation of atoms and molecules by ultrashort laser pulses", XV Int. School of Quantum Electronics, 15-19 Sept., Burgas, Bulgaria, Abstracts, p.75-76 (2008).

Title: Generation and interfacing of single-photon light with matter and control of ultrafast atomic dynamics for quantum information processing

Abstract: We develop a robust and realistic mechanism for the generation of indistinguishable single-photon (SP) pulses with identical frequency and polarization. They are produced on demand from a coupled double-Raman atom-cavity system driven by a sequence of laser pump pulses. This scheme features a high efficiency, the ability to produce a sequence of narrow-band SP pulses with a delay determined only by the pump repetition rate, and simplicity of the system free from complications such as repumping process and environmental dephasing.

We propose and analyze a simple scheme of parametric frequency conversion for optical quantum information in cold atomic ensembles. Its remarkable properties are minimal losses and distortion of the pulse shape, and the persistence of quantum coherence and entanglement. Efficient conversion of frequency between different spectral regions is shown. A method for the generation of frequency-entangled single photon states is discussed.

We suggest a robust and simple mechanism for the coherent excitation of molecules or atoms to a superposition of pre-selected states by a train of femtosecond laser pulses, combined with narrow-band coupling field.

The theory of quantum beatings in the generation of ultra-violet radiation via a four wave mixing in pump-probe experiments is developed. The results are in good agreement with experimental data observed in Rb vapor when the laser phase fluctuations are significant.

Key words: Cavity quantum electrodynamics, single-photon generation, quantum frequency conversion, parametric interaction, selective excitation, atomic coherence, quantum beatings, four-wave-mixing process

Titre : Génération et interfaçage de lumière à photon unique et contrôle de la dynamique atomique ultra-rapide pour l'information quantique

Résumé : Nous développons un mécanisme robuste et réaliste pour la génération de photons uniques indiscernables avec des impulsions de fréence et de polarisation identiques. Ils sont produits à la demande à partir d'un système couplé atome-cavité double-Raman en interaction avec une séquence d'impulsions laser de pompe. Ce processus combine un rendement élevé, la capacité de produire une séquence d'impulsions de photons uniques à bande étroite avec un retard déterminé seulement par le taux de répétition de la pompe, avec la simplicité du système libre de complications comme le repompage et le déphasage de l'environnement.

Nous proposons et analysons un schéma simple de conversion paramétrique de fréence pour l'information quantique optique dans des ensembles atomiques froids. Ses propriétés remarquables sont des pertes réduites, une distorsion de la forme des impulsions minimale, ainsi que la persistance de la cohérence quantique et de l'intrication. Une conversion efficace de fréquence entre les différentes régions spectrales est montrée. Une méthode de génération d'états caractérisant des photons uniques intriqués en fréquence est discutée.

Nous proposons un mécanisme robuste et simple d'excitation cohérente de molécules et d'atomes en une superposition d'états pré-sélectionnés par un train d'impulsions laser femtoseconde, combinée avec un champ de couplage à largeur de bande étroite.

La théorie des battements quantiques pour la génération du rayonnement ultra-violet par mélange à quatre ondes dans des expériences pompe-sonde est développée. Les résultats sont en bon accord avec les données expérimentales observées dans la vapeur de Rb lorsque les fluctuations de phase laser sont importantes.

Mots clefs : Electrodynamique quantique en cavité, génération de photons uniques, conversion de fréquence quantique, interaction paramétrique, excitation sélective, cohérence atomique, battements quantiques, processus de mélange à quatre ondes.